NASA/TM-2006-213677

2004 Research Engineering Annual Report

Compiled by
Patrick Stoliker, Bradley Flick, and Everlyn Cruciani
NASA Dryden Flight Research Center
Edwards, California

June 2006

NASA STI Program ... in Profile

Since its founding, NASA has been dedicated to the advancement of aeronautics and space science. The NASA scientific and technical information (STI) program plays a key part in helping NASA maintain this important role.

The NASA STI program is operated under the auspices of the Agency Chief Information Officer. It collects, organizes, provides for archiving, and disseminates NASA's STI. The NASA STI program provides access to the NASA Aeronautics and Space Database and its public interface, the NASA Technical Report Server, thus providing one of the largest collections of aeronautical and space science STI in the world. Results are published in both non-NASA channels and by NASA in the NASA STI Report Series, which includes the following report types:

- TECHNICAL PUBLICATION. Reports of completed research or a major significant phase of research that present the results of NASA programs and include extensive data or theoretical analysis. Includes compilations of significant scientific and technical data and information deemed to be of continuing reference value. NASA counterpart of peer-reviewed formal professional papers but has less stringent limitations on manuscript length and extent of graphic presentations.

- TECHNICAL MEMORANDUM. Scientific and technical findings that are preliminary or of specialized interest, e.g., quick release reports, working papers, and bibliographies that contain minimal annotation. Does not contain extensive analysis.

- CONTRACTOR REPORT. Scientific and technical findings by NASA-sponsored contractors and grantees.

- CONFERENCE PUBLICATION. Collected papers from scientific and technical conferences, symposia, seminars, or other meetings sponsored or cosponsored by NASA.

- SPECIAL PUBLICATION. Scientific, technical, or historical information from NASA programs, projects, and missions, often concerned with subjects having substantial public interest.

- TECHNICAL TRANSLATION. English-language translations of foreign scientific and technical material pertinent to NASA's mission.

Specialized services also include creating custom thesauri, building customized databases, and organizing and publishing research results.

For more information about the NASA STI program, see the following:

Access the NASA STI program home page at *http://www.sti.nasa.gov*.

- E-mail your question via the Internet to help@sti.nasa.gov.

- Fax your question to the NASA STI Help Desk at (301) 621-0134.

- Phone the NASA STI Help Desk at (301) 621-0390.

- Write to:
  NASA STI Help Desk
  NASA Center for AeroSpace Information
  7121 Standard Drive
  Hanover, MD 21076-1320

NASA/TM-2006-213677

2004 Research Engineering Annual Report

Compiled by
Patrick Stoliker, Bradley Flick, and Everlyn Cruciani
NASA Dryden Flight Research Center
Edwards, California

National Aeronautics and
Space Administration

Dryden Flight Research Center
Edwards, California 93523-0273

June 2006

NOTICE

Use of trade names or names of manufacturers in this document does not constitute an official endorsement of such products or manufacturers, either expressed or implied, by the National Aeronautics and Space Administration.

Available from the following:

NASA Center for AeroSpace Information
7121 Standard Drive
Hanover, MD 21076-1320
(301) 621-0390

National Technical Information Service
5285 Port Royal Road
Springfield, VA 22161-2171
(703) 605-6000

2004 RESEARCH ENGINEERING REPORT

Table of Contents

2004 Research Engineering Directorate Staff

Director	Patrick Stoliker
Deputy Director (Acting)	Bradley Flick
Associate Director	Ron Young
Administrative Officer	Everlyn Cruciani

*__Branch Codes and Chiefs__

RA – Aerodynamics (Acting)	Greg Noffz
RC – Controls and Dynamics	Joe Pahle
RF – Flight Systems	Bob Antoniewicz
RI – Flight Instrumentation	Glen Bever
RP – Propulsion and Performance	Dave Lux
RS – Aerostructures	Tom Horn

THE X-43A (HYPER-X) FLIES INTO THE RECORD BOOKS

Summary

The goal of the Hyper-X research program, conducted jointly by the NASA Dryden Flight Research Center and the NASA Langley Research Center, was to demonstrate and validate the technology, experimental techniques, and computation methods and tools for design and performance predictions of a hypersonic aircraft with an airframe-integrated, scramjet propulsion system. Three X-43A airframe-integrated, scramjet research vehicles were designed and fabricated to achieve that goal by flight test: two test flights at Mach 7 and one test flight at Mach 10. The first flight, conducted on June 2, 2001, experienced a launch vehicle failure and resulted in a 9-month mishap investigation. A two-year return-to-flight effort ensued and concluded when the second Mach 7 flight was successful on March 27, 2004. Just eight months later, on November 16, the X-43A successfully completed the third and final flight. These two flights were the first flight demonstrations, at Mach 7 and Mach 10 respectively, of an airframe-integrated, scramjet-powered, hypersonic vehicle.

Objective

The primary objective of the X-43A project was to demonstrate the performance of an airframe-integrated, scramjet-powered vehicle at selected test conditions. Data were acquired to verify scramjet, aerodynamics, and stability and control performance predictions as well as to perform flight correlation of the ground-based experimental data. In addition, data were acquired to verify the hypersonic vehicle structural integrity and system design.

Approach

The X-43A missions were designed such that the maximum amount of data could be obtained to demonstrate and validate the technology, design tools and techniques.

Mission Overview

Following release from the NASA B-52B (The Boeing Company, Chicago, Illinois) airplane, tail number 008, the Hyper-X Launch Vehicle (HXLV), a modified first stage Pegasus® (Orbital Sciences Corporation, Dulles, Virginia) rocket booster, launched the X-43A to the predetermined research test conditions (fig. 1). After separation from the HXLV and during the engine test phase, the X-43A engine ignited and operated for approximately 10 s. Following the Mach 7 engine operation, a parameter identification (PID) maneuver was performed. Subsequent to the engine sequence, the X-43A performed a recovery maneuver to begin the controlled predetermined descent trajectory. During the descent, PID, push-over-pull-up, and frequency sweep maneuvers were performed to assess aerodynamic characteristics and open-loop frequency response.

EC04-0092-32

Figure 1. Hyper-X Launch Vehicle boost.

Mach 7 and Mach 10 Flight Results

For both the Mach 7 and Mach 10 missions, the HXLV maintained nominal attitude throughout the boost, closely followed the predicted trajectory, and delivered the X-43A to the desired separation conditions well within the specified tolerance. After issuing the “separate” command, the X-43A successfully separated from the HXLV and achieved stable flight. The adapter cameras looking at the aft end of the X-43A captured the separation event, as shown in figure 2. Following separation, the engine sequence began. During the powered flight of the Mach 7 mission, scramjet engine performance was within 3 percent of the preflight predictions and sufficient to overcome additional airframe drag and produce net positive thrust (fig. 3). The maximum powered Mach number achieved was 6.8. For the Mach 10 mission, the vehicle achieved a cruise condition with a maximum powered Mach number of 9.6. For both flights, the X-43A remained controlled from separation through the engine test and descent and successfully completed the descent maneuvers. All systems on both the launch vehicle and the X-43A performed well and extensive research quality data was acquired throughout the flight.

Status

Although the project concluded with the completion of the Mach 10 flight, the data continues to be analyzed.

050048-2

Figure 2. Adapter camera view of X-43A separation.

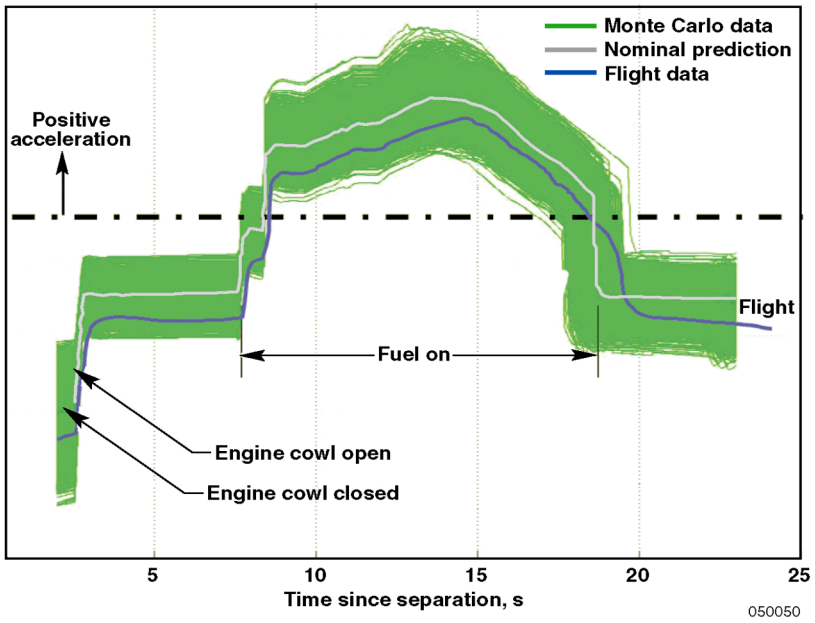

Figure 3. Mach 7 axial acceleration profile during the engine test.

Contacts

Laurie Grindle, DFRC, Code R, (661) 276-2988
Catherine Bahm, DFRC, Code R, (661) 276-3123

THE X-43A FLIGHT SYSTEM HIGHLIGHTS AND CHALLENGES FOR THE SECOND AND THIRD FLIGHTS

Summary

The following sections summarize tests that were performed on the X-43A Hyper-X Research Vehicle (HXRV) and Hyper-X Launch Vehicle (HXLV) in preparation for two flight tests in 2004. The first section covers the first flight at Mach 7 and the second section covers the flight at Mach 10. The challenges encountered during the verification and validation effort are presented, along with results and highlights.

Flight 2 Highlights and Challenges

After the loss of the first X-43A Hyper-X Research Vehicle (HXRV) booster stack on June 2, 2001, a number of return-to-flight activities were formulated to increase the mission success of the program. Some of these activities involved tests that were applicable to both the Hyper-X Launch Vehicle (HXLV) and the X-43A HXRV. The flight systems group supported the HXRV activities by developing and conducting the actuator compliance, timing, and calibration tests, in addition to nominal and off-nominal aircraft-in-the-loop (AIL) tests. The compliance and timing tests were new characterization tests for the second vehicle. The calibration and AIL tests were refined to a higher fidelity to thoroughly validate the systems.

The compliance test measured the elastic deformation of the entire actuation system when the surfaces are under load. One contributing factor to the mishap was the inaccurate modeling of compliance in the HXLV fin actuation system. As much as 90 percent of total compliance can occur outside the servo loop, the region from the actuator to the linkages that cannot be detected by the position feedback sensor. To model the system accurately, compliance inside and outside the servo loop should be measured using the representative hardware. For the HXRV, total wing compliance was, on average, 0.75° at ±1780 in-lb torque. Of this value, approximately 80 percent is outside the servo loop. Average rudder compliance was approximately 0.4° at ±470 in-lb. Approximately 75 percent of the rudder compliance is outside the loop. Simulation analyses indicated no problems for the HXRV. Planning, staging, and conducting this test was quite challenging, because it involved cross-discipline support, facilities, and specialized equipment such as a laser tracker, custom cable-extension transducers, and accurate hydraulic loading equipment all operating simultaneously.

The timing test measures the time between actuator command and initial surface motion. It also provides timing of the position feedback loop to the flight control computer. The data is used to quantify time delays within a system and is modeled in the X-43A simulation.

For the first HXRV, surfaces were calibrated using a digital inclinometer and custom fabricated protractors. To obtain higher fidelity data for the remaining vehicles, a laser tracker was used to measure angles with accuracies better than ±0.001°. The AIL tests were refined through the use of updated actuator and timing models. Nominal and off-nominal tests were conducted with simulated or real actuator feedback in the loop.

The second X-43A flight occurred on March 27, 2004, and flew successfully, gathering scramjet data for approximately 11 s. It accelerated to a maximum Mach number of 6.83 during free flight at an altitude of approximately 94,000 ft. All systems remained functional up to ocean impact. The average wing compliance inside the servo loop during boost was approximately 19.5 percent more than ground test measurements. The point loading technique used in ground testing is a possible explanation for the discrepancy. The actuator command and feedback matched well throughout the entire mission. The vehicle set a new Guinness World Record for speed in an air-breathing aircraft. Figure 1 shows the second HXRV moments before free flight.

050048-2

Adapter camera view of the HXRV number 2.

Flight 3 Highlights and Challenges

The third HXRV flight required software changes to enhance the performance of the propulsion, guidance, and controller systems. While it was in the process of being updated, hardware testing continued with the help of test equipment that was specifically designed to interface with the HXRV, the adapter, and the HXLV at any configuration stage. Activities such as stack integration progressed without the delay of waiting for the software. When the final version of the flight code was released, validation testing was conducted using slight modifications to the original test setup to match the current configuration of the assembled vehicles.

The captive carry flight proved to be challenging. The first two attempts were cancelled because of B-52B hydraulic pack problems. In the third attempt, a longer than expected power transfer from ground power to B-52B airplane power caused the HXRV flight control computer to reject global positioning system (GPS) data. During the normal transfer process, which takes approximately 3–4 min, the GPS signal is removed from the HXRV flight control computer, and is restored when the transfer is complete. For this mission, the transfer took approximately 6 min, which caused the internal HXRV GPS time to drift. After the signal was restored, the true GPS data did not fall within the lagged Kalman filter estimates, causing the flight control computer to reject the true GPS signal for use in blended (GPS + inertial) navigation. The project personnel decided to proceed, since the primary captive carry objectives were to demonstrate that the HXRV oxygen intrusion levels were below 1.5 percent (to reduce the possibility of the silane igniter creating a fire hazard), and that there were no electromagnetic interference (EMI) or electromagnetic compatibility (EMC) problems.

Once airborne, the HXRV navigation and related parameters were invalid. An inflight power cycle did not clear the problem. After the postflight investigation, a temporary backup battery was used during the power transfer to solve the GPS blackout issue.

The first attempt for the third flight was aborted because of delays caused by an electronically scanned pressure module and the aft transmitter. The second attempt, on November 16, 2004, resulted in the successful accomplishment of the flight objectives. The vehicle achieved cruise

conditions at a maximum Mach number of 9.68, at an altitude of approximately 109,000 ft. Navigation systems performed nominally. Right wing compliance within the servo loop was about 16.6 percent more than ground test data, and the left wing was 6.28 percent less, because of slight asymmetrical hinge moments during boost. In the postengine experiment phase, a pressure signal input exceeded the multiplexer limits, causing a spillover effect onto other flight control computer input channels. This effect resulted in a temporary bias on three actuator feedback signals, but did not affect their performance. A second speed record was awarded by the Guinness World Records organization to the Hyper-X team.

Contacts

Yohan Lin, DFRC, Code RF, (661) 276-3155

HYPER-X RESEARCH VEHICLE MACH 7 AND MACH 10 MISSION GUIDANCE, NAVIGATION, AND CONTROL PERFORMANCE

Summary

The Hyper-X program culminated in two successful flights in 2004 of the X-43A, also known as the Hyper-X Research Vehicle (HXRV). The first flight of 2004 occurred on March 27 and reached a top speed of Mach 6.9. During this mission, the HXRV demonstrated the first inflight operation of an airframe-integrated scramjet engine. All of the objectives for the Mach 7 mission were accomplished including separation from the HXLV, vehicle acceleration during the scramjet test, and controlled flight to an impact in the Pacific Ocean. The second mission, to Mach 10, occurred on November 16, 2004. The HXRV achieved a maximum Mach number of 9.7. All of the mission objectives for the Mach 10 mission were accomplished.

Objective

The NASA Dryden Flight Research Center (DFRC) Guidance, Navigation, and Control (GNC) team supported the Mach 7 mission flight test. Data from the Mach 7 mission were examined for approximately one month; subsequently, three months were allocated for the GNC team to update the HXRV software for the Mach 10 mission. The software update team included team members from DFRC, Analytical Mechanics Associates, Inc. (AMA), The Boeing Company, and the NASA Langley Research Center. A software update was required because the HXRV guidance and control system algorithms had not been designed for use above Mach 7.5. Additionally, lessons learned from examining the data from the Mach 7 mission needed to be incorporated. There were also several unique aspects of the Mach 10 mission to be addressed. For example, the engine fueling profile was significantly different between the Mach 7 and Mach 10 missions, resulting in an update to the engine on elevator loop feed-forward terms.

Data from the successful Mach 7 mission provided confidence in the analysis tools and techniques used to model the HXRV control system and performance. The analysis tools included linear models and a nonlinear simulation, which could be used for Monte Carlo analysis. The inflight performance of the HXRV during the Mach 7 flight validated these tools and analysis techniques. This confidence in the models and tools allowed the HXRV software to be quickly updated for the Mach 10 mission.

After the software update for the Mach 10 mission, the GNC team supported the flight test and analyzed the flight data.

Results

For both missions, the HXRVs successfully separated from the HXLV, were within the desired engine test conditions, completed the recovery maneuver, flew a controlled descent to a splashdown in the Pacific Ocean, and conducted parameter identification (PID) maneuvers at every integer Mach number. The inflight vehicle performance was generally within the preflight Monte Carlo simulation predictions, however, several unique events were seen in each mission. The HXRVs both experienced a large amplitude bank angle excursion slightly below Mach 1. During the Mach 7 mission, the HXRV experienced a small amplitude angle of attack oscillation during the recovery maneuver. The cause of the oscillation is still under investigation and was not seen at any time during the Mach 10 mission. During the Mach 10 mission, the HXRV failed to track the normal acceleration (Nz) command and experienced a rocking in bank angle of ±10° growing to ±20° about the command. The HXRV began following the commands shortly prior to the Mach 8 PID maneuver. Flight data is indicating that air was unexpectedly flowing through the engine at this time, and this is the likely cause for the HXRV not tracking the Nz and bank angle commands.

Status

The GNC team is in the process of documenting the flight results in papers and flight reports. Data from the Mach 7 and Mach 10 missions is continuing to be evaluated.

050048-2

Aft view of the HXRV during the Mach 7 mission separation event.

Contacts

Ethan Baumann, DFRC, Code RC, (661) 276-3417
Cathy Bahm, DFRC, Code RC, (661) 276-3123
Brian Strovers, AMA, (661) 276-5415

THE X-43A FORCE AND MOMENT ANALYSIS

Summary

Airframe accelerations and rotational rates measured during force and moment analysis maneuvers provided a continuous record of the vehicle body axis aerodynamic forces and moments. These maneuvers were conducted in a Mach range of 9.60 to 0.76, at an altitude range of 110,000 ft to sea level, with a dynamic pressure range of 1100 to 550 psf, and an observed angle of attack range of 3 to 9 deg. These flight measurements were then compared with preflight predictions based on wind tunnel test data. The comparisons covered topics such as stability and control characteristics, static margins, longitudinal and lateral-directional characteristics, and aerodynamic characteristics in this flight regime.

Objective

The primary objective of the analysis was to compare the force and moments generated from flight with the preflight predictions. This data would then be used to refine the preprediction tools used for the analysis and design of hypersonic vehicles.

Approach

Frequency sweeps and modified Schroeder sweeps were performed throughout the X-43A cowl-closed descent phase. Extraction of the Hyper-X Research Vehicle (HXRV) cowl-closed aerodynamics from flight is based on manipulation of the body axis system (BAS) 6-degree-of-freedom (DOF) equations of motion. Specifically, flight-measured kinematic state measurements, onboard accelerometer and rate gyro readings, and mass property model data are used to deduce BAS 6-DOF aerodynamic forces and moments. The figure below shows the BAS system used during the analysis.

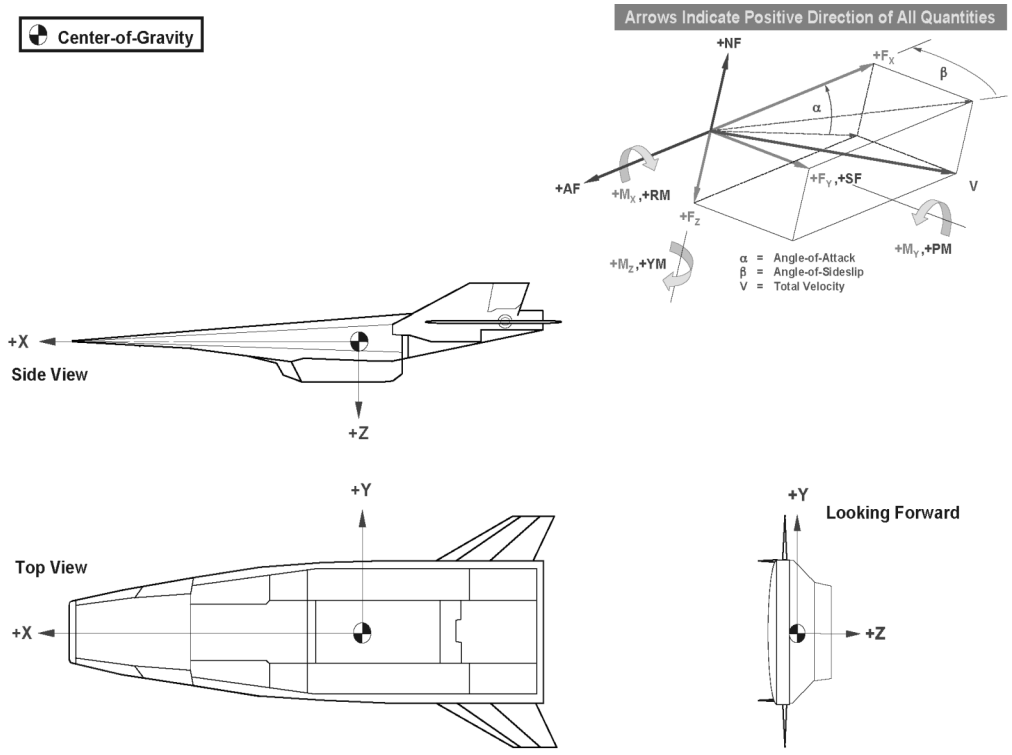

Coordinate system used for the force and moment analysis.

Status

The analysis for flight 2 is complete and the analysis for flight 3 is approximately 95 percent complete. Two reports are in the process of being written. The report for flight 2 is currently in peer review and the third report is currently being written. The flight 2 report is titled “Flight Test-Determined Aerodynamic Force and Moment Characteristics of the X-43A Research Vehicle at Mach 7.0” and the flight 3 report is titled “Flight Test-Determined Aerodynamic Force and Moment Characteristics of the X-43A Research Vehicle at Mach 10.0.”

Contacts

Mark Davis, DFRC, Code RA, (661) 276-2241

THE X-43A AND B-52B TUNNEL TEST

Summary

A low speed wind tunnel test was performed with a 3-percent-scale model of the Orbital Sciences Corporation (Dulles, Virginia) Pegasus® booster rocket mated to the X-43A research vehicle and the B-52B (The Boeing Company, Chicago, Illinois) airplane. The test was conducted both in freestream [for the Hyper-X Launch Vehicle (HXLV)] and in the presence of a partial model of the B-52B launch vehicle. The objectives of the test were to obtain force and moment data to generate structural loads affecting the pylon of the B-52B and to determine the aerodynamic influence of the B-52B on the HXLV for evaluating launch separation characteristics. The data gathered was used to develop loads models and for use in engineering simulations.

Objective

The primary objective of the test was to characterize the aerodynamic influences of the B-52B airplane on the X-43A stack. The resulting data was then used to generate aerodynamic loads tables for use in verifying the B-52B pylon capabilities.

Approach

A low speed wind tunnel test was conducted to gather crucial data. This data was difficult to gather using analytical methods because of the complex flow fields. The figure below shows the models used in testing.

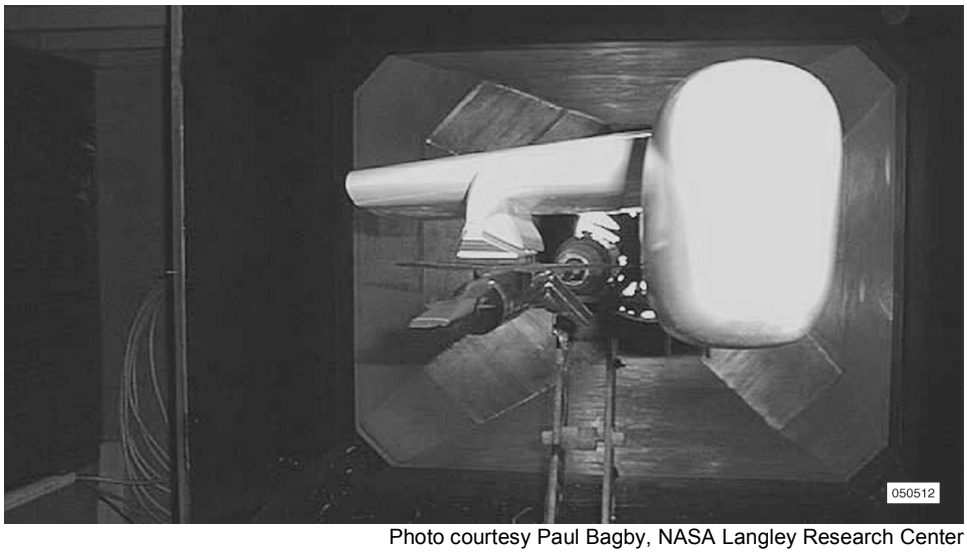

Photo courtesy Paul Bagby, NASA Langley Research Center

The B-52B with the HXLV in the low-speed tunnel test section.

Status

The tests have been completed. The data were used to develop an aerodynamic loads database and were used in an engineering based simulation. A NASA Technical Memorandum was written along with an American Institute of Aeronautics and Astronautics (AIAA) presentation. The title of the report is “Wind Tunnel Results of the B-52B with the X-43A Stack.”

Contacts

Mark Davis, DFRC, Code RA, (661) 276-2241

THE X-43 PARAMETER IDENTIFICATION RESEARCH

Summary

Initial analyses of flights 2 and 3 have been completed. Analysis covered longitudinal and lateral/directional analysis. The results of the flight 2 parameter identification (PID) led to the desire to make updates to the PID maneuvers used by the X-43A Hyper-X Research Vehicle (HXRV). The data from flight 2 was used in conjunction with simulations to redefine and redesign the PID maneuvers used for flight 3. For both flight 2 and 3, the descent PID maneuvers were nominal.

Objective

The primary object of the PID analysis was to extract aerodynamic coefficients and aerodynamic performance data from the X-43A HXRV during the nonpowered portion of the flight. This data will then be used to update the aerodynamic database for hypersonic vehicles.

Approach

The approach taken was to have both the NASA Dryden Flight Research Center (DFRC) and the NASA Langley Research Center (LaRC) work together to develop the maneuvers used for PID research. Then each center would analyze the data using different methods. The DFRC used a time-domain, output-error program called pEst while LaRC used a frequency domain method. Finally, the results from the two methods were compared and a paper was written on the findings.

Status

Initial analyses of flights 2 and 3 have been completed. Both LaRC and DFRC have presented papers on the results at a Joint Army, Navy, NASA, Air Force (JANNAF) conference. The paper presented was titled “Aerodynamic Parameter Estimation for Flight 2 of the X-43A." A second paper to present the data from flight 3 is currently in progress.

Contacts

Mark Smith, DFRC, Code RA, (661) 276-3177

THE X-43A FLUSH AIRDATA SENSING RESEARCH

Summary

A flush airdata sensing (FADS) system was flight tested on two X-43A Hyper-X Research Vehicle (HXRV) missions, providing a unique opportunity to validate the system in the hypersonic flight regime. The FADS system was used on three flight tests from Mach 0.8 to Mach 9.6, with an angle of attack ranging from –6 to 15 deg and an angle of sideslip ranging from ±3°. The FADS system provided estimation of angle of attack, angle of sideslip, and dynamic pressure.

Objective

After several years of performing ground tests, the FADS system was flight tested in hypersonic flight conditions. The FADS system was flown at Mach 7.0 and at Mach 9.6. The third flight (the Mach 9.6 test point) was faster than any tests conducted on the ground and all preflight data prior to the third flight was obtained using only analytical methods. This flight data will be analyzed to verify the functionality and performance of the FADS system.

Approach

The approach was to develop, ground test, and flight test a FADS system on the X-43A HXRV. The data obtained will be compared to the inertial flight data, the data obtained through trajectory reconstruction, and all preflight analysis. From this analysis, the calibration used for flight will be reevaluated. The vehicle configuration necessitated modification of the FADS system from the flight 2 configurations to a smaller system for flight 3. The systems architecture for flight 2 and flight 3 are shown in the following figure:

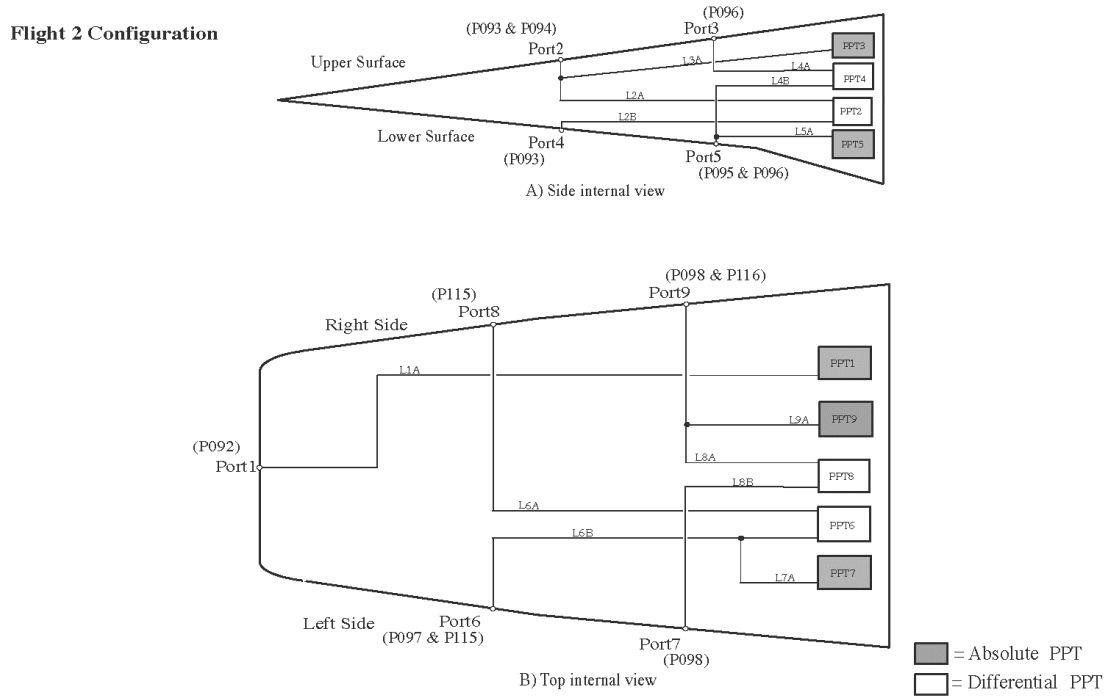

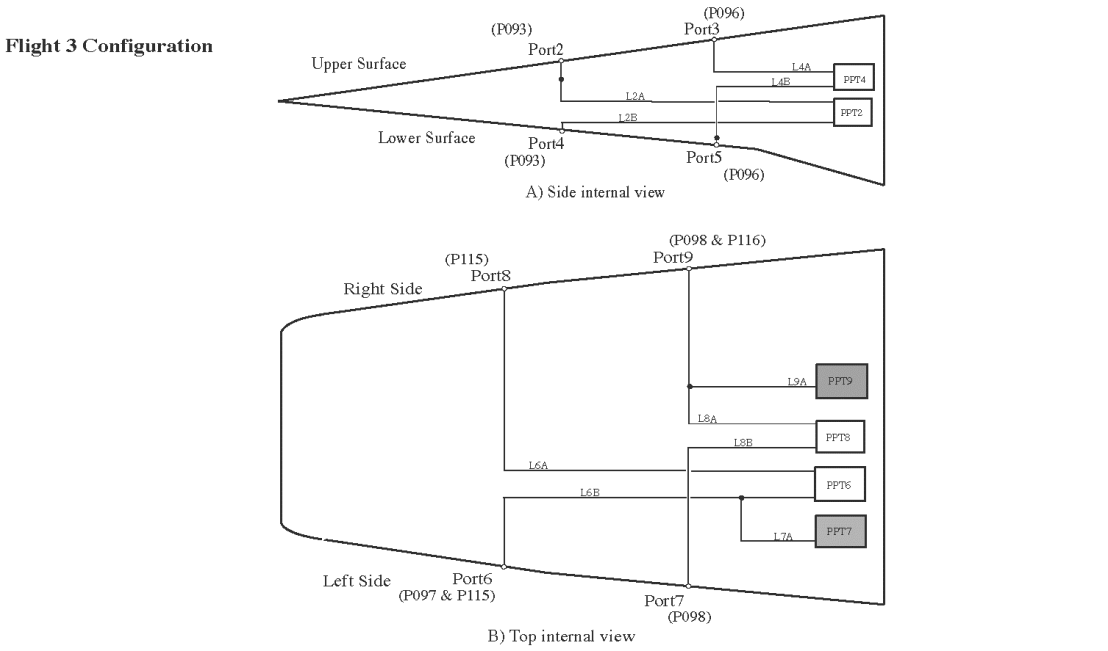

The flush airdata sensing layout for flight 2 and flight 3.

Status

Currently, the FADS data from both flight 2 and flight 3 are being analyzed.

Contacts

Mark Davis, DFRC, Code RA, (661) 276-2241
Ethan Baumann, DFRC, Code RC, (661) 276-3417

FLIGHT TEST OF THE ENGINE FUEL SCHEDULES OF THE X-43A HYPER-X RESEARCH VEHICLES

Summary

The Hyper-X program flew two X-43A Hyper-X Research Vehicles (HXRVs) in 2004, referred to as Ship 2 and Ship 3. The scramjet engine of the X-43A research vehicle was autonomously controlled in flight to track a predetermined fueling schedule. Ship 2 flew at approximately Mach 7 and Ship 3 flew at approximately Mach 10.

Objective

The objective of the flight test was to control the fuel equivalence ratio of the scramjet engine. If not controlled properly, scramjets are prone to two unfavorable phenomena: unstarts and flameouts. The primary control is fuel equivalence ratio (ϕ_e), defined as the actual fuel-to-air ratio divided by the stoichiometric fuel-to-air ratio. Flameouts can occur with low fuel equivalence ratios (fuel lean) and unstarts tend to occur with high fuel equivalence ratios (fuel rich). Between these two limits, increasing fuel equivalence ratios generally tends to generate increased engine thrust. Flameouts and unstarts result in the immediate loss of thrust from the scramjet engine and the subsequent deceleration of the scramjet-powered vehicle. Therefore, the control of the fuel equivalence ratio of scramjet engines is crucial to the overall performance of scramjet-powered vehicles.

Approach

There were separate fuel schedules for each vehicle. The fuel schedule was used to ensure correct delivery of fuel to maintain an adequate fuel-to-air ratio in the engine. The equivalence ratio was varied during the time of engine operation to increase the probability of proper ignition and positive acceleration as well as to decrease the probability of engine unstart. The fuel used for the X-43A was hydrogen gas. A gas mixture (80:20 by volume) was used as an igniter that consisted of hydrogen and a pyrophoric gas, silane, which ignites on contact with air. The fueling schedule includes the injection of the igniter gas.

Figure 1 shows the Mach 7 flight fuel schedule and the silane mole fraction of the igniter mixture. The Mach 7 fuel schedule was developed during wind tunnel testing in the NASA Langley Research Center 8-Foot High Temperature Tunnel (refs. 1 and 2). This fueling profile was a compromise between desired fueling test points, fueling transitions, and hardware capabilities. For example, step inputs during ignition were required because of an undesirable low flow rate condition of the pressure regulators (ref. 3). This fueling profile resulted in three stable fueling instances or plateaus, with a ϕ_e of 0.75 (with igniter), 0.9 (hydrogen only) and with a goal value of 1.3 (hydrogen only). This same fueling profile also allowed slow transitions between stable fueling instances to reduce the risk of an engine-out condition. Further risk reduction for unstarts was accomplished through a set of unstart protection algorithms, which became active only above a ϕ_e of 0.9.

Figure 2 shows the fuel schedule for the Mach 10 flight, which did not include lean fueling ϕ_e plateaus (excluding ignition). This omission was made to match wind tunnel test points and to expedite the fuel schedule to the more important rich ϕ_e data points, where positive vehicle acceleration was more probable. The lean fueling data (without igniter below ϕ_e of 1.0) was placed at the end of the schedule because of the risk of flameout at low ϕ_e values. A number of tests at the NASA HYpersonic PULSE (HYPULSE) Facility located at and operated by the GASL Division of Allied Aerospace Industries, Inc., Ronkonkoma, New York, were performed to anchor the analysis tools for the scramjet engine (refs. 4 and 5).

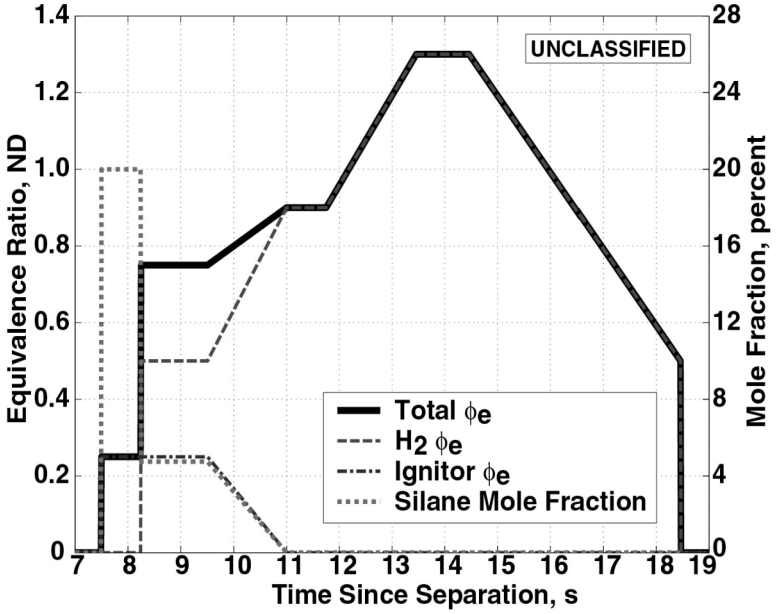

Figure 1. Mach 7 fuel schedule.

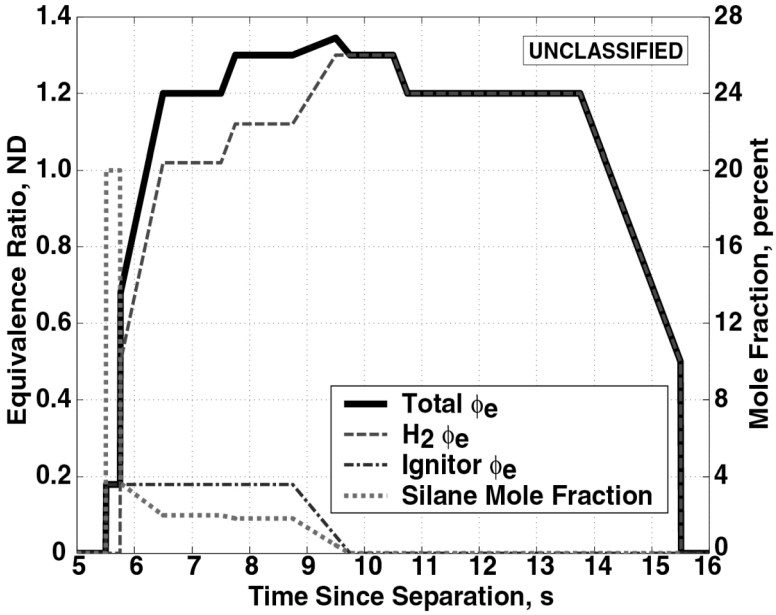

Figure 2. Mach 10 fuel schedule.

Results

The fuel schedules described above were implemented into the propulsion system controllers (PSCs) for the Mach 7 and Mach 10 flight tests. Rock (ref. 6) provides a discussion of the development and testing of the PSC, and Jones and Baumann (ref. 7) discuss further software testing and validation using a Monte Carlo technique with a six degree-of-freedom batch simulation. Although the details of the engine performance are classified, the PSC did adequately control the engine along the predetermined fuel schedules for both Ship 2 and Ship 3 without an unstart or flameout event. The installed engine performance was within

preflight predictions for both flights. Jones et al. (ref. 8) give a summary of the PSC performance.

Status and Future Work

Shortly following the flight of X-43A Ship 3, the project was ended and all follow-on projects, such as X-43B and X-43C, were terminated. The United States Air Force, however, is going forward with their flight program, a scramjet engine demonstrator. Further research is required, however, to progress the scramjet engine technology. More flight tests of unstart protection algorithms are needed to provide a better understanding of the unstart phenomenon. Flight test of hydrocarbon-fueled engines to evaluate the performance differences with hydrogen is also needed. The ramjet to scramjet transition needs study to evaluate transition combustion stability. Flight test at unsteady test points (over Mach and qbar) is required to evaluate real life engine operability. Many of these tasks can and should be performed using small scale flight tests with a high flight rate. This would help drive the technology and reduce the cost of testing.

References

1. Voland, R. T., K. E. Rock, L. D. Huebner, D. W. Witte, K. E. Fischer, and C. R. McClinton, “Hyper-X Engine Design and Ground Test Program,” AIAA-98-1532, April 1998.
2. Huebner, L. D., K. E. Rock, D. W. Witte, E. G. Ruf, and E. H. Andrews, “Hyper-X Engine Testing in the NASA Langley 8-Foot High Temperature Tunnel,” AIAA-2000-3605, July 2000.
3. Lugbauer, J., C. Christy, and M. Mizukami, “X-43 Fluid Systems: Design and Development,” Proceedings of the JANNAF CS/APS/PSHS Joint Meeting, Monterey, CA, CPIA-Publ-703-vol-2, pp. 43–45, November 2000.
4. Bakos, R. J., C. Y. Tsai, R. C. Rogers, and A. T. Shih, “The Mach 10 Component of NASA’s Hyper-X Ground Test Program,” ISABE Paper 99-7216, September 1999.
5. Bakos, R. J., C. Y. Tsai, R. C. Rogers, and A. T. Shih, “Hyper-X Mach 10 Engine Flowpath Development: Fifth Entry Test Conditions and Methodology,” AIAA-2001-1814, April 2001.
6. Rock, K. E., M. R. Nugent, J. S. Orme, and J. F. Calleja, “Propulsion Subsystem Control Law Development for the Hyper-X Mach 7 Flight Test,” CPIA-Publ-692-Vol-2, pp. 205–226, October 1999.
7. Jones, T. P., and E. Baumann, “Evaluation of the X-43A Scramjet Engine Controller Performance by Monte Carlo Technique,” NASA/TM-2003-212036, 2003.
8. Jones, T. P., K. Rock, K. Cabell, M. Nugent, and L. Miranda, “Flight Test Performance Summary of the Propulsion System Controller for the X-43A Vehicles,” Presented at the JANNAF 40th CS, 28th APS, 22nd PSHS, and 4th MSS Joint Meeting, Charleston, SC, June 13–17, 2005.

Contacts

Thomas Jones, DFRC, Code RP, Thomas.P.Jones@nasa.gov

EVALUATION OF ACTIVE AEROELASTIC WING FLIGHT CONTROLS TECHNOLOGY

Summary

Flight tests of research control laws on the Active Aeroelastic Wing (AAW) airplane have been accomplished. Eighteen low-altitude transonic and supersonic test points were specifically selected by the project to evaluate AAW technology. In the first part of the three and one-half month flight test program, flight tests concentrated on safely addressing open questions about the aerodynamic modeling used for flight control design. Once those issues were put to rest, new overlays were developed in the last month of flying to allow additional testing at 13 of the 18 test points.

Objective

Flight tests were conducted to prove the ability of the research control laws to roll the F/A-18 (McDonnell Douglas Corporation, St. Louis, Missouri and Northrop Corporation, Newbury Park, California) airplane using wing control surfaces only. The project expected that the selected flight conditions would span the AAW design space, from conventional roll control to fully reversed trailing edge control. Secondary objectives included testing maneuver load control used to reduce bending and torsion loads at the wing root and fold at elevated g.

Approach

Research flights were conducted on a specially modified F/A-18 airplane. A research flight control system (RFCS) allowed the new control laws to be evaluated at each of the 18 test points. Considerations of cost and schedule drove the design efforts to point designs rather than a full-envelope flight control system. Figure 1 shows the AAW airplane on its first flight using the newly designed research flight control laws.

EC04-0361-02

Figure 1. The F/A-18 airplane during the second phase of the Active Aeroelastic Wing program.

Results

Flight test results showed the AAW airplane was able to roll effectively utilizing wing-only control throughout its planned test envelope. Some of the subsonic test points showed low performance, but were still able to achieve a Level 2 roll performance requirement. Loaded rolls and wind-up turns were also accomplished as part of the planned testing. Comparisons of the flight test data with simulation prediction have been made and good agreement has been found, albeit aerodynamic updates from previous parameter estimation flight tests were necessarily added to the simulation model.

Figure 2 shows a control room display that was developed to aid the pilot in maintaining the test point conditions. This display showed the status of the RFCS in the upper left corner, the AAW airplane sensed impact and static pressure (used for test point gain selection) plotted against RFCS disengage envelopes in the center of the display, and digital presentation of the individual impact and static pressure measurements in the lower right corner. The digital strip chart in the upper right corner showed a time history of the RFCS arm–engagement status.

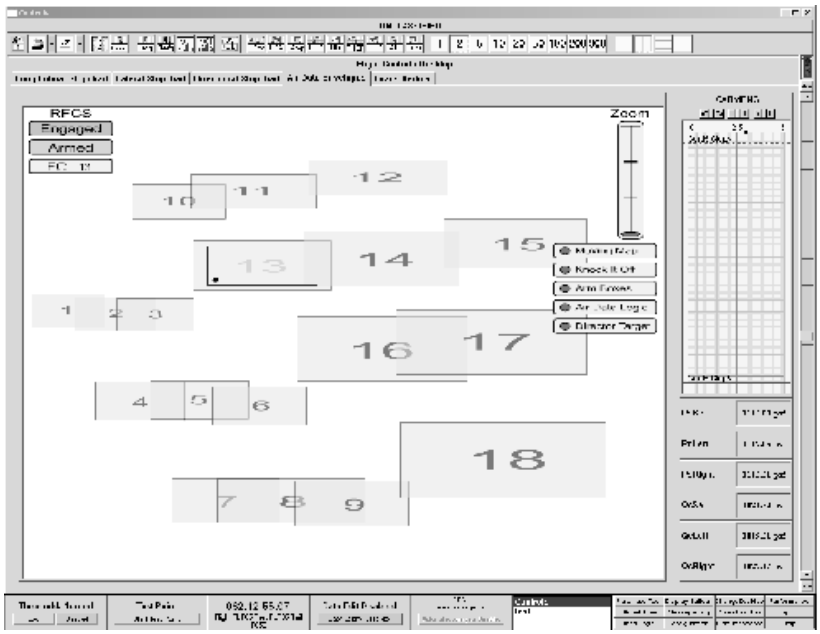

Figure 2. Control room IADS® display showing the RFCS status and 18 test point envelopes.

Status

All planned flight activities are complete as of March 2005. Analysis of the flight data and reporting of the results are in work. Some of this work was presented at the Aerospace Flutter and Dynamics Council (AFDC) Spring 2005 meeting and more is planned for a special session at the 2005 AIAA Atmospheric Flight Mechanics Conference and Exhibit that will be held in San Francisco, California in August 2005.

Contacts

Robert Clarke, DFRC, Code RC, bob.clarke@nasa.gov, (661) 276-3799
Michael Allen, DFRC, Code RC, michael.j.allen@nasa.gov, (661) 276-2784
Ryan Dibley, DFRC, Code RC, ryan.p.dibley@nasa.gov, (661) 276-5324

VERIFICATION OF THE ACTIVE AEROELASTIC WING AERODYNAMIC MODEL WITH FLIGHT TEST RESULTS

Summary

During phase II of the Active Aeroelastic Wing (AAW) project, test flights were conducted using control laws designed using an aerodynamic model developed at the NASA Dryden Flight Research Center. These flights allowed a unique opportunity to evaluate the accuracy and adequacy of the aerodynamic model. Aerodynamic responses from flight were compared with responses from the F-18 airplane simulation using the aerodynamic model. Overall, the aerodynamic model was found to be adequate for control law design and as a predictive tool for aircraft behavior.

Objective

The objective of this research was to verify the adequacy of the aerodynamic model created for the AAW F/A-18 (McDonnell Douglas Corporation, St. Louis, Missouri and Northrop Corporation, Newbury Park, California) airplane.

Approach

The verification process involved analyzing the data from maneuvers performed in flight and comparing the responses from these maneuvers with responses from the F/A-18 simulation using the AAW aerodynamic model. The comparison between the two responses concentrated on the degree to which the simulation responses matched the flight response trends as well as the absolute differences between the two responses. The results from the various maneuvers at the different flight conditions were gathered, and the accuracy of the aerodynamic model was evaluated at each flight condition.

Status

The Active Aeroelastic Wing program has been completed. The aerodynamic model proved to be an adequate model and sufficient for the purposes of the AAW project. The significant improvement of the AAW aerodynamic model over the baseline F-18 aerodynamic model showed that existing F/A-18 models could be significantly improved through extensive parameter identification testing. An American Institute of Aeronautics and Astronautics (AIAA) paper entitled “Active Aeroelastic Wing Aerodynamic Model Development and Validation for a Modified F/A-18A” has been presented and a NASA Technical Memorandum is in the publication process.

Contacts

Stephen Cumming, DFRC, Code RA, (661) 276-3732

THE C-17 THROTTLES-ONLY CONTROL EVALUATION AND SIMULATION VALIDATION

Summary

Throttles-only control (TOC) has been used several times by pilots whose airplanes have suffered degraded control or a loss of hydraulics. Throttles-only control involves throttle manipulation to change heading, control pitch oscillations, turn and bank, and direct all other aspects of control. Fortunately, the twinjet configuration popular in today's commercial fleet [such as the Boeing 757 and 767 (The Boeing Company, Chicago, Illinois), the Airbus A319 (Airbus, Hamburg, Germany), and the Airbus 320 (Airbus, Toulouse, France)] is especially responsive to TOC. The response of TOC on a four-engine configuration such as that of the 747 (The Boeing Company, Chicago, Illinois) and the C-17 (The Boeing Company, Chicago, Illinois) has been the subject of much debate. The NASA Dryden Flight Research Center (DFRC) conducted both simulation and flight tests using TOC to control a C-17 and develop TOC procedures specific to a 4-engine configuration. The flight tests demonstrated more ease of use than the simulation suggested, and further ground research would require a validation of the simulation using flight data.

EC01-0325-8

The Boeing C-17 airplane in flight.

Objective

The primary objective of this research is to validate the DFRC C-17 simulator through comparison of data with actual flight test results. Specifically, data pertaining to the airplane response to throttle inputs will be acquired, analyzed, and used to update the DFRC C-17 simulator. This simulator will then be used to develop TOC procedures for the C-17.

Approach

The first step toward acquiring flight data was determining the appropriate maneuvers and flight conditions. Several simulation runs were performed using the DFRC C-17 simulation to generate the requirements. These C-17 simulator tests showed that a survivable TOC landing

was almost impossible. A DFRC pilot with extensive C-17 experience thought the simulators were "too pessimistic," which underscored the necessity of simulator validation for TOC.

The second step toward acquiring flight data was clearing the desired maneuvers and conditions for flight. This was done during the Boeing flight hardware simulation (FHS). The pilots refined the maneuvers and prepared for the TOC flights in two FHS sessions during the fall of 2004. The experience and data acquired by the team was a large step toward preparing for flight. Documents were written and reviews were performed on behalf of the Air Force Flight Test Center, Edwards Air Force Base, California, NASA DFRC, Edwards, California, and The Boeing Company, Long Beach, California.

During the spring of 2005, the C-17 test flights took place at Edwards Air Force Base, California. Three flights were performed over a range of flight conditions, and the data showed that TOC in flight was much more successful than that experienced in the simulations. The DFRC pilots made successful TOC approaches in turbulence, and the airplane exhibited better Dutch roll damping in flight. Flight data also suggested that both the simulators (NASA and FHS) underestimated the inflight drag.

Status

The simulation-to-flight data comparison is nearly complete, and the simulation modifications will be performed in the upcoming months.

Contacts

Jennifer Hansen, DFRC, Code RA, (661) 276-2052
Shaun McWherter, DFRC, Code RC, (661) 276-2530
Bill Burcham, Analytical Services & Materials, Inc.

DAMAGE EMULATION IN THE DRYDEN C-17 SIMULATION ESTIMATING MAXIMUM TORQUE TOLERANCE

Summary

One of the goals of the Damage Adaptive Control Systems (DACS) project is to develop and integrate high-fidelity damage models into various commercial aircraft simulations. These damage models are to be representative of a wide variety of instances of shoulder-launched-missile-inflicted damage. The goal of this study was to explore a method of emulating damage not through exact modeling, but rather through determining maximum tolerable aerodynamic effect for a variety of system failure scenarios in a simulation environment. This phase of the study is considered a preliminary assessment and was performed in the NASA Dryden Flight Research Center (DFRC) C-17 simulator.

Simulation

The current lack of aerodynamic data representative of damage to civilian and cargo class aircraft poses a significant obstacle to modeling such effects in a simulated environment and to developing mitigating control methodologies. Until such high-fidelity damage models are determined, the approach described herein will attempt to emulate the effect of damage as an external aerodynamic effect added to a failure of systems such as control surfaces and engines, or judicious combinations of these that could reasonably be caused by a missile impact. The external aerodynamic effect is incorporated in this first phase as a single moment about each body axis. The idea is to determine the maximum torque tolerable about each body axis for each failure scenario and what pilot control techniques were employed for the upset recovery, followed by controlled flight and an approach and survivable landing.

The Dryden C-17 simulation code was modified to introduce the following failures:

- Full hydraulic system failure: mechanical mode
- Left wing failure: aileron float, flaps fixed
- Left wing failure and outboard engine failure
- Left wing failure and inboard engine failure

The C-17 simulation aerodynamic moment equations were modified to introduce external moments about each axis individually:

- L_AeroNew = L_aero + L_external
- M_AeroNew = M_aero + M_external
- N_AeroNew = N_aero + N_external

During the simulation sessions, the aircraft was set up at a nominal flight condition. After approximately 10 s of flight, a particular failure scenario was initiated. One second after the failure was initiated, an external moment was also applied about a body axis. The pilot was expected to recover the upset with any feasible combination of control power and then perform an emergency approach and landing. This procedure was repeated to determine the maximum moment tolerable in each body axis for each predefined failure scenario. The maximum moment and piloting recovery and landing technique were noted for each scenario and body axis moment.

Approach

Some simplifying assumptions are made in this approach, the most obvious being that the aerodynamic effect of damage can be represented with single constant torques applied in each axis separately, whereas in reality, the effect would be a dynamic-pressure-dependent cross-coupled effect in each axis. The assumption was considered workable in that the method would be expanded in stages moving closer to replicating the general characteristics of certain types of damage determined in the actual damage modeling done within the DACS program. The simplifying assumption also allowed the rapid creation of a framework for damage implementation into a simulation environment. An advantage of this approach, compared with performing high-fidelity damage modeling up front, is that meticulous damage modeling only creates models for specific damage scenarios for a specific aircraft. The approach described herein provides a framework for generalizing specific damage models to other aircraft of similar configuration and damage cases of similar type. It does so by assuming only the general characteristics of the damage, but ultimately attempts to discover the maximum boundaries of a generalized damage effects envelope. No structural limitations were taken into consideration in this phase. Structural limitations were ignored so that the study could progress to determine the viability of the method with the idea that structural limitations could be incorporated in later stages of increasing fidelity.

Status

The study has been completed for the damage scenarios defined and for constant torques in each axis. Data analysis and report generation is in process. When data analysis is complete, the method will be assessed and improved. The next phase of improvements may include increasing the fidelity of damage emulation through introducing cross-coupling characteristics based on preliminary studies done at DFRC using asymmetric vortex lattice (AVL), or by incorporating the NASA Langley Research Center damage modeling results. It is planned to implement the method in the NASA Ames Research Center Advanced Cab Flight Simulator (ACFS) to evaluate the method on a configuration resembling a civilian commercial aircraft.

Contacts

Shaun McWherter, DFRC, Code RC, shaun.c.mcwherter@nasa.gov, (661) 276-2530

THE NASA F-15 INTELLIGENT FLIGHT CONTROL SYSTEMS – GENERATION II

Summary

The Second Generation (Gen II) control system for the F-15 Intelligent Flight Control System (IFCS) program implements direct adaptive neural networks to demonstrate robust tolerance to faults and failures. The direct adaptive tracking controller integrates learning neural networks (NNs) with a dynamic inversion control law. The term "direct adaptive" is used because the error between the reference model and the aircraft response is being compensated or "directly adapted" to minimize error without regard to knowing the cause of the error. No parameter estimation is needed for this direct adaptive control system.

In the Gen II design (fig. 1), the feedback errors are regulated with a proportional-plus-integral (PI) compensator. This basic compensator is augmented with an online NN that changes the system gains via an error-based adaptation law to improve aircraft performance at all times, including normal flight, system failures, mispredicted behavior, or changes in behavior resulting from damage.

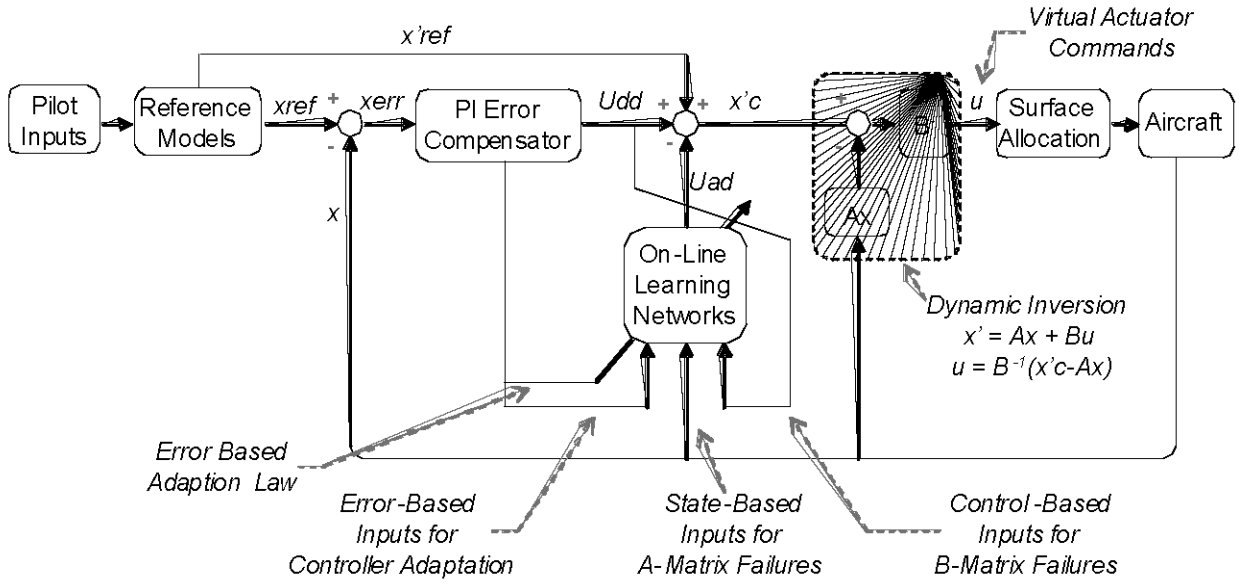

Figure 1. Direct-adaptive, neural network flight control.

Objective

The Gen II inflight performance shall be evaluated under both nominal configurations and in the presence of simulated surface failures (hold or bias).

Justification

Intelligent Flight Controls improves flight safety and mission completion for manned and unmanned vehicles. The technology can be applied to multichannel fly-by-wire control systems so that they can automatically compensate for off-nominal conditions, increasing aircraft performance over nonadapting control systems.

Approach

Flight performance comparisons will be made between Gen II controllers with and without the neural networks activated at the same conditions and in the presence of the same failures. Performance results will be evaluated against accepted handling qualities standards such as the Cooper-Harper Handling Qualities Rating Scale. All flight test conditions will be coordinated with simulation evaluations to validate in flight that the system performs as expected.

Failures are limited to those that can be accomplished safely (as determined by handling qualities and structural load considerations) in a subsonic flight envelope. No control surfaces will actually be failed; simulated failures will be implemented by software inserting a command to hold or bias surfaces at specified values. All simulated failure candidates will be pretested on a piloted simulation.

Results

Failures are designed to show controller adaptation to unknown aerodynamics (A matrix) and to control surface failures (B matrix). For A matrix failures, the symmetric canard command is biased by introducing a gain between 0.8 and –0.5. For B matrix failures, the right stabilator is held at trim, ±2° from trim, and ±4° from trim.

The NN architecture is designed to minimize transients upon failure introduction while improving tracking performance (fig. 2). The adaptation also reduces cross-axis coupling during the failure. Piloted simulations show notable handling quality improvements in the presences of failures.

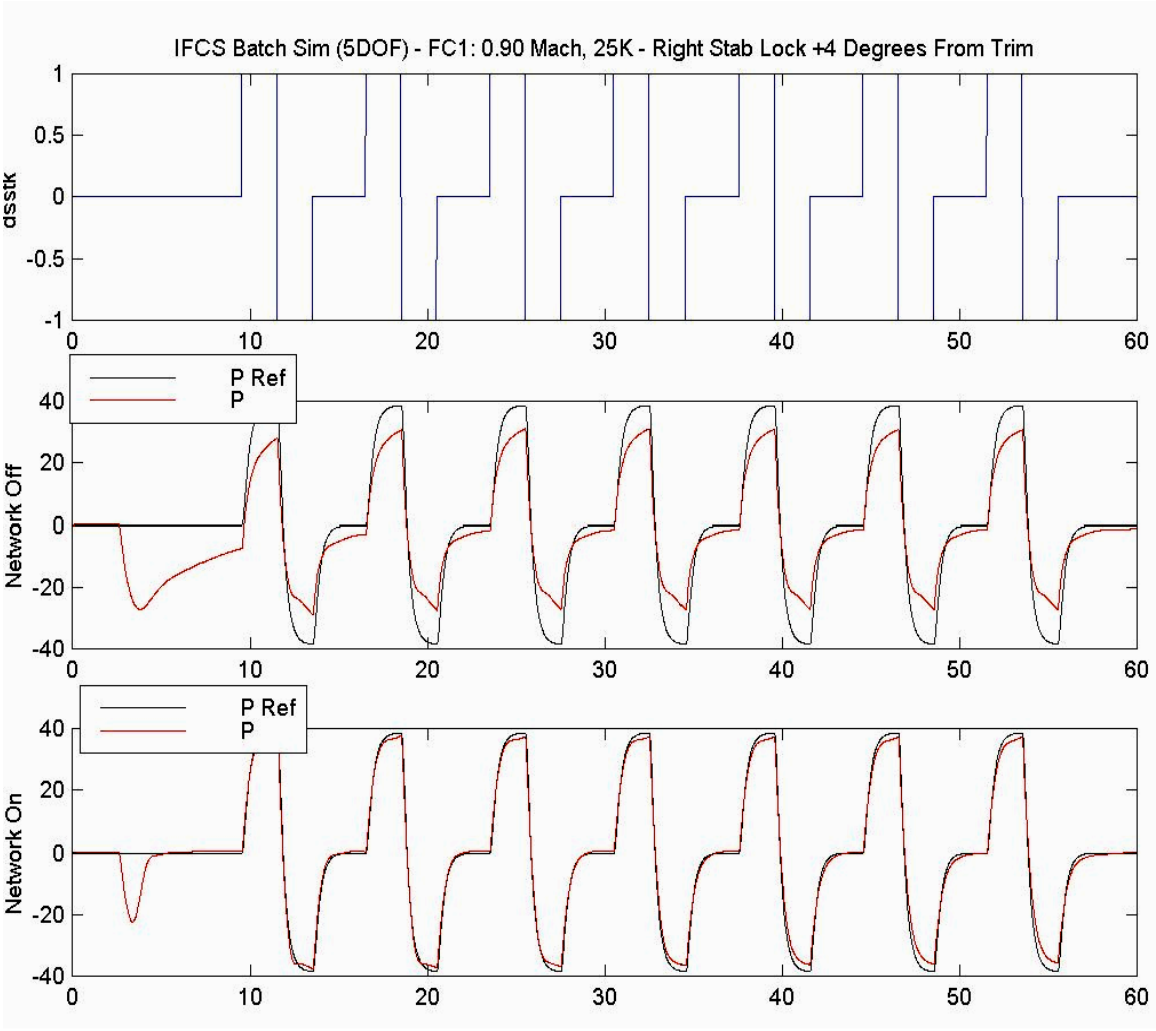

Figure 2. Improved roll performance example.

Status

The Critical Design Review was held in September, 2004, and the Gen II controller design is now complete. Onboard safety monitor software is nearing completion. Embedded software development is under way. Flight tests are expected to begin in September, 2005.

Contacts

Mark Buschbacher, IFCS Lead Flight Controls Engineer, DFRC, Code RC, (661) 276-3838
John Bosworth, IFCS Chief Engineer, DFRC, Code RC, (661) 276-3792

VERIFICATION AND VALIDATION OF NEURAL NETWORKS IN FLIGHT CONTROL SYSTEMS

Summary

The Strategic Methodologies for Autonomous & Robust Technology Testing (SMART-T) project is developing verification and validation tools and guidelines for use with neural networks and other adaptive control systems.

Objective

The objective of the project is to address issues with the design, analysis, verification, validation, and certification of autonomous and adaptive control systems.

Approach

The technology of current interest is the application of neural networks to flight control systems. The SMART-T project has developed several tools and techniques to evaluate the performance and stability of those neural networks. The NASA Dryden Flight Research Center is partnering with the NASA Ames Research Center, Boeing Phantom Works in St. Louis, Missouri, the Institute for Scientific Research (ISR), and Case Western Reserve University in this endeavor.

The confidence and envelope tools calculate a confidence interval around the outputs of the neural network based on a Bayesian statistical model. The sensitivity tool performs a sensitivity analysis of the neural network to ensure a region of stability as prescribed by the Lyapunov second method for stability of nonlinear complex systems. The sensitivity analysis tool interface is shown below.

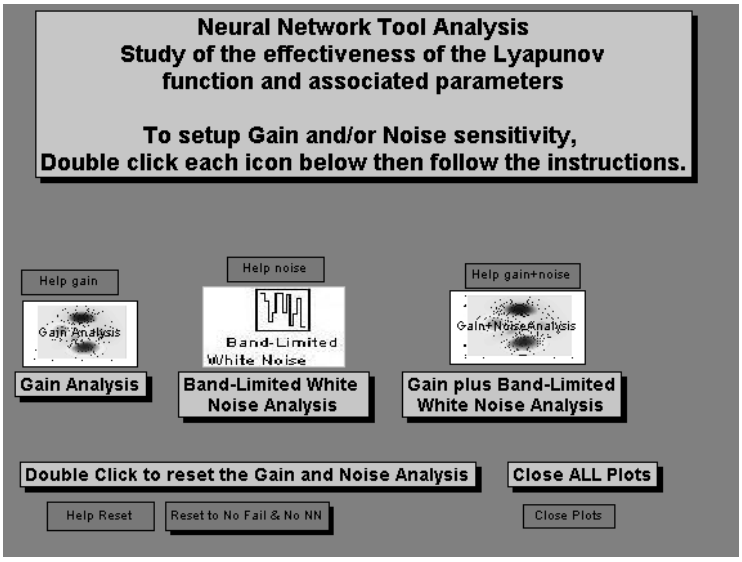

Sensitivity analysis tool interface.

The Automated Neural Controller Test (ANCT) tool was designed to help engineers test adaptive flight controllers in various flight conditions, quantify performance, and determine regions of stability. The SMART-T project is working with the Intelligent Flight Control System (IFCS) project to demonstrate the usefulness of these neural network evaluation tools.

A study of the effects of neural network learning on aircraft handling qualities is also being undertaken.

Phase I seeks to demonstrate automated handling qualities determination from a simple control system and longitudinal aircraft model. Control Designer's Unified Interface (CONDUIT) and other Matlab (The MathWorks, Natick, Massachusetts) scripts will be used to predict handling qualities by calculating the control anticipation parameter (CAP) and bandwidth for the system. Phase II will look at the effects of nonlinearities introduced by a neural network in the flight control system and a more detailed F-15 aircraft model. Phase III will correlate the output of the confidence and sensitivity tools with changes in handling qualities during failure recovery and neural network adaptation.

The SMART-T project has also been working with the Boeing Development and Modification Center, Wichita, Kansas, to examine the current gaps and hurdles to Federal Aviation Administration (FAA) certification of adaptive flight control systems. The IFCS project documentation will be reviewed by an expert in FAA certification to determine adequacy. Sections of the IFCS flight control software containing neural networks will also be evaluated against certification standards.

Status

Tool development and testing are ongoing. Research flights of the highly modified IFCS F-15 (McDonnell Douglas Corporation, St. Louis, Missouri) test bed aircraft will begin in the fall of 2005. The confidence tool will be flown onboard the aircraft, and the output will be evaluated postflight.

Phase I of the handling qualities study is complete. A screen shot of the results from CONDUIT are shown below.

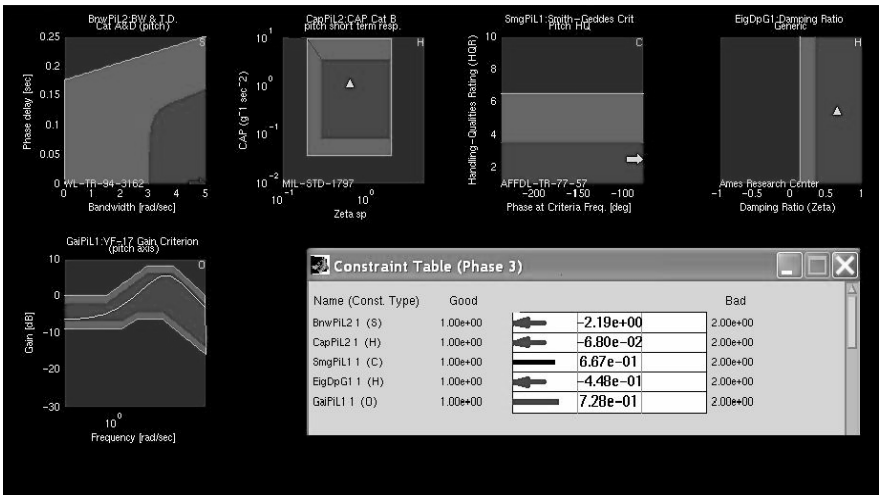

CONDUIT screen shot.

More detailed and complex models are now being incorporated for Phase II.

The FAA certification gap analysis of adaptive flight control systems is under way and should be complete in late 2005. “Verification and Validation of Adaptive Control Systems – Flight Control Software V&V Guidelines for Learning Systems” will also be released in 2005.

Contacts

Michael Richard, DFRC, Code RC, (661) 276-3543
Kurt Guenther, Analytical Services & Materials, Inc., Code RF, (661) 276-2179
John Hodgkinson, Spiral Technology, Code RC, (661) 276-2727
Fola Soares, Contek Research, Inc., Code RF, (661) 276-5536

GENERIC GUIDANCE AND CONTROL LAW DEVELOPMENT FOR SIX DEGREE-OF-FREEDOM (DOF) SIMULATION TO SUPPORT CONCEPTUAL AIRCRAFT DESIGN

Summary

Early stages of aircraft design often use trade studies involving simulation and analysis to determine the best design to meet requirements. Typically, models, such as aerodynamics, mass properties, sensors, and actuators frequently and significantly change as various aircraft configurations are studied. The frequency and significance of model variations require large control law changes if 6-DOF simulations are used in this phase of design. Developing a generic set of control laws that require no modifications based on model configuration changes would enhance the 6-DOF simulation as a conceptual aircraft design tool.

Approach

Two types of generic control laws were developed using dynamic inversion: nonlinear dynamic inversion (NDI) and simplified dynamic inversion (SDI). Both methods employ a technique to estimate the aerodynamics, which is then inverted to cancel out the bare airframe aircraft dynamics. The control law designer then has the ability to provide the desired dynamics. The SDI control laws employed a simplified approach to dynamic inversion, where state acceleration feedback is used in the aerodynamic cancellation process. The SDI was primarily focused on a piloted, real-time simulation. The NDI was primarily developed for batch simulation, although piloted real-time simulation was possible, with focus on outer-loop guidance law developments. With NDI, the user could also control the aircraft to fly to a user-defined latitude, longitude, and altitude, or to a defined bank angle, angle-of-attack, and speed command. Both SDI and NDI used a direct control allocation approach for commanding control effectors.

Both generic control laws were evaluated using two distinctly different 6-DOF simulations: a high fidelity fighter aircraft model and an air-breathing hypersonic model at Mach 6. By modifying only the interfaces, the same set of control laws, including the desired dynamics, was applied to both simulations. Both NDI and SDI methods were evaluated by comparing inner-loop response dynamics. Stability characteristics and the handling qualities of the pilot-in-the-loop simulation, using a research test pilot, were also evaluated. For NDI, the ability of both simulations to follow guidance commands was tested at all outer-loop levels.

Status

Figure 1 depicts the step responses of both simulations in the pitch axis. The results are similar for both NDI and SDI controllers. Despite the wide disparity in aircraft configuration and flight condition between the simulations, the responses appear nearly identical to the same step input. Similar results were obtained for the other axes. This indicates that the technique successfully cancels out the bare airframe dynamics and replaces them with the desired dynamics. It also illustrates the utility of the approach for wide selections of conceptual aircraft configurations. For these examples, the technique had adequate stability margin, and handling qualities were good to adequate, depending on the task. The NDI control laws were used with both simulations to successfully command guidance control variables at all levels. Figure 2 shows the fighter simulation intersecting a waypoint, turning, and then re-intersecting the same waypoint.

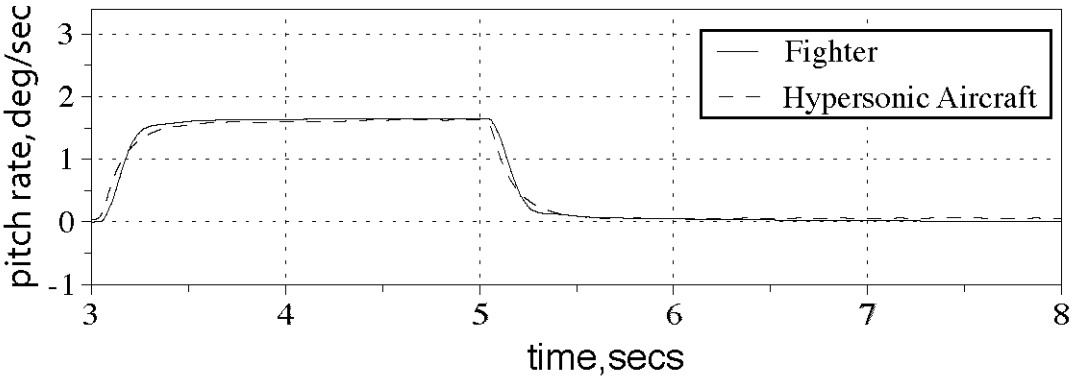

Figure 1. Step response comparison of fighter and hypersonic vehicle.

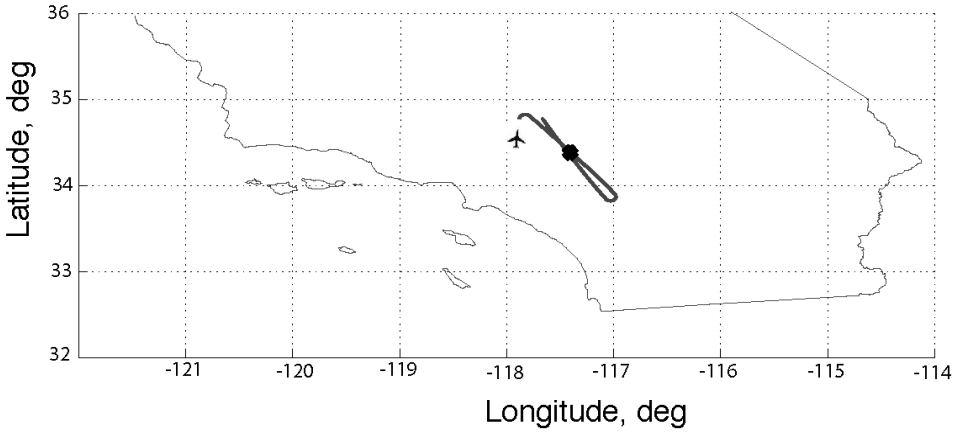

Figure 2. Waypoint intersection using fighter simulation.

Conclusion

A generic set of control laws was developed to promote the use of 6-DOF simulations in the conceptual aircraft design phase. The utility of the control laws was demonstrated through successful application to two distinct, disparate simulation models.

References

1. Cox, T. H. and M. C. Cotting, “A Generic Inner-Loop Control Law Structure for Six-Degree-of-Freedom Conceptual Aircraft Design," NASA/TM-2005-212865, 2005.
2. Cotting, M. C. and T. H. Cox, “A Generic Guidance and Control Structure for Six-Degree-of-Freedom Conceptual Aircraft Design," NASA/TM-2005-212866, 2005.

Contacts

Timothy H. Cox, DFRC, Code RC, timothy.h.cox@nasa.gov, (661) 276-2126
M. Christopher Cotting, ccotting@mail.gov

NETWORKED UNMANNED AERIAL VEHICLE TEAMS (NUAVT)

Summary

A partnership between the NASA Ames Research Center and the NASA Dryden Flight Research Center (DFRC) explored the ability of small unmanned aircraft to support forest fire fighting using teaming behavior. The Networked UAV Teams project flight tested mission planning algorithms for multi-UAV cooperative transit, area search, and waypoint time-of-arrival that might someday allow the early detection of developing forest fires and support the gathering of images and atmospheric samples to help improve predictions of the future behavior of established fires.

Objective

The primary objective of the project was to demonstrate, in a flight environment, the potential usefulness of multiple coordinated UAVs for forest fire fighting applications. Two UAVs were launched in support of an imaginary forest fire fighting activity. The airplanes were tasked to cooperatively search for new forest fires and to gather air samples, using virtual sensors for both.

Approach

The DFRC owns and operates two APV-3 UAVs, manufactured by RnR Products of Milpitas, California. The UAVs (pictured below) have 12-foot wingspans, weigh 30 lb empty and can carry up to 25 lb of combined fuel and payload. Both UAVs are outfitted with Piccolo® (Cloud Cap Technology, Inc., Hood River, Oregon) avionics and are operated via a Cloud Cap ground control station (GCS). Software was developed by NASA to perform real-time multi-vehicle dynamic mission planning on a second ground computer interfaced with the GCS. Bird android (Boid) algorithms provided the UAVs with behaviors similar to flocking birds and dynamic search algorithms provided the UAVs with the ability to work cooperatively to efficiently search an area. Four-dimensional navigation control ensured that the locations of the UAVs were coordinated in space and time.

EC05-0043-42

Figure 1. The NASA DFRC APV-3s in flight.

Results

Figure 2 below the ground tracks for both UAVs using Boid algorithms to flock together while traveling from the lower-right corner of the flight test range to the upper left. The airplanes successfully avoided two virtual obstacles that were placed in their paths and arrived at their destination waypoints.

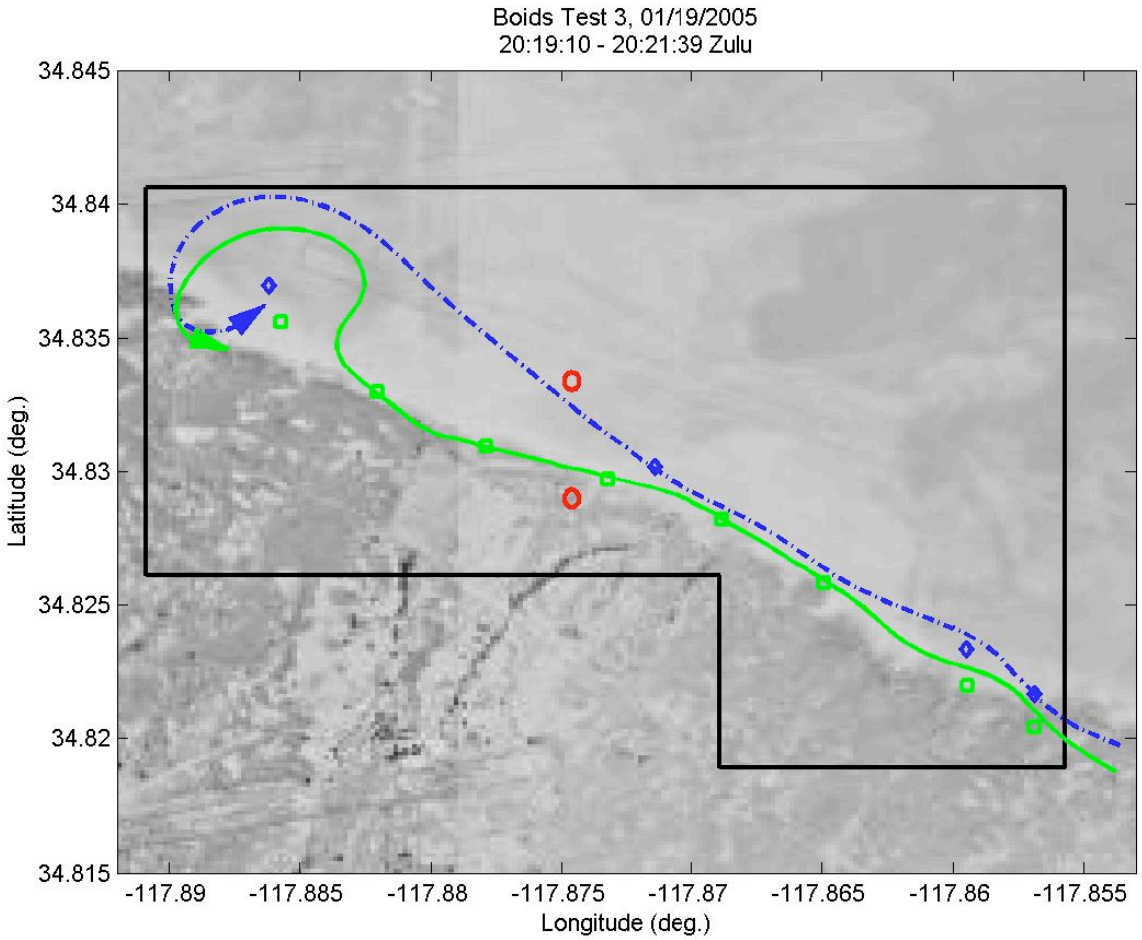

Figure 2. Boids test ground track.

Results from a cooperative search flight test are shown in figure 3. Initial mission planning divided the search area evenly between both aircraft. Soon after the search began, one of the aircraft located a virtual forest fire and entered an orbit to gather more information. The second aircraft was then retasked and completed the remaining unsearched waypoints.

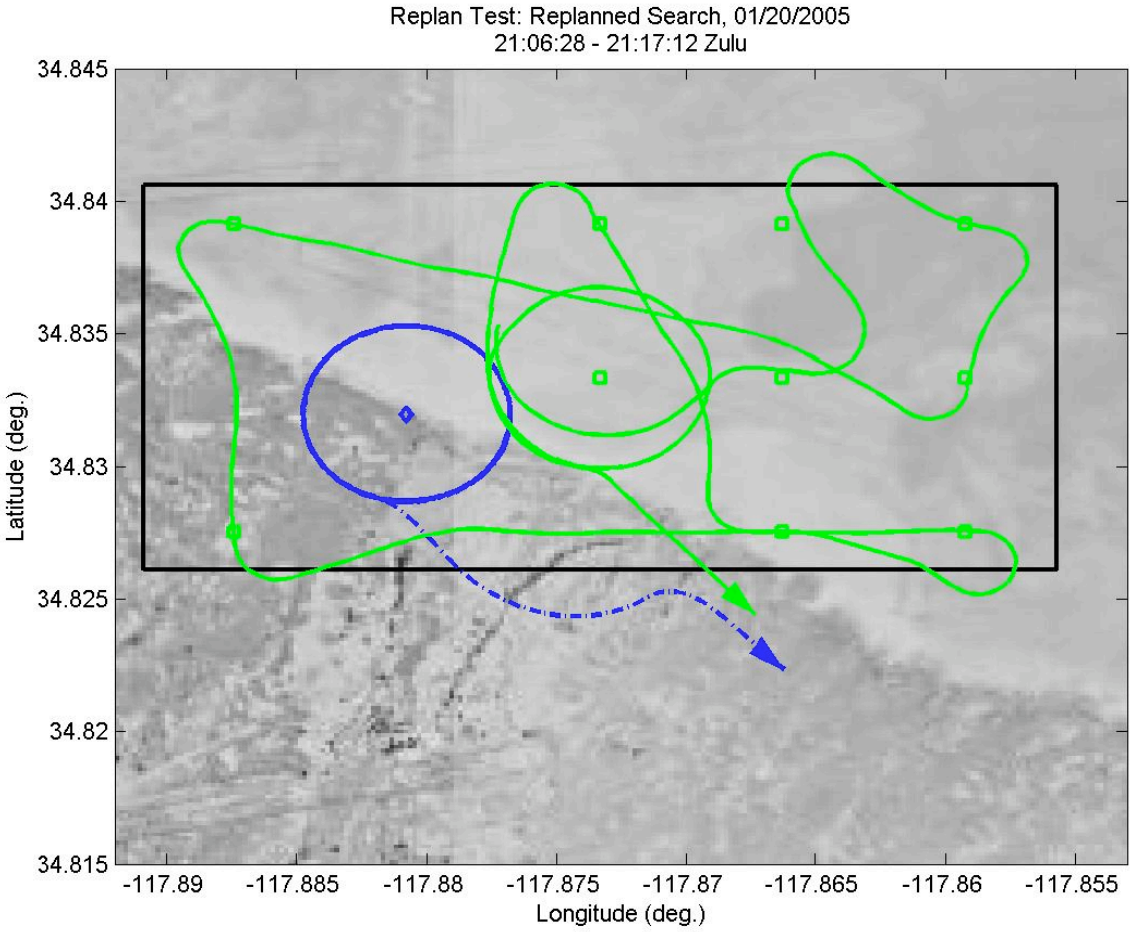

Figure 3. Replan test ground track.

Contacts

Jack Ryan, Principle Investigator, DFRC, Code RC, (661) 276-2558
Curt Hanson, DFRC, Code RC, (661) 276-3966
Steve Jacobson, DFRC, Code RC, (661) 276-7423

AUTONOMOUS SOARING FOR SMALL UNMANNED AERIAL VEHICLES (UAVs)

Summary

One relatively unexplored way to improve the performance of an autonomous aircraft is to use buoyant plumes of air found in the lower atmosphere called thermals or updrafts. Updrafts are commonly used by glider pilots and birds to improve range, endurance, and cross-country speed. A small electric-powered UAV can extend its maximum duration 7 times longer using updrafts (ref. 1). Average endurance was found to be 4 times longer in simulation. The objective of this effort is to flight test autonomous soaring algorithms on a small UAV.

Approach

A small UAV, nicknamed CloudSwift, will be used to flight test the autonomous soaring algorithms. The CloudSwift is an electric motor glider with a 14 ft-wingspan and a weight of 15 lb. The aircraft is controlled with Piccolo-plus® (Cloud Cap Technology, Inc., Hood River, Oregon) autopilots having global positioning system (GPS), static and total pressure, 3-axis accelerations, and 3-axis angular rate measurements. New algorithms for the Piccolo-plus are autocoded from Matlab and Simulink (The MathWorks, Natick, Massachusetts).

Simulation

The development of autonomous soaring guidance and control laws was performed with a Simulink model of the Piccolo® autopilot and aircraft. The Simulink model uses a linear aircraft dynamics model with nonlinear Euler angle and inertial position calculations. A hardware-in-the-loop (HIL) simulation [that was based on the NASA Dryden Flight Research Center (DFRC) APEX sailplane simulation] has also been developed for this system. Both simulators include an updraft model developed at DFRC from meteorological and flight data (ref. 2).

Onboard Updraft Identification

Identification of the updraft size and position is used by the soaring algorithms to calculate a circular flightpath command that is centered on the updraft and has a radius that is determined by the estimated updraft size. Updraft size estimation was performed by fitting a Gaussian curve to a 40-s history of aircraft position and total energy rate-of-change. Updraft position was performed using a centroid calculation.

Results

Flight tests are currently under way. Initial flight test results show that the aircraft can soar autonomously for extended periods of time using multiple updrafts. On September 7, 2005, the CloudSwift added 60 min to its endurance by soaring autonomously in thermals. The UAV also climbed from a cruise altitude of 1,000 ft to a maximum altitude of 3,800 ft autonomously, without using the electric motor. Figure 1 shows the performance of the autonomous soaring algorithms in flight.

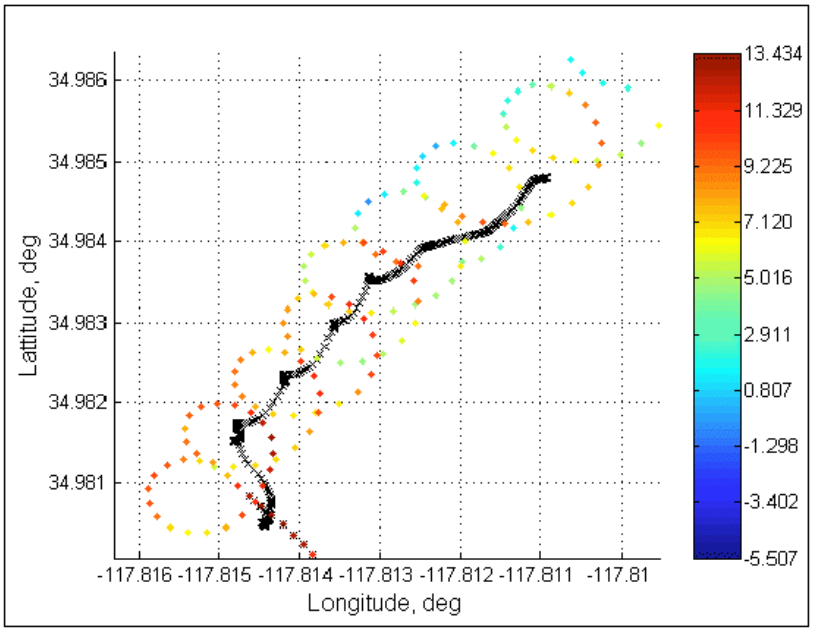

Figure 1. Autonomous soaring flight data.

Future Plans

Flight testing will end September 23, 2005. Results will be used to update the aircraft simulation and updraft models. The updated simulation will be used to investigate cooperative soaring for multi-UAV flocks and swarms.

Conclusion

The design of guidance and control algorithms for autonomous soaring has been completed. These algorithms are currently being flight tested.

References

1. Allen, Michael J., “Autonomous Soaring for Improved Endurance of a Small UAV,” AIAA-2005-1025.
2. Allen, Michael J., “An Updraft Model for the Development of Autonomous Soaring UAVs,” to be presented at the AIAA Aerospace Sciences conference in January, 2006.

Contacts

Michael Allen, DFRC, Michael.J.Allen@nasa.gov, (661) 276-2784

METEOROLOGICAL SUPPORT FOR THE PATHFINDER-PLUS AEROELASTIC RESEARCH FLIGHTS

Summary

During the summer and autumn of 2004, the Pathfinder-Plus (AeroVironment, Inc., Monrovia, California) solar-powered unmanned aerial vehicle (UAV) was deployed to the NASA Dryden Flight Research Center (DFRC) for a series of flight tests. The purpose of these flight tests was to better understand the aeroelastic properties of an aircraft with a flexible span loaded structure while flying in turbulence. The project required meteorological support from the NASA DFRC Research Aerodynamics (RA) branch who aided from the conceptual design of the Atmospheric Turbulence Measuring System (ATMS) to the operational, inflight, weather forecasting and analysis.

Objective

The objective of these flights was to safely fly the Pathfinder-Plus into atmospheric turbulence with sufficient intensity and duration to gather meaningful data from the ATMS and spar strain gage payloads to facilitate the development of a model for use in the design of future high-altitude, long-endurance (HALE) class vehicles.

Approach

The DFRC sound detecting and ranging (SODAR) wind profiler and rawinsonde balloons were used to find altitudes of modest wind shearing, usually found near the top of the inversion layer, and thermal activity; the flight plan was to fly at altitudes of likely turbulence or over the northeast edge of the lakebed, where turbulence was encountered in previous flight tests of Centurion (AeroVironment, Inc., Monrovia, California) and Helios (AeroVironment, Inc., Monrovia, California).

EC04-0277-11

Figure 1. Pathfinder-Plus aircraft with ATMS booms (7 total).

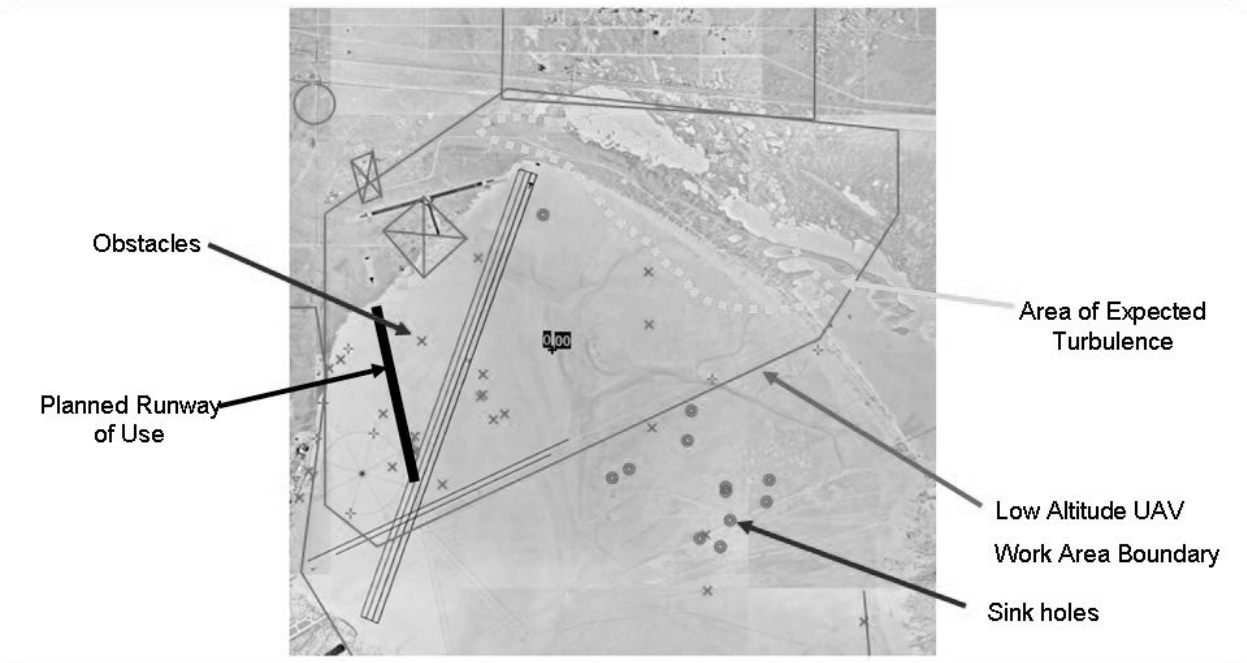

Figure 2. Pathfinder-Plus flight plan and test area.

Status

The flight test was delayed indefinitely because of heavy rainfall the night before the first flight attempt on October 20, 2004. The lakebed was “red,” or unusable, for the remainder of the year. The flight team will stand down until summer 2005, or until the lakebed is “green.”

Contacts

Casey Donohue, DFRC, Code RA, (661) 276-2768

GROUND TESTING OF DIVOT EJECTION SYSTEMS FOR THE LIFTING INSULATING FOAM TRAJECTORY (LIFT) PROGRAM

Introduction and Objective

The loss of the Space Shuttle Columbia because of debris shed from the external tank (ET) has prompted an extensive effort to understand how and why debris is shed and what happens to it after enters the flow field. A spray-on, insulating foam forms the bulk of the thermal protection system (TPS) of the ET. The primary function of TPSs on most launch vehicles is to protect the vehicle from ascent heating. On the Shuttle ET, however, the primary purpose of the foam TPS is to prevent or reduce the formation of ice on the exterior of the tank after it is filled with liquid hydrogen and liquid oxygen, reducing the exposure of the Shuttle to ice shed during launch. Unfortunately, during the course of the program, it was discovered that some of the foam itself is shed during virtually every launch because of a variety of physical mechanisms (ref. 1). The shedded foam consistently takes the shape of a truncated cone called a “divot.”

The objective of the LIFT program was to eject foam divots from the F-15 Flight Test Fixture (FTF) at between 10 and 100 ft/s transverse to the flow field and record the trajectory with high-speed video. This research review summarizes the ground testing of candidate divot ejection systems prior to selection and integration with the aircraft.

Approach

Four distinct systems were designed, fabricated, and tested. Three were essentially large “air rifles” that used pressurized nitrogen to accelerate premanufactured foam divots to the desired speeds. These systems allowed precise control of divot size and shape. The fourth system used pressurized nitrogen to fail a foam sheet glued to a metal plate. This system was more true to the actual failure mechanism on the ET, but resulted in more irregularly shaped divots.

Originally, the requirement for divot ejection speed was 300 ft/s. Given the thin (approximately 8 in.) profile of the FTF, the requirement dictated a higher pressure and faster acting system that could accelerate the divots over such a short distance. The solution was a burst disk system, shown in figure 1. The system was pressurized to approximately 80 percent of the rated burst disk, a solenoid valve was closed, and the pressure behind it was raised to approximately 120 percent of the burst value. When the solenoid valve was opened, the burst disk would fail and the divot would eject. Unfortunately, this system would shatter the divot at burst disk pressures above 50 psi, which was the pressure required to attain the ejection speed.

Fortunately, the ejection speed requirement was eased to a range of 10 to 100 ft/s allowing the design of systems that did not necessitate attaining such high accelerations. The integrated piston–reservoir system (fig. 2) consisted of a prepressurized reservoir behind a piston that was held by a claw retention mechanism. When the claw was released the piston would accelerate down the cylinder, driving the divot out. At the end of the stroke, the piston was retained by a guide bearing support. Divot ejection speed was controlled by the amount of pressurization, but ejection speeds higher than 100 ft/s would have resulted in unacceptably high piston accelerations.

Another system made possible by the easing of the ejection speed requirement was the needle-guided or “kabob” system (fig. 3). This system was simply an aluminum tube with a concentric needle that kept the axis of the divot and the tube coincident. The back of the tube contained ports into which the propellant gas, controlled by a solenoid valve, entered. A reservoir–burst disk arrangement was not required because the divots were accelerated over a longer distance relative to the burst disk system described above and shown in figure 1. During testing, it was

discovered that the kabob would “whip” downstream of the divot and prevent ejection. More tests were conducted with the kabob removed and system performed to specification.

The pressure-failed sheet system consisted of a foam sheet bonded to a metal plate with ports for nitrogen propellant. The nitrogen was controlled with the same solenoid valve as was used in the kabob system. The system was pressurized, the valve was opened, and the foam would fail and pop off. Divot dimensions could be controlled by varying foam thickness and void size (if any).

Summary

Approximately 70 tests were performed in September and October, 2004. All four divot ejection systems performed to specification with some requiring small modifications. Roughly half of the 70 tests were performed with the pressure-failed sheet system. All four could have performed in flight, but the pressure-failed sheet system was deemed the easiest to implement into the FTF. After a final briefing to the NASA Johnson Space Center (JSC) on November 7, 2004, ground testing was complete and the go-ahead was given to fly the pressure-failed sheet system.

Status

The LIFT program continued toward flight in early 2005. The first flight was on February 14, 2005, and 10 flights were completed within the next 5 weeks. The program was completed on March 17, 2005, and high-speed video and photogrammetry data was provided to JSC for model verification.

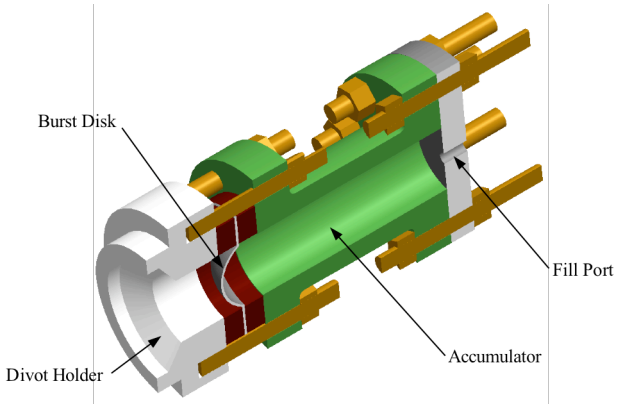

Figure 1. Burst disk system.

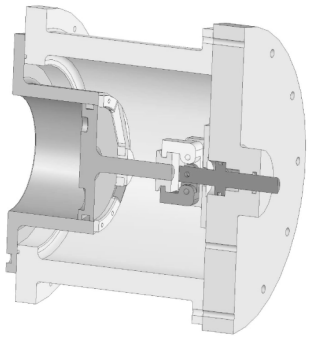

Figure 2. Integrated piston–reservoir.

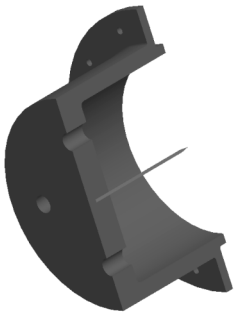

Figure 3. Needle-guided system.

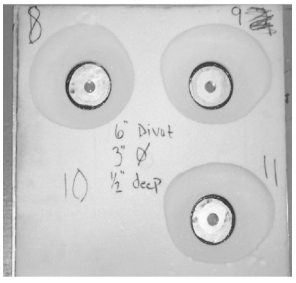

Figure 4. Pressure-failed sheet.

Contacts

Greg Noffz, DFRC, Code RA, (661) 276-2417
Kimberly Vaughn, DFRC, Code RA, (661) 276-5972
Ryan Lefkofsky, DFRC, Code OE, (661) 276-3944
Nathan Palumbo, formerly Code RP

SHAPED SONIC BOOM EXPERIMENT

Summary

The most significant technology barrier for unrestricted supersonic flight is the loudness of the sonic boom. The validated ability to shape aircraft to lower the resulting ground disturbance caused by the sonic boom is a major breakthrough for potential future development of environmentally acceptable supersonic aircraft. The 2004 Shaped Sonic Boom Experiment (SSBE) was designed to build on the success of the Defense Advanced Research Projects Agency (DARPA), NASA, and Northrop Shaped Sonic Boom Demonstration (SSBD) in 2003.

Objective

The SSBD aircraft, in limited flights in marginally acceptable weather, provided an initial validation of the theory of the shaped sonic boom. In contrast, the objective of the SSBE was to provide a proof of the robustness of the shaped sonic boom through the real atmosphere.

Approach

Figure 1 shows the SSBE design and a summary of the data taken.

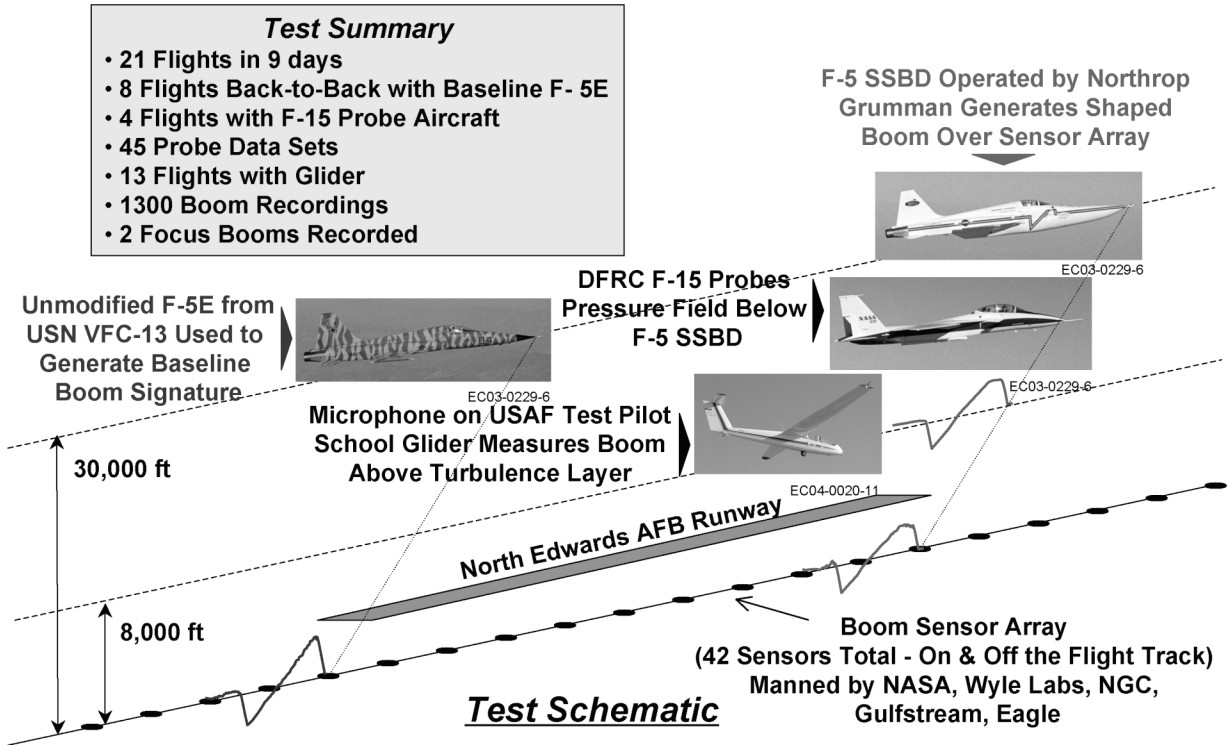

Figure 1. Successful test provides extensive validation of persistence of shaped sonic booms.

The SSBD and unmodified F-5E (Northrop, now the Northrop Grumman Corporation, Los Angeles, California) aircraft were flown over an array of ground sensors while a glider-borne microphone measured booms above the ground turbulence. On every flight of the SSBD aircraft, a shaped sonic boom was measured, including off-design Mach and altitude flight conditions and in different atmospheres, proving the robustness of sonic boom shaping. On separate flights, the NASA Dryden Flight Research Center F-15B (McDonnell Douglas

Corporation, St. Louis, Missouri) airplane probed the shockwaves of the SSBD in the near-field to validate computational fluid dynamics (CFD) predictions. After CFD adjustment, good to excellent CFD-to-flight agreement was achieved. Figure 2 shows typical flight results from SSBE, including near-field probing data, glider microphone data, and ground-level microphone data. These data have been, and are being, used to validate computational methods.

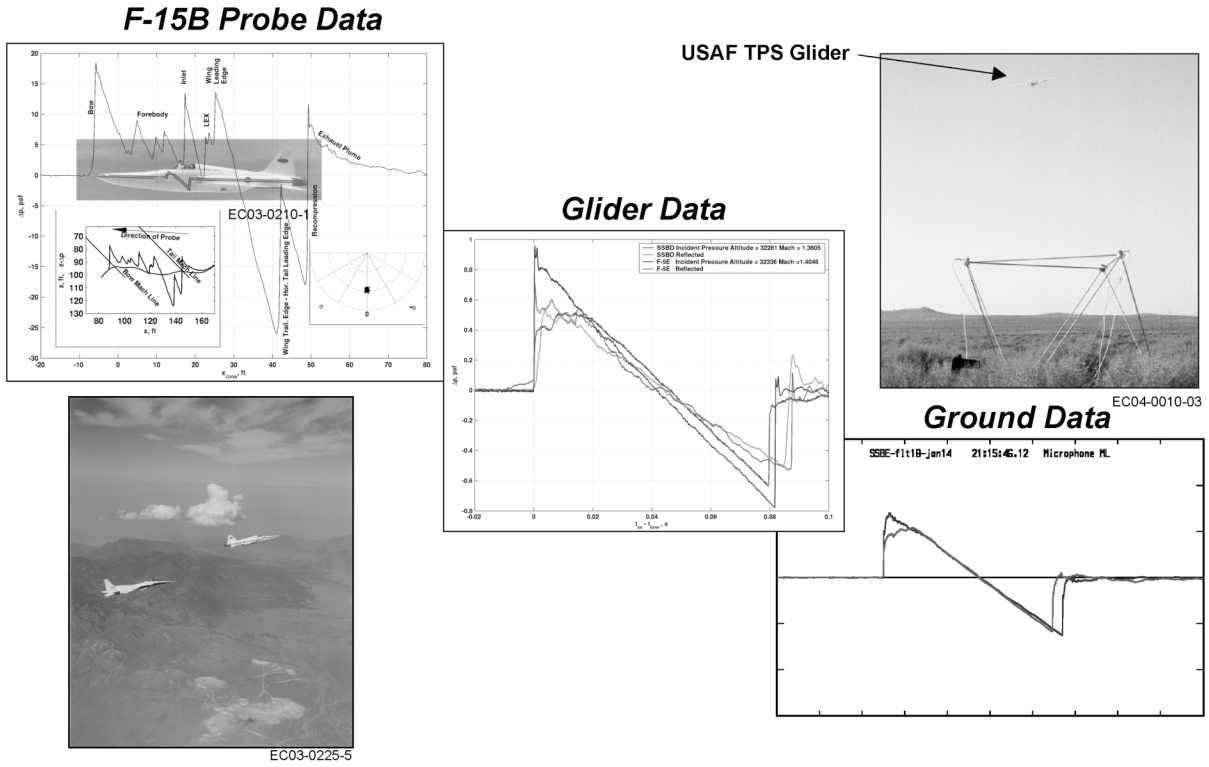

Figure 2. Typical SSBE flight results used to validate CFD and sonic boom propagation codes.

Status

The vast amount of data collected during this test is invaluable to future supersonic aircraft designs in that it will allow designers to proceed with confidence in the ability to predict, and thereby control, sonic booms. These data are currently being used in industry concept exploration studies for low sonic boom vehicles.

As soon as space is available, the U.S. Navy plans to induct the F-5 SSBD aircraft into the National Museum of Naval Aviation in Pensacola, Florida. In the meantime, it will be on loan to the Valiant Air Command Warbird Museum in Titusville, Florida near the Kennedy Space Center.

Contacts

Edward A. Haering, Jr., DFRC, Code RA, (661) 276-3696
Peter G. Coen, LaRC, (757) 864-5991

THE F-15B EMBEDDED GLOBAL POSITIONING SYSTEM/INERTIAL NAVIGATION SYSTEM INSTRUMENTATION SYSTEM UPGRADE

Summary

An embedded global positioning system/inertial navigation system (GPS/INS) has been incorporated into the existing instrumentation system of the NASA Dryden Flight Research Center F-15B (McDonnell Douglas Corporation, St. Louis, Missouri) airplane. This system provides aircraft state information as part of the aircraft pulse coded modulation (PCM) stream and is available in the control room in real time and through the flight data access system (FDAS) postflight.

Objective

In many flight experiments, the aircraft state must be accurately measured, telemetered, and made available to researchers in real time and postflight. The primary objectives of this upgrade were to integrate an embedded GPS/INS into the F-15B airplane and to merge the required data with the existing instrumentation system PCM stream.

Approach

A hybrid navigation system blending inertial navigation and global positioning technologies is blended in a Kalman filter, providing a tightly coupled GPS/INS solution. The inertial navigation subsystem provides medium accuracy, 0.8 nmi/hr circular error probability (CEP), utilizing an optically biased zero lock gyroscope. The embedded GPS receiver (EGR) subsystem is a 5-channel C/A-P(Y) code receiver which provides a 16-m spherical error probability (SEP) performance.

The unit was installed in the aircraft gun bay, with angular offsets relative to the aircraft subsequently quantified with a laser-based measuring system. These offsets are internally compensated for and the navigation solution is reported in the vehicle frame.

A 3U VME-based Mil-Std-1553 bus controller was developed for initializing the GPS/INS and for requesting navigation data in flight. A PCM slave stack was also added to acquire this data and merge it with the existing instrumentation system PCM stream.

Photo courtesy Russ Franz

Figure 1. GPS/INS and 1553 bus controller.

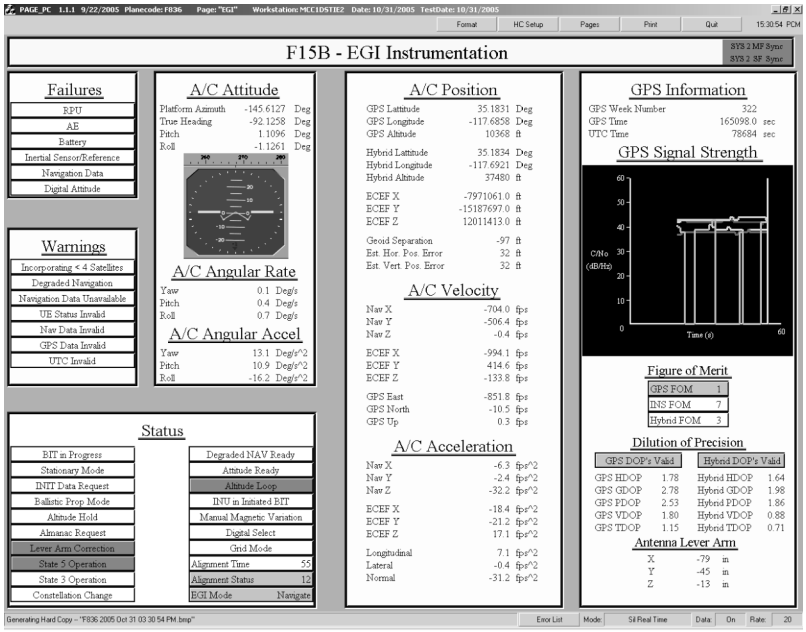

Figure 2. Control room PAGE display.

Status

The complete system has been installed on the aircraft and is awaiting flights for validation.

Contacts

Russ Franz, DFRC, Code RI, (661) 276-2022

HIGHER RESOLUTION STRAIN GAGE DATA ACQUISITION

Summary

Higher resolution and quieter strain gage measurements have been accomplished by means of new in-house electrical circuit board designs.

EC98-44511-1

Figure 1. The NASA F-15 airplane, tail number 837.

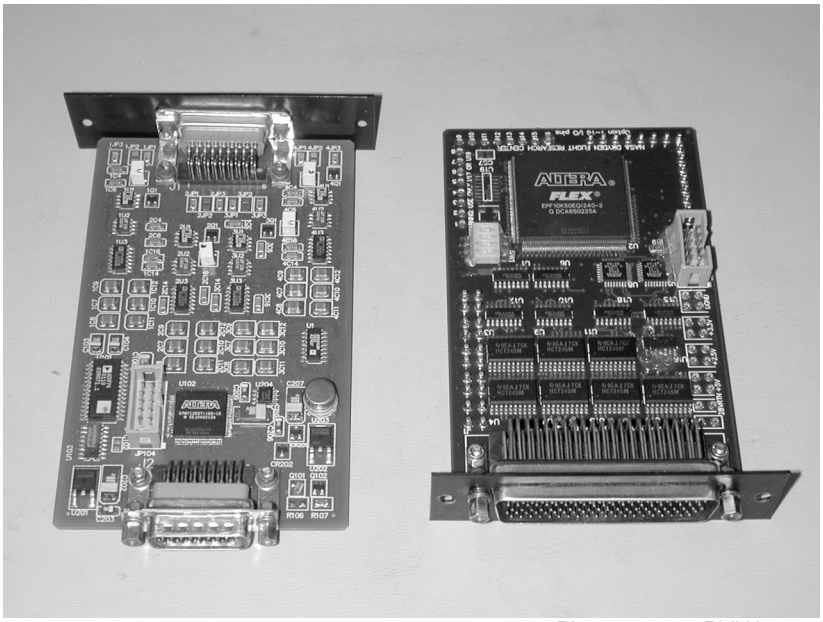

Photo courtesy Phil Hamory

Figure 2. The KK-756 digital strain gage card (left); the KK-748 general purpose EPLD board (right).

Objective

The objective of this undertaking was to obtain strain gage measurement data with up to 16-bit resolution and to minimize the number of wires required to implement the measurements.

Approach

A 16-bit analog-to-digital converter was integrated onto the strain gage signal-conditioning circuit board, locating the signal-conditioning board as close to the strain gages as possible to keep noise to a minimum. Multiple signal-conditioning boards were connected to a master controller card over a single bus to keep wires to a minimum. The master controller card was used to deliver the data to the aircraft pulse code modulation (PCM) system. A block diagram of the relationship between the data acquisition components is shown in figure 3.

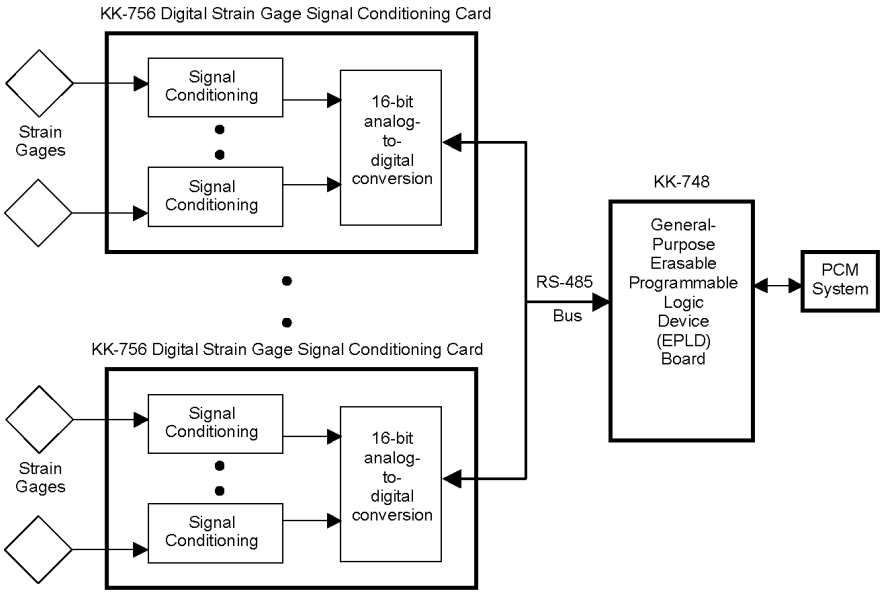

Figure 3. Simplified block diagram showing relationship between the data acquisition components.

Status

A system of these cards is installed on the NASA Dryden Flight Research Center F-15 (McDonnell Douglas Corporation, St. Louis, Missouri) airplane, tail number 837 (F-15/837) and has been supporting the structural loads model validation (SLMV) flights of the Intelligent Flight Control Systems (IFCS) project since June, 2005. The system supports 20 full-bridge strain measurements and uses one KK-748 and five KK-756 cards interfaced to a Vector 800 PCM system. Flight data shows close correlation between counterpart digital and analog strain gage measurements. The present design allows for up to 32 full-bridge, half-bridge, or quarter-bridge strain gages on a single RS-485 bus through the use of up to eight KK-756 cards.

Contributors

Tony Branco, Harry Chiles, Phil Hamory, Victor Lin, Kendall Mauldin, Matt Reaves

Contact

Phil Hamory, DFRC, Code RI, Philip.J.Hamory@nasa.gov, (661) 276-3090

INTERNET PROTOCOL OVER TELEMETRY TESTING FOR EARTH SCIENCE CAPABILITY DEMO SUMMARY

Summary

The development and flight tests described here focused on utilizing existing pulse code modulation (PCM) telemetry equipment to enable on-vehicle networks of instruments and computers to be a simple extension of the ground station network. This capability is envisioned as a necessary component of a global range that supports test and development of manned and unmanned airborne vehicles.

Objectives

The Hi-rate Wireless Airborne Network Demonstration (HiWAND) project was established to meet the following five main objectives:

1. Demonstrate transparent use of Telemetry (TM) Band for bidirectional Internet Protocol (IP) communications
2. Demonstrate capability of existing telemetry hardware to support bidirectional IP communications
3. Remotely initiate processes and collect results using IP over existing TM Band
4. Demonstrate capability for line-of-sight data links between ground and aircraft systems
5. Evaluate system performance during flight testing up to a 150-mile range

Approach

The approach adopted by the project was to populate an existing equipment rack that was previously flown on the NASA Dryden Flight Research Center (DFRC) King Air, tail number 801 (NASA 801). The rack included similar equipment to the ground-based equipment located at the Aeronautical Tracking Facility (ATF) at the NASA DFRC Western Aeronautical Test Range (WATR), Edwards, California. Since only one shaped offset quadrature phase-shift keying (SOQPSK) transmitter was available, pulse code modulation/frequency modulation (PCM/FM) at 5 Mbps was used for the uplink and SOQPSK modulation at 10 Mbps was used for the downlink.

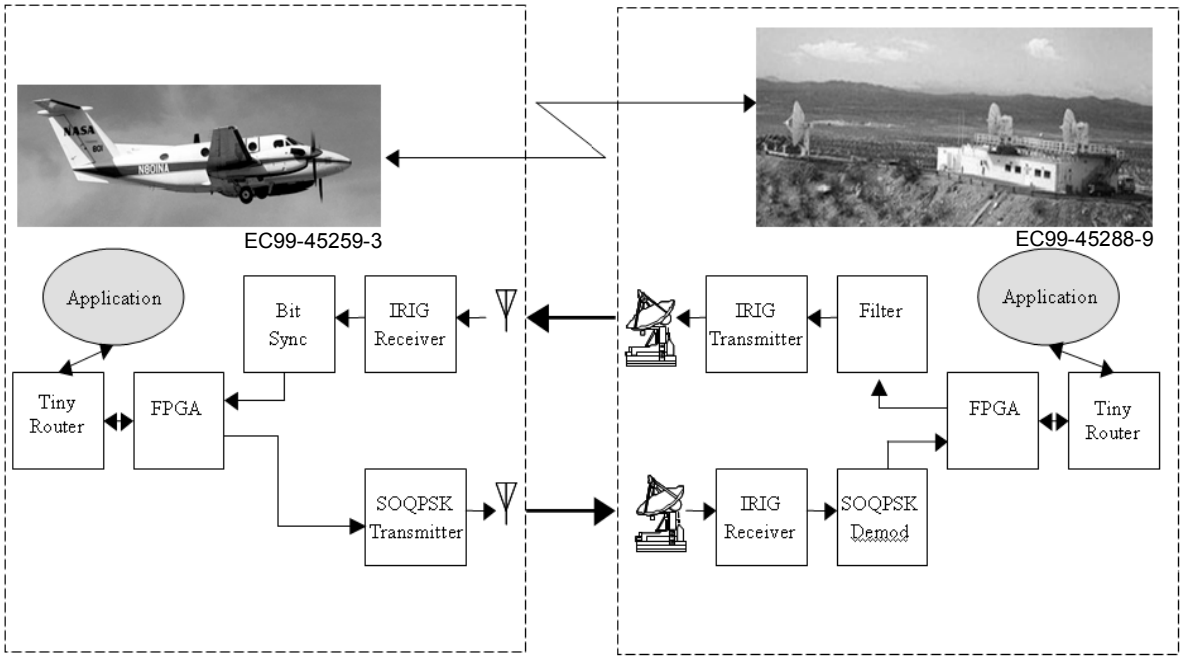

Figure 1. Flight test configuration.

System performance was quantified in the following ways:

1. Data throughput – file transfer protocol (FTP) file transfers, and transmission control protocol (TCP) and user datagram protocol (UDP) throughput tests
2. Packet loss – Transmission of UDP packets at various bit rates
3. Latency – Ping tests with various size data payloads
4. Repeatability – The above tests were repeated at the same flight conditions.

A custom graphic user interface (GUI) (fig. 2) was developed to automate testing, record results, allow for remote initiation of tests, and provide “chat-like” communications between the ground and aircraft test conductors.

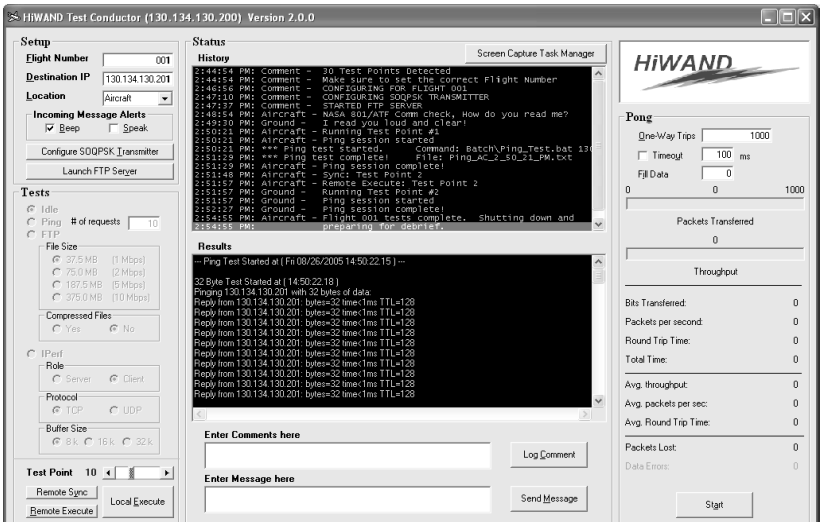

Figure 2. Test conductor graphic user interface.

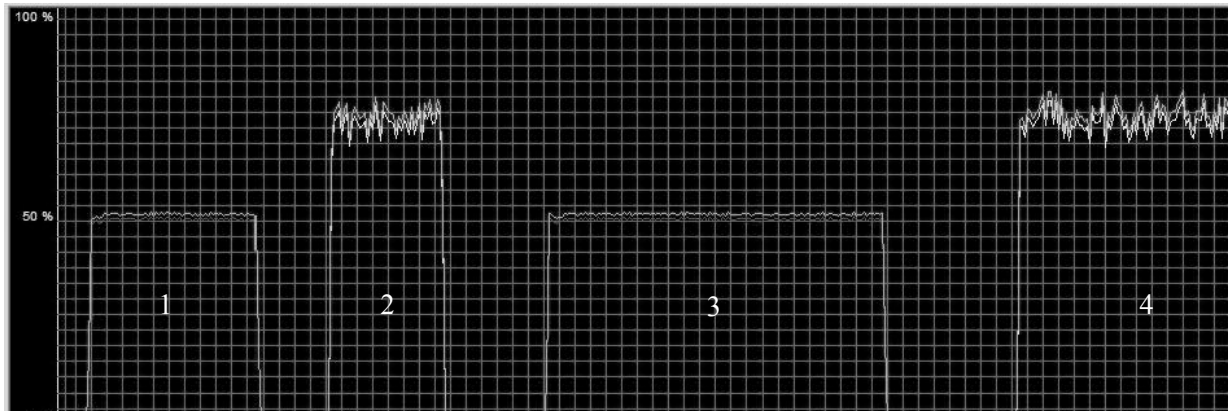

Figure 3. Flight test data throughput.

The throughput test results are depicted in figure 3, where 100 percent is based on 10 Mbps. The graphs labeled 1 through 4 are results from a 37.5 MB FTP transfer uplink and downlink and a 187.5 MB FTP transfer uplink and downlink, respectively.

Status

A total of seven flights were conducted, the last of which culminated in a UDP throughput of 9.4 Mbps, and TCP throughput of 7.2 Mbps at a range of 165 miles. Internet connectivity was also established in flight allowing for World Wide Web surfing, downloading satellite imagery, and sending e-mail. Future work for system miniaturization and aircraft-to-aircraft testing is being discussed.

Contacts

Russ Franz, DFRC, Code RI, Principle Investigator, (661) 276-2022
Mark Pestana, DFRC, Code OF, Project Manager, (661) 276-2519
Shedrick Bessent, DFRC, Code RI, Instrumentation Engineer, (661) 276-3663
Richard Hang, DFRC, Code RI, Instrumentation Engineer, (661) 276-2090
Howard Ng, DFRC, Code RI, Instrumentation Engineer, (661) 276-3803

LOW COST KU-BAND SATELLITE TRANSMITTER SYSTEM

Summary

The NASA Space-based Telemetry and Range Safety (STARS) program has tested a low-cost Ku-Band transmitter alternative for Tracking and Data Relay Satellite System (TDRSS) applications based on an existing inter-range instrumentation group-106 (IRIG-106) shaped offset quadrature phase-shift keying (SOQPSK) transmitter. The data collected indicates that IRIG-based hardware should be capable of providing a low-cost TDRSS option for Ku-Band and S-Band TDRSS return link applications. The existing transmitter hardware is not currently space qualified, however, it can satisfy TDRSS transmitter requirements for suborbital applications such as uninhabited aerial vehicles (UAVs), a significant area of interest at the NASA Dryden Flight Research Center, Edwards, California.

Objective

The SOQPSK also offers the advantage of a spectrally efficient transmitter that is already qualified for the aircraft environment and is compatible with the current IRIG-106 standard Tier 2 transmitter hardware. Prior simulations have demonstrated that SOQPSK (Version B) offers a TDRSS implementation loss advantage over other versions of SOQPSK. The system implementation loss characterizes compatibility issues the TDRSS receivers may have with the transmit system utilized.

Approach

The SOQPSK transmitter selected was an L-Band unit with the radio frequency (RF) amplifier removed. This lower output power simplified development of the up-converter and reduced vehicle electromagnetic interference (EMI) and radio frequency interface (RFI) concerns. The up-converter utilizes a local oscillator (LO), which, when mixed with a transmitter output, results in a frequency component at 15.0035 GHz. Although the nominal TDRSS center frequency is 15.0034 GHz, the TDRSS receiver can be tuned to 15.0035 GHz, making use of the low-cost system feasible.

The low-cost SOQPSK transmitter was compatibility tested with the integrated receiver (IR) at the NASA White Sands Complex, Las Cruces, New Mexico. The resulting basic encoding rules (BER) were collected at data rates of 1 Mbps, 3 Mbps and 5 Mbps.

Status

The Ku-band TDRSS compatibility test results indicate that the proposed low-cost approach is feasible and can result in an order of magnitude cost savings. Although testing has not been completed to date, it is likely that current IRIG Tier 2 S-Band transmitters can be used with TDRSS, with minor firmware modifications, resulting in a very low-cost and readily available option for S-Band TDRSS. These transmitters are also an especially interesting low-cost option for future UAV applications.

Photo courtesy of the NASA Space Network TDRSS Compatibility Test Van

Figure 1. Low cost Ku-band transmitter test setup at NASA Goddard Space Flight Center, Greenbelt, Maryland.

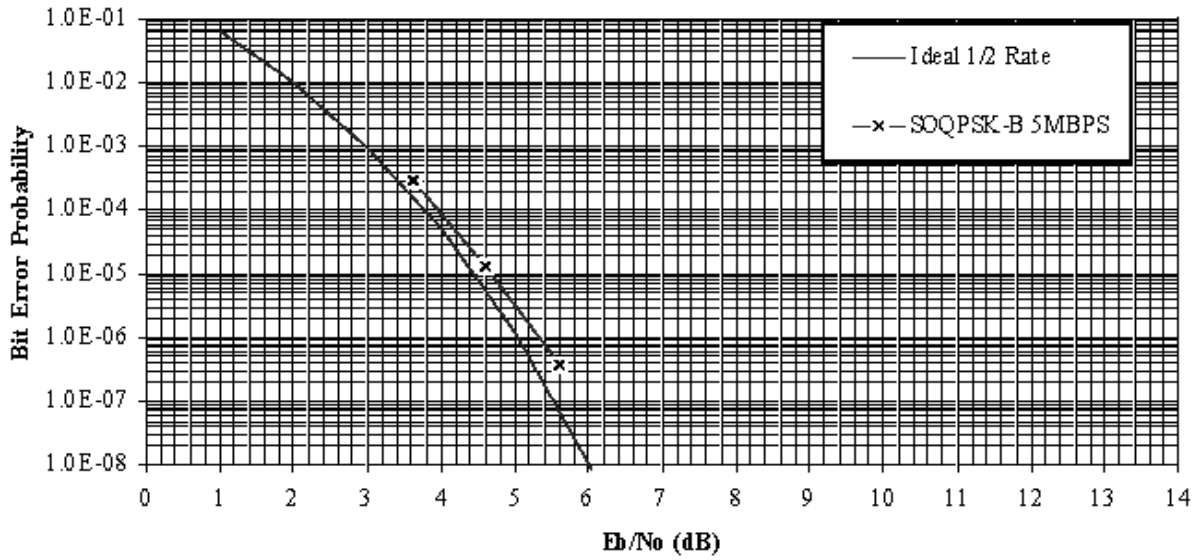

Figure 2. STARS Transmitter RTN Mode 2 Non-Coherent SOQPSK (NRZ-M) 1/2 Rate Conv.

Contacts

Don Whiteman, DFRC, Code RI, donald.e.whiteman@nasa.gov, (661) 276-3385

RECONFIGURABLE INSTRUMENTATION SIGNAL CONDITIONING

Summary

The schematic design of new signal conditioning circuitry for increasing flight research productivity is 80 percent complete. The new design maintains the functionality and research quality performance of existing designs and in addition, enables the remote adjustment of the gain, offset, and filtering settings.

Objective

The objective of the project is to design a printed circuit board that does not require physical access or replacement of components when the fine tuning of circuit performance is required.

Justification

Sensor signal conditioning is an important part of instrumentation data acquisition. Traditional signal conditioning is based on hardware designs that use analog circuit components to condition measurement signals into a format suitable for data acquisition processing. The traditional approach is extremely costly, time-consuming, and requires component-level tailoring of each individual signal channel. Drawbacks exist that impede the instrumentation processing and operational readiness. Initial fabrication time has an extremely long lead time and requires tailoring designs on a channel-by-channel basis. This requires knowledge of individual sensor types and characteristics which may not be readily available early in the design cycle. The NASA Dryden Flight Research Center data systems can include hundreds of sensors. Often, signal conditioning requirements are changed because of sensor replacement or changing requirements in signal characteristics. Modifications are implemented with component-level changes to the hardware; this adds the risk of damaging the hardware.

Approach

The investigation of modern analog, digital, and mixed signal devices with built-in, reconfigurable intelligent systems is under way.

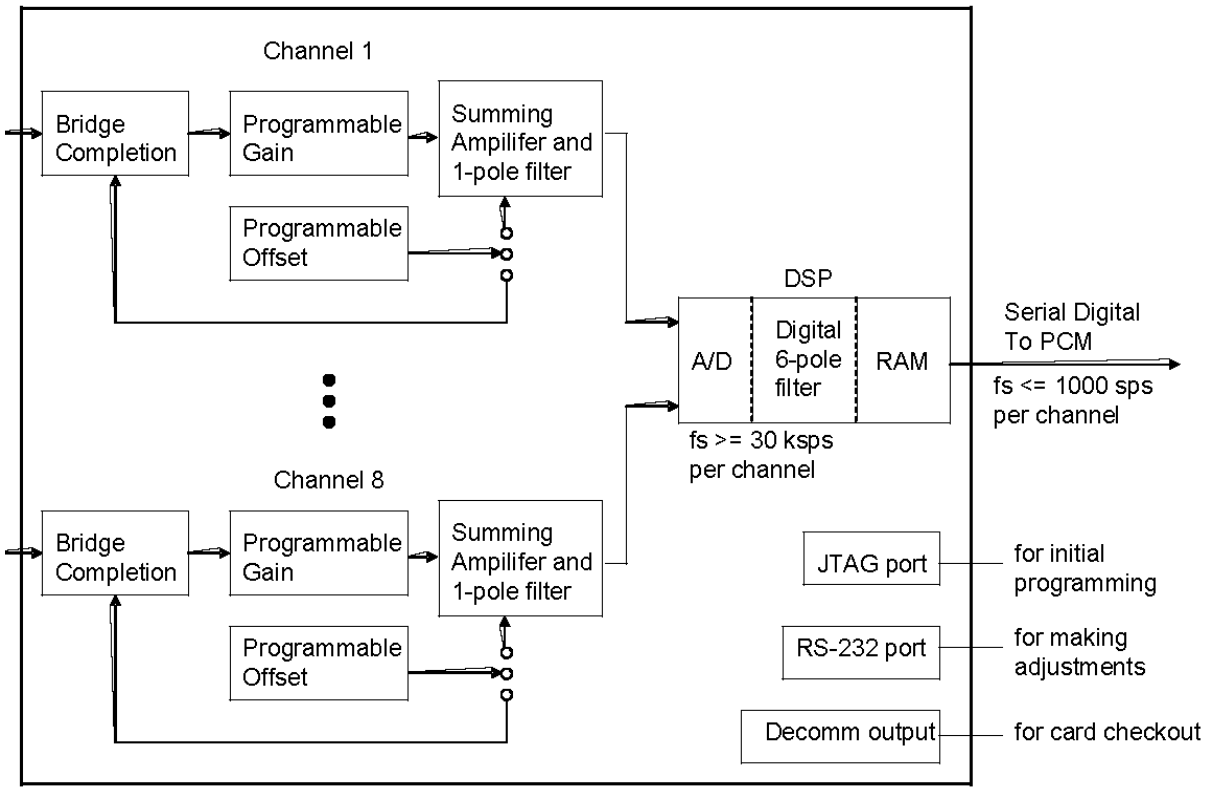

RISC Simplified Block Diagram

Results

The TMS320F2811 digital signal processor (Texas Instruments, Dallas, Texas) was selected as the core element. Development kits and other candidate components were purchased and evaluated. Good quality was observed, and correct functionality was demonstrated when the unit was connected to Dryden pulse code modulation (PCM) systems. Design reviews were held in July and September, 2005.

Benefits

The ability to reprogram signal conditioning without the need for physical access and without the need to replace components is a high payoff enhancement because of savings in time, manpower, and potential damage to parts caused by rework efforts.

Status

Eighty percent of the components for the new design have been purchased. Manufacturing and assembly of the new design is expected to be complete in November, 2005. If funding is available, laboratory, environmental, and flight testing will follow.

Contributors

Phil Hamory, Dmitriy Bekker, Richard Hang

Contacts

Phil Hamory, DFRC, Code RI, Philip.J.Hamory@nasa.gov, (661) 276-3090
Richard Hang, DFRC, Code RI, Richard.Hang@nasa.gov, (661) 276-2090

SPACE-BASED TELEMETRY AND RANGE SAFETY (STARS) PHASED ARRAY ANTENNA CONTROLLER

Summary

A phased array antenna controller (PAAC) has been developed for tracking a Tracking and Data Relay Satellite System (TDRSS) satellite from a maneuvering aircraft. This system leverages work accomplished for the F-15B Embedded GPS/INS Instrumentation System Upgrade project.

Objective

The primary objective was to develop a real-time antenna controller that could fly on the F-15B (McDonnell Douglas Corporation, St. Louis, Missouri) airplane and maintain tracking of a satellite. The beam width of the antenna is 2 deg and the aircraft maneuvering would be initially limited, with increasing maneuvering on successive flights. It was also an objective for the controller to communicate certain information via ethernet for demonstration of routable data distribution.

Approach

Proper pointing of an antenna requires knowledge of certain real-time information. For instance, the position and attitude of the airplane and the position of the satellite must be accurately known. An onboard global positioning system/inertial navigation system (GPS/INS) is used to provide the position and attitude of the airplane and the GPS time. The satellite position is approximated as a function of time and is computed by the PAAC from inter-range instrumentation group B (IRIG-B) time code input. The PAAC tasks were combined with the Mil-Std-1553 bus controller tasks that initialize, orient, boresight, align, and request navigation data from the GPS/INS. Data collected from the GPS/INS, calculated parameters, and antenna commands and status are transmitted in fixed-length frames via ethernet and RS-422 data transmission.

Photo courtesy Russ Franz

Figure 1. Phased array antenna with GPS/INS during TDRSS test.

Status

The complete antenna controller system successfully tracked a TDRSS satellite during a ground test near the Aeronautical Tracking Facility (ATF) at the NASA Dryden Flight Research Center Western Aeronautical Test Range (WATR), Edwards, California. Flight testing is planned for the F-15B airplane during the spring of 2006.

Contacts

Russ Franz, DFRC, Code RI, (661) 276-2022

TWO SERIAL DATA TO PULSE CODE MODULATION SYSTEM INTERFACES

Summary

Two pulse code modulation (PCM) system interfaces for asynchronous serial data are described. One interface is for global positioning system (GPS) data on the NASA Dryden Flight Research Center (DFRC) F-15B (McDonnell Douglas Corporation, St. Louis, Missouri) airplane, tail number 836 (F-15B/836). The other is for flight control computer data on the duPont Aerospace (La Jolla, California) DP-1, a 53-percent scale model of the duPont Aerospace DP-2.

Photo courtesy duPont Aerospace

Figure 1. The duPont Aerospace DP-1.

EC99-44862-12

Figure 2. The NASA F-15B airplane in flight.

Objective

Digital data from various aircraft computers are frequently required to be downlinked with other measurements obtained by flight research instrumentation systems. The RS-232 format is a standard format for communicating data between computers. Having an easily deployable and reconfigurable interface unit can address a wide range of needs.

Approach

For several years, the DFRC has had experience using Tattletale® (Onset Computer Corporation, Bourne, Massachusetts) data loggers for analog and digital data acquisition and control tasks. The Tattletale Models 7 and 8 are based on the 68332 microcontroller which has an onboard coprocessor called the time processing unit (TPU). The TPU is well suited for handling digital waveforms such as the RS-232. Data is passed to the PCM system as 8-bit parallel words under the control of the timing signals from the PCM system.

The Tattletale system on the F-15B/836 receives five blocks of data from the Ashtech Z-12 GPS receiver (Thales Navigation, Santa Clara, California), cross-checks two of the blocks for the correct time, extracts the desired parameters, converts most values from American Standard Code for Information Interchange (ASCII) characters to the Institute of Electrical and Electronics Engineers (IEEE) 754 floating-point numbers, and passes them to the PCM system.

Data conversions are not required for the DP-1 system. This frees processing time for the Tattletale to handle data at a higher transfer rate, as shown in table 1.

Table 1. Selected specifications for the two interfaces.

Item	F-15B/836 interface	DP-1 interface
Block data rate	2 blocks per second	20 blocks per second
Block length	345 bytes	500 bytes
Real-time data conversion	Yes	No
RS-232 Bd rate	19,200	115,200

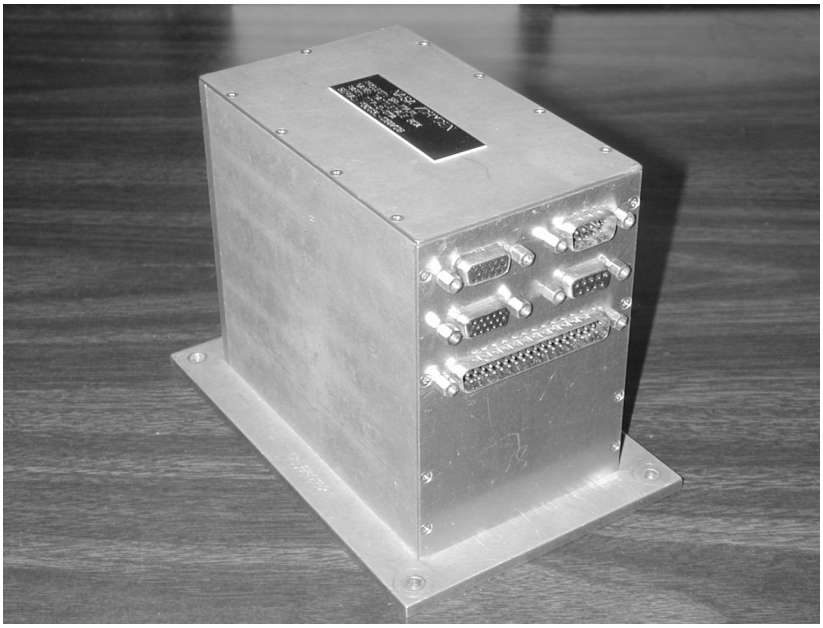

Photo courtesy Phil Hamory

Figure 3. Photograph of the Tattletale system for the DP-1.

Status

The GPS interface has been flying on the F-15B/836 since 2001. The flight control computer interface for the DP-1 has been fully checked out at DFRC and is at duPont Aerospace waiting for aircraft installation. Lab tests have shown that the TPU can support RS-232 rates of at least 230,400 Bd. The RS-422 and Serial Peripheral Interfaces (SPI)® (Motorola, Incorporated, Schaumburg, Illinois) are available as well.

Contributors

Ryan Heine (former co-op student from Saint Louis University), Phil Hamory, Victor Lin

Contact

Phil Hamory, DFRC, Code RI, Philip.J.Hamory@nasa.gov, (661) 276-3090

STUDY OF THE NEW AIR-LAUNCHED SMALL MISSILE (ALSM) PHOENIX HYPERSONIC FLIGHT RESEARCH TEST BED

Summary

A new test bed for hypersonic flight research is proposed. Named the Air-Launched Small Missile (ALSM) Phoenix hypersonic flight research test bed, it was conceived to help address the current lack in hypersonic flight research capabilities. The Phoenix ALSM test bed results from the utilization of two unique and very capable flight assets: the U.S. Navy Phoenix AIM-54 guided air-to-air missile and the NASA Dryden Flight Research Center F-15B (McDonnell Douglas Corporation, St. Louis, Missouri) flight research airplane.

Preliminary studies indicate that the Phoenix missile is a highly capable platform. When launched from a high-performance aircraft, the guided Phoenix missile can boost research payloads to low hypersonic Mach numbers, enabling cost-effective, quick-turnaround flight research in the supersonic-to-hypersonic transitional flight envelope. Experience gained from developing and operating the ALSM Phoenix test bed will be valuable for the development and operation of future higher-performance ALSM hypersonic flight test beds as well as responsive microsatellite and small-payload air-launched space boosters.

Objective

The principal objectives of this effort are to conduct initial feasibility study and preliminary performance estimates for the ALSM Phoenix hypersonic flight research test bed.

Approach

The availability of hundreds of surplus Phoenix AIM-54 long-range, guided, air-to-air missiles from the U.S. Navy has presented an excellent opportunity for converting this valuable flight asset into a new hypersonic flight test bed. This cost-effective new platform will fill an existing gap in the test and evaluation of current and future hypersonic systems for flights at Mach numbers ranging from 3 to 5.

In the proposed ALSM test platform, the modified Phoenix missile is used as a high-Mach, precision-guided booster for flight research experiments at low hypersonic Mach numbers. When the missile's radar seeker, attendant signal processing equipment, target detector, and warhead are removed, it is possible to have a research payload volume of more than 7 ft^3 and an allowable weight of up to 250 lb. In addition, the performance of the standard Phoenix missile can be significantly increased by launching it from a high-performance carrier aircraft such as the NASA F-15B flight research airplane.

Status

Preliminary study and performance analysis have been conducted. The results indicated excellent feasibility of the proposed new ALSM test bed. Several briefings have also been made to the hypersonic research community at the NASA Langley Research Center, the NASA Glenn Research Center, and the Air Force Research Laboratory regarding the new ALSM test bed. Valuable technical input was provided by various hypersonic researchers at these briefings. In general, the research community showed high interest in the proposed ALSM test bed. Key Phoenix missile hardware, including F-14 airplane adapter pylons, launch rails, inert missile rounds, and other support hardware have been obtained from the U.S. Navy for more detailed design studies.

Contacts

Trong Bui, DFRC, Code RP, trong_bui@mail.dfrc.nasa.gov, (661) 276-2645

THE DRYDEN AEROSPIKE ROCKET TEST

Summary

The Dryden Aerospike Rocket Test Director Discretionary Fund Project conducted atmospheric flight research of the aerospike rocket nozzle using high-power rockets. Although the advantages of the aerospike rocket nozzles are well understood through analysis and ground testing, the lack of flight test data has precluded the use of these nozzles in the current generation of aerospace vehicles. Commercial high-power rockets provided a convenient, inexpensive test bed to conduct aerospike flight research. The conventional nozzles in high-power solid rocket motors were replaced by aerospike nozzles, and the instrumented rockets were then flown, resulting in the first known supersonic flights of aerospike rockets.

Objective

The principal objective of this effort is to conduct atmospheric flight research of aerospike rocket nozzles using commercial high power rockets.

Approach

A comprehensive effort was undertaken with analysis, ground testing, and flight testing, all conducted in a complementary and integrated manner. The flowpath for the aerospike nozzles was designed at the NASA Dryden Flight Research Center, Edwards, California in collaboration with the Air Force Flight Test Center, Edwards Air Force Base, California. The blacksky Corporation (Carlsbad, California) designed and fabricated the rocket test bed vehicle. The blacksky Corporation also coordinated development of the experimental aerospike nozzles and solid propellant motors used in the tests with Cesaroni Technology Inc. (Gormley, Ontario, Canada).

Status

During this research effort, one conventional conical nozzle and three aerospike rocket nozzles were test-fired on the ground. Three rockets were also successfully flown. Two aerospike rockets were flown successfully on two consecutive flights on March 30 and 31, 2004, at the Pecos County Aerospace Development Corporation Flight Test Range in Fort Stockton, Texas. The conventional rocket was successfully flown on May 18, 2005, in Fort Stockton, Texas. All flight data were recovered and analyzed.

The ground and flight test results were presented at the 41st AIAA/ASME/SAE/ASEE [American Institute of Aeronautics and Astronautics (AIAA), American Society of Mechanical Engineers (ASME), Society of Automotive Engineers (SAE), and American Society of Engineering Education (ASEE)] Joint Propulsion Conference & Exhibit in July 2005 (AIAA Paper 2005-3797). Flight data showed that all of the rockets successfully reached supersonic speeds with a maximum Mach number of 1.6 and a peak pressure altitude of nearly 30,000 ft. The aerospike nozzle efficiency was determined to be 0.96 from computational fluid dynamics (CFD) analysis. The rocket chamber pressures and thrusts of the aerospike rocket motors were lower than the conventional rocket motors, both in the ground- and flight-tests. Because the same propellant formulation was used in all of the rocket motors, the discrepancy in rocket chamber pressure and thrust was most likely caused by a larger actual aerospike nozzle throat area than the designed throat area.

Contacts

Trong Bui, DFRC, Code RP, trong_bui@mail.dfrc.nasa.gov, (661) 276-2645

DEVELOPMENT OF PORTABLE FIBER BRAGG GRATING INTERROGATION SYSTEM

Summary

A portable ground-based interrogation system was developed for the study and characterization of fiber Bragg gratings. The system utilizes tunable microelectromechanical system (MEMS) laser technology with fiber Bragg gratings to measure surface strain. A modified wavelength-to-strain algorithm was implemented based on research initiated at the NASA Langley Research Center to maximize computational efficiency. To validate this technology and system, laboratory tests were performed with fiber optic sensors and collocated conventional strain gages. Testing on a cantilever beam showed that the fiber optic strain sensors correlated to within 3–5 percent. Overall, test results show that the system represents a viable laboratory interrogation tool for fiber Bragg gratings.

Objective

The objective of the project is to develop a portable fiber Bragg grating interrogation system applicable for use in a laboratory environment. The system should be consistent in performance with a previously developed desktop interrogation system. To achieve portability, it should be lightweight, exhibit a small form factor, and have low power consumption. The system should also be designed to measure strain over a 20-ft segment of sensor fiber at a rate of one sample per second. Information from the interrogation system should be recorded locally, and a subset of that information should be sent to a monitoring notebook computer via an ethernet connection.

Approach

A redesign of an existing fiber optics interrogation system was performed considering weight, size, power limitations, and cost. The previous design was proven in the Flight Loads Laboratory using a desktop personal computer (PC) with a tabletop C-band tunable laser (fig. 1).

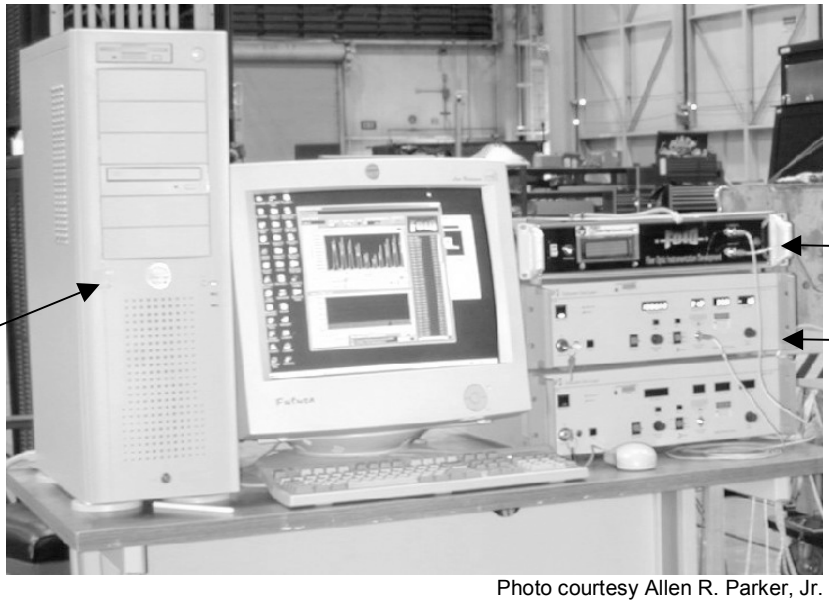

Photo courtesy Allen R. Parker, Jr.

Figure 1. Previously developed interrogation system.

The subcomponents that comprise this system include a C-band tunable laser, an optical network, an optical-to-electrical (O/E) amplifier/converter, a high-speed analog-to-digital (A/D) converter, and a host PC with large mass storage capacity. The host PC collected and processed data from the fiber optic sensor as well as displayed the results graphically. Great emphasis was placed on reducing the size of the PC and laser, which measured 17 in. W x 18 in. L x 5 in. H, weighed 35 lb, and cost $45,000.

The redesign included exchanging the desktop PC for a compact PC/104+ form factor central processing unit (CPU), measuring 4 in. W x 4.5 in. L which collects and processes data from the fiber optic sensors. Also, the desktop A/D card was exchanged for a compact PC/104+ A/D card that attaches directly to the new CPU. The tabletop laser was replaced with an innovative MEMS technology C-band tunable laser measuring 2 in. W x 3 in. L x 0.5 in. H and costing only $10,000. The subcomponents mentioned were integrated into a 17 in. W x 12 in. L x 3.5 in. H box and identified as the Fiber Optics Instrumentation Development (FOID) system (fig. 2). The FOID system also has a 40-GB hard disk to record the collected data, along with an ethernet port to communicate with a host notebook PC for control and graphical data display.

Photo courtesy Allen R. Parker, Jr.

Figure 2. FOID System with notebook central processing unit.

Status

A version of this system is being developed for wing shape monitoring on unmanned aerial vehicles (UAVs) where power, weight, and size limitations are more restrictive. The design will include a low power 133-MHz host CPU with a 233-MHz digital signal processing (DSP) processor, which will allow for lower power consumption while maintaining an adequate sampling rate. Multichannel systems are also being considered for large-scale testing as well as higher sampling systems.

Contacts

Allen R. Parker Jr., DFRC, Code RS, (661) 276-2407
Lance Richards, DFRC, Code RS (661) 276-3562
Anthony Piazza, DFRC, Code RS (661) 276-2714
Gary Williams, DFRC, Spiral Technology, (661) 276-2791

FIBER OPTIC SENSOR ATTACHMENT DEVELOPMENT AND PERFORMANCE EVALUATIONS

Summary

Research conducted in the Flight Loads Laboratory (FLL) at the NASA Dryden Flight Research Center has subjected fiber optic (FO) sensors to hostile environments for inflight applications and hot-structures ground testing (hypersonic/reentry vehicles). Sensor attachment of both fiber Bragg gratings (FBG) and silica based extrinsic Fabry-Perot interferometers (EFPI) have been accomplished on metallic and composite substrates. The FO sensors have been successfully demonstrated:

- At room and elevated temperatures (to 1850 °F)
- With combined applied thermal–mechanical loads
- And on both small laboratory coupons and large-scale structures for ground testing

Further development is required to increase the upper temperature limits to 3000 °F for sapphire EFPI sensors.

Objective

Project objectives are to develop attachment techniques and evaluate FO strain–temperature sensor performance for structural health monitoring aerospace applications. Sensor evaluation main tasks include:

1. Characterization of apparent strain (Eapp) of gold-coated EFPIs for posttest corrections of indicated strain values
2. Surface attachment and correction of thermal output of FBG to 500 °F and
3. Develop attachment techniques for sapphire strain sensors for applications that exceed the maximum operating temperature of the current silica EFPI sensor.

Approach

Thermal-sprayed sensor attachment procedures were developed and tested for both carbon/carbon (C/C) and carbon/silicon carbide (C/SiC) substrates. Testing of EFPI sensors to 1850 °F were performed to evaluate attachment integrity and sensor performance. Dilatometer tests compared substrate expansion with sensor output and generated Eapp correction curves for X-37 (Boeing Phantom Works, Huntington Beach, California) Orbital Vehicle tests. The FBG were attached to tubes for high altitude, long endurance (HALE) wing shape monitoring system tests performed in the FLL.

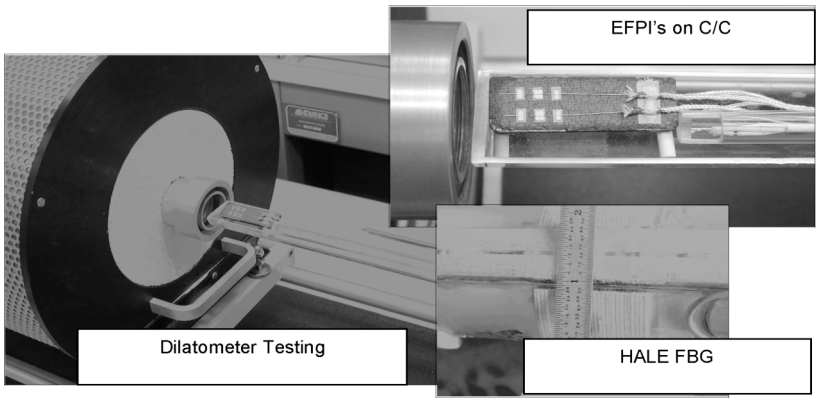

Photos courtesy Anthony Piazza

Laboratory sensor characterization testing of fiber optics.

Status

Future work with gold-coated EFPI sensors will address sensor-to-sensor scatter on ceramic composites (for example, C/C) and refinement of thermal corrections. The FBGs will be attached and characterized for applications to 500 °F.

A preliminarily evaluation of a multimode system has been accomplished for a future sapphire sensor prototype. A NASA Phase II Small Business Innovation Research (SBIR) was awarded for sensor development (TRL2). Thermal-spray attachment investigation will be initiated on both C/C and C/SiC substrates for temperatures approaching 3000 °F.

Contacts

Anthony Piazza, DFRC, Code RS (661) 276-2714
Larry Hudson, DFRC, Code RS (661) 276-3925
Lance Richards, DFRC, Code RS (661) 276-3562

AEROELASTIC FLIGHT DATA ANALYSIS WITH THE HILBERT–HUANG ALGORITHM

Summary

This research investigates the utility of the Hilbert–Huang Transform (HHT) for the analysis of aeroelastic flight data. It is well known that the classical Hilbert transform can be used for time-frequency analysis of functions or signals. Unfortunately, the Hilbert transform can only be effectively applied to an extremely small class of signals, namely those that are characterized by a single frequency component at any instant in time. The recently developed Hilbert–Huang algorithm addresses the limitations of the classical Hilbert transform through a process known as empirical mode decomposition. Using this approach, the data is filtered into a series of intrinsic mode functions, each of which admits a well-behaved Hilbert transform. In this manner, the Hilbert–Huang algorithm affords time-frequency analysis of a large class of signals. This powerful tool has been applied in the analysis of scientific data, structural system identification, mechanical system fault detection, and even image processing. The purpose of this research is to demonstrate the potential applications of the Hilbert–Huang algorithm for the analysis of aeroelastic systems, with improvements such as localized–online processing. Applications for correlations between system input and output, and among output sensors, characterize the time-varying amplitude and frequency correlations present in the various components of multiple data channels. Online stability analyses and modal identification are new applications for the algorithm, particularly in the area of aeroelastic and aeroservoelastic systems analysis.

Objective

An objective of signal-adaptive basis function derivations using the Hilbert–Huang algorithm is to yield intrinsic mode functions (IMF) giving instantaneous frequencies as functions of time that permit identification of imbedded structures. Instantaneous frequency is a quantity critical for understanding nonstationary and nonlinear processes. An empirical mode decomposition (EMD) process responds to the dilemma surrounding the applicability of instantaneous frequency from the Hilbert transform of a general multicomponent signal. The EMD decomposes a multicomponent signal into its associated monocomponents, called IMFs, while not obscuring or obliterating the physical essentials of the signal, and allows the traditional definition of instantaneous frequency to be complete by being applicable to signals of both mono- and multicomponent. To follow the true frequency evolution within a multicomponent signal, it is necessary to break down the components into individual and physically meaningful intrinsic parts. The adaptive and nonarbitrary decomposition using EMD produces an orthogonal set of intrinsic components, each retaining the true physical characteristics of the original signal. The monocomponents or intrinsic modes satisfy the conditions for a well defined notion of instantaneous frequency.

There is a multiresolution quality in the EMD process which deals with intermittency by allowing multiple time-scales within an IMF, but not allowing a similar time-scale simultaneously with other IMFs. System identification in the IMF subcomponent environment is a practical endeavor in the domain of multiresolution system identification. The concept of exploiting local properties for signal analysis applies to spatial data as well as temporal data with frequency and scale (translation and duration) variations. From the concept of empiquency to describe oscillations in images based on extrema points there are potential applications for general time-space-frequency-scale signal processing. Modern intelligent control and integrated aerostructures require control feedback signal processing cognizant of system stability and health. Time-varying linear or nonlinear modal characteristics derived from flight data are all within the realm of HHT. Further research will investigate these issues and HHT connections between localized

instantaneous dynamics, health diagnostics, and global system stability and performance for monitoring and prediction.

Approach

Correlations are made between Hilbert-transformed IMFs of various signals given the associated complex analytic signals $Z_x(t)$ and $Z_y(t)$ from original signals $x(t)$ and $y(t)$

$$Z_x(t) = x(t) + ix_H(t); \qquad Z_y(t) = y(t) + iy_H(t)$$

where $x_H(t)$ and $y_H(t)$ are Hilbert transforms of signals $x(t)$ and $y(t)$, respectively. A measure of the local correlation between components, in terms of simultaneous changes in instantaneous amplitude or frequency (phase) between analytic signals, is the Hilbert Local Correlation Coefficient, *HLCC*, from which we get instantaneous transfer function (*ITF*), its instantaneous magnitude (*IM*), and its instantaneous phase (*IP*).

$$ITF(t) = Z_{xy}(t) / Z_{xx}(t); \qquad IM(t) = |ITF(t)|; \qquad IP(t) = \cos^{-1}[HLCC(t)]$$

Now the concept of the using the essentially-orthogonal analytic IMFs from the inputs and outputs is pursued to establish a multiloop connotation of input IMFs to output IMFs for correlation and even stability properties. The input IMFs are interpreted as an orthogonal decomposition of the input(s), and the same for output IMFs for output(s). This can be generalized to multi-input-multi-output (MIMO) signal analysis where in reality each signal is represented by its Hilbert-transformed EMD. A singular value analysis of the operator between Hilbert-transformed IMFs represents relative contributions from the principal cross-correlation analytic IMFs as a result of correlation of all input analytic IMFs to all output analytic IMFs over the entire time span. The maximum singular value of this input-output operator corresponds to the structured singular value with a full-complex uncertainty block structure, and similarly for scalar uncertainty structures using the spectral radius. Hence, for time-domain MIMO signal analysis, it is most appropriate to combine complex uncertainty blocks (either full or scalar) for each input-output into a multiblock structure, where each complex sub-block corresponds to an input-output analytic IMF complex uncertainty structure. This is analogous to frequency-domain robust stability analysis, except that now at each point in time there is instantaneous frequency information and there results a time-dependent robust stability analysis.

Status

Application of the Hilbert–Huang algorithm for system signal decompositions, studying the effect of enhancements such as local–online behavior, understanding filtering properties, and especially investigation of correlations between input-output and between sensors in terms of instantaneous system identification, is still being investigated. System input-output signal analysis characterizes the time-varying amplitude and frequency components of multiple data channels, including input-to-output and distributed sensors, in terms of the IMFs of the HHT. These procedures are significant departures from Fourier and other time-frequency or time-scale wavelet approaches. Linear and nonlinear system identification using the IMFs is ongoing.

Contact

Marty Brenner, DFRC, Code RS (Aerostructures Branch), Martin.J.Brenner@nasa.gov,
(661) 276-3793

PREDICTIONS OF AEROSTRUCTURES OPERATIONAL FLIGHT LIFE USING THE HALF-CYCLE CRACK GROWTH PROGRAM

Summary

The half-cycle crack growth theory was incorporated into the Ko closed-form aging theory for the predictions of operational flight life of failure-critical aerostructural components. A new crack growth computer program was written to determine the maximum and minimum loads of each half-cycle from the random loading spectra for crack growth calculations. The outputs from this program were used to generate crack growth curves. The unified theories were then applied to calculate the number of flights permitted for the B-52B (The Boeing Company, Chicago, Illinois) airplane pylon hooks and the Pegasus® (Orbital Sciences Corporation, Dulles, Virginia) adapter pylon hooks to carry the Pegasus rocket–X-43 for air launching. A crack growth curve for each hook was generated for visual observation of the crack growth behavior during the entire air-launching flight. It was found that taxiing, takeoff run, and landing induced major portion of the total crack growth per flight.

Objective

The Ko operational life equation for the calculations of the number of flights, F_1^*, was established as

$$F_1^* = \frac{1 - f^{m-2}}{1 - \left(1 + \dfrac{\Delta a_1}{a_c^p}\right)^{1-\frac{m}{2}}} \tag{1}$$

In equation (1), $a_1\ (= a_c^p + \Delta a_1)$ is the crack size at the end of the first flight, and Δa_1 is the amount of crack growth induced by the first flight; a_c^p is the initial crack size, *m* is the material constant, and f is the operational load factor. The objective is to calculate the unknowns Δa_1 and f in equation (1).

Approach

The crack growth computer program reads the random flight loading spectra to determine the maximum and minimum loads of each half-cycle and calculate the incremental crack growth using the Walker crack growth equation. The accumulated crack growth, Δa_1, and the operational load factor, f, are then obtained for the calculations of the number of flights, F_1^*, from equation (1).

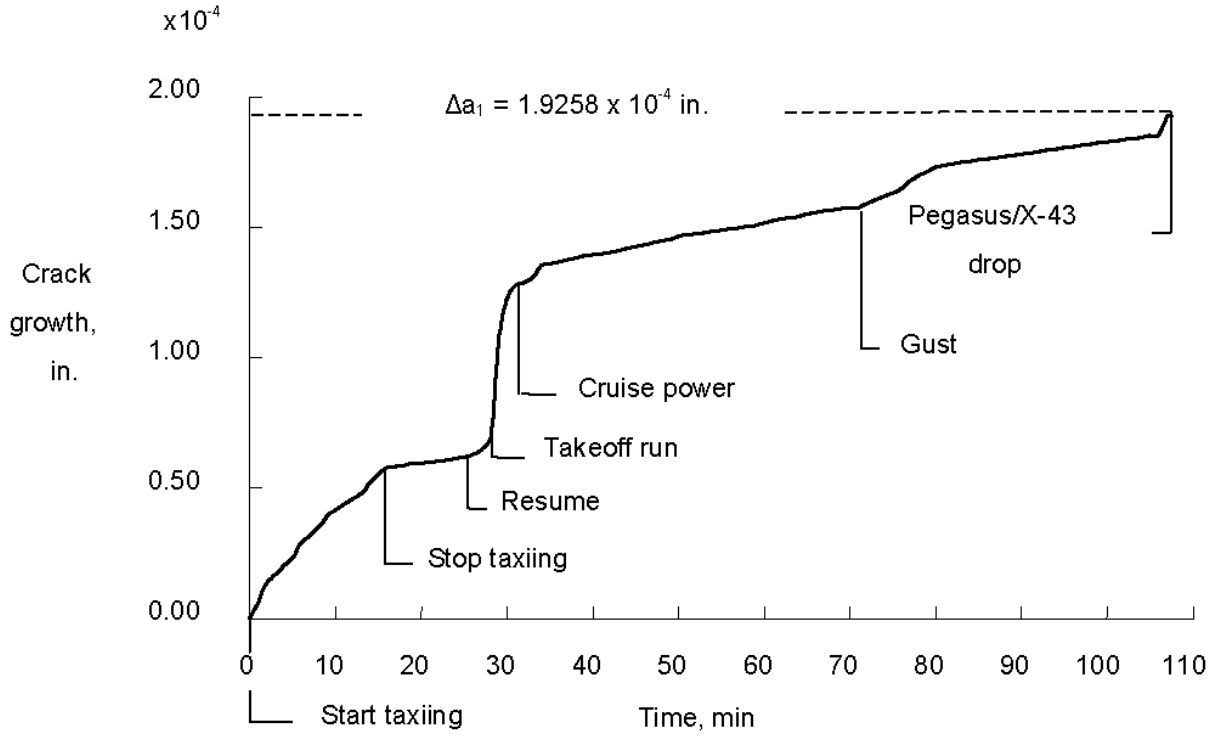

Figure 1. Crack growth curve generated for B-52B pylon front hook carrying Pegasus–X-43.

Status

The developed crack growth computer program is currently functional, but it will be modified to include spike removal. When interfaced with the existing Control Room equipment, this program can be a powerful tool for flight tests for visually monitoring the inflight crack growth behavior of airborne failure-critical structural components.

Contacts

Dr. William L. Ko, DFRC, Code RS, (661) 276-3581
Van T. Tran, DFRC, Code RS, (661) 276-3929

UPDATING THE FINITE ELEMENT MODEL TO MATCH GROUND VIBRATION TEST DATA

Summary

A simple and efficient approach for updating analytical finite element models (FEM) to match analytical frequencies and mode shapes to the experimental ground vibration test (GVT) data is introduced in this study. The proposed model updating procedure is based on a series of optimizations. This approach has been successfully applied to create an equivalent beam FEM for the inboard and outboard B-52H (The Boeing Company, Chicago, Illinois) airplane engines and the X-37 Advanced Technology Demonstrator Drogue Chute Test Fixture (DCTF) with the X-planes pylon. The goal was a simple model capable of being analyzed in a captive-carry configuration with the B-52H mother ship. This study has shown that natural frequencies and corresponding mode shapes from the updated FEM achieved at the final optimization iteration have excellent agreement with corresponding measured modal frequencies and mode shapes.

Objective

The primary objective of this study is to develop and validate a simple and efficient technique for including the measured GVT data into the analytical FEM. If measured mode shapes are to be associated with a FEM of the structure, the FEM will likely need to be adjusted to reduce the structural dynamic modeling errors in the flutter analysis; by so doing, flight safety can be improved as well.

Approach

Discrepancies between the GVT and the analytical results are common. In this approach, discrepancies in frequencies and mode shapes are minimized using the series of optimization procedures. Three optimization steps were used in turn to refine each model: the mass properties were set, the mass matrix was orthogonalized, and the natural frequencies and mode shapes were matched. Design variables for the optimization can include structural sizing information (thickness, cross-sectional area, area moment of inertia, torsional constant, etc.), point properties (lumped mass, spring constant, etc.), and material properties (density, Young's modulus, etc.).

B-52H Mother Ship

Frequencies and modal assurance criteria (MAC) values before and after model updating are given in table 1. It should be noted that a maximum of 14 percent frequency error before model updating is reduced to a maximum of 0.03 percent frequency error after model updating. In table 1, the minimum MAC value after model updating is 83. Therefore, we may conclude that analytical frequencies and mode shapes for the inboard and outboard engine nacelles have excellent agreement with the engine nacelle component GVT data. The FEM for the remaining B-52H structural components will be used in an "as is" condition, since the GVT data is unavailable.

X-Planes Pylon and X-37 DCTF Model

Frequencies less than 5 Hz are in the range of interest for the captive carry flutter analysis. The number of modes matched varied depending on the number of frequencies below 20 Hz (4 times higher than the frequency of interest) and with the ease with which the mode shape could be matched. Frequencies and MAC values after the model updating are shown in table 2. The GVT frequencies are also given in table 2. Overall, excellent matching for the frequencies and mode shapes was accomplished in this model updating procedure.

Status

The equivalent beam model that resulted from this study, while consisting of only about one percent of the number of nodes of the full detailed model, matches the first four natural frequencies and mode shapes of the GVT data. The model complexity is on the same order as that of the B-52H airplane, which makes combining them mathematically viable.

The first three frequencies of the X-planes pylon and the X-37 DCTF structures are close to the frequency range of the captive carry flutter analysis, therefore it is required to perform the model validation and model updating for the high fidelity flutter analysis. The B-52H airplane with the X-planes pylon and the X-37 DCTF is flutter-free within the flight envelope.

Table 1. Frequencies and modal assurance criteria values for the B-52H engine nacelles before and after model updating.

Frequencies (Hz)										
Mode	Inboard Engine Nacelle					Outboard Engine Nacelle				
	Before	Error	After	Error	GVT	Before	Error	After	Error	GVT
1	1.856	8.3%	2.025	0%	2.025	1.917	7.6%	2.075	0%	2.075
2	3.572	14%	4.139	0.02%	4.140	3.550	6.2%	3.784	0.03%	3.785
3	4.960	3.7%	5.150	0%	5.150	4.910	4.7%	5.149	0.02%	5.150

MAC Values						
Mode	Inboard Engine Nacelle			Outboard Engine Nacelle		
	Before	After	GVT	Before	After	GVT
1	98.95	98.98	100	97.79	97.92	100
2	96.37	98.30	100	97.99	99.33	100
3	92.22	89.16	100	88.77	82.71	100

Table 2. Frequencies and modal assurance criteria values after model updating.

Mode	Equivalent Beam (Hz / percent error)		MAC	GVT (Hz)
	Guyan Reduction	Full Order		
1	4.919 / – 0.04	4.917 / – 0.08	94.4	4.921
2	7.218 / – 0.01	7.217 / – 0.03	84.7	7.219
3	7.940 / – 0.01	7.939 / – 0.03	50.6	7.941
4	25.08 / – 0.05	24.05 / – 4.1	82.3	25.09

Contacts

Chan-gi Pak, DFRC, Code RS, (661) 276-5698

THE F-15B BASELINE GROUND VIBRATION TESTING

Summary

The NASA Dryden Flight Research Center (DFRC) uses a modified F-15B (McDonnell Douglas Corporation, St. Louis, Missouri) airplane, tail number 836, as a test bed for a variety of flight research experiments mounted underneath the airplane fuselage. This F-15B was selected to fly Gulfstream Aerospace Corporation's Quiet Spike (QS) project; however, this experiment is very unique and unlike any of the previous test bed experiments. The experiment involves the addition of a relatively long QS boom attached to the radar bulkhead of the airplane. This QS experiment is a stepping stone to airframe structural morphing technologies designed to mitigate sonic boom strength. Prior to flying the QS on the F-15B, the QS modal characteristics and coupling effects with the F-15B need to be understood. One of the first steps to understanding these effects is conducting a baseline ground vibration test (GVT) of the F-15B.

Objective

The objective of this baseline F-15B GVT was to measure the frequency, modal damping, and mode shape of primary structural modes for fully fueled, gear up, and gear down aircraft configurations. The GVT data will be used to create a baseline beam finite element model (FEM) of the NASA F-15B which will be used for future flutter analyses.

Approach

The GVT testing was conducted in a DFRC hangar with the aircraft fully fueled (41,268 lb) and in flight-ready condition. For this particular GVT, no soft support system was used because of conflict with the new self-jacking soft support system. Instead, the aircraft was supported at the three standard aircraft jacking locations with standard F-15 aircraft jacks. Acquiring usable GVT data with the airplane on jacks was possible only if the jacks were modeled analytically along with the rest of the aircraft. This way, once the analytical FEM was updated using GVT data, the jacks could be analytically removed to properly represent the aircraft in the free-free flight configuration for the flutter analysis. The aircraft was jacked upward just high enough to enable the landing gear to extend and retract without coming in contact with the hangar floor. The orientation of the jacks and thread length was critical for modeling purposes. No primary aircraft hydraulics (PC1 and PC2) could be used for the GVT because of an interface clearance issue with the gear landing and the external primary hydraulic system hookup locations. The flaps were faired and locked in place with no free play. The ailerons were allowed to droop to their fully extended position and bungee cords were installed with lead shot bags to remove the free play in the surface. The horizontal stabilizers were leveled and locked with wooden blocks placed in the actuator arms. The rudders were manually moved to the faired position for testing. During testing, a total of 205 degrees of freedom was measured. The aircraft was instrumented with 199 external accelerometers and the aircraft jacks with 6 accelerometers. Figure 1 illustrates the GVT test model created from the accelerometer locations. The aircraft was configured in three different ways for testing; landing gear up with no hydraulics, landing gear down with no hydraulics, and landing gear down with utility hydraulics. Each aircraft configuration had several different shaker configurations. All shaker locations and excitation were symmetric from the left to the right side of the aircraft. The aircraft was excited with burst random inputs from two 150-lb shakers vertically and at a 45º angle at different places on the aircraft. A total of 38 test runs was conducted, but the majority of the data sets gathered were in the aircraft configuration with landing gear up and no hydraulics because the results from these data sets were to be used for creating the F-15B FEM.

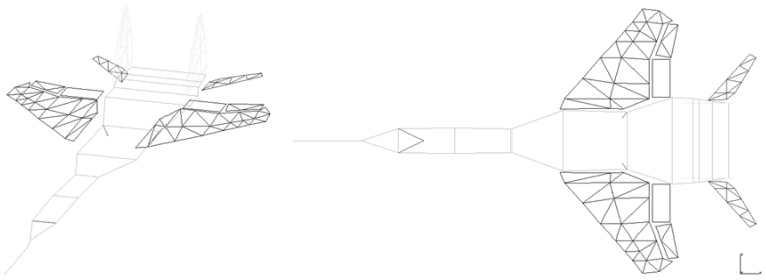

The F-15B airplane ground vibration test Integrated Design Engineering Software (I-DEAS) test model.

After numerous data curve fits from 2–30 Hz, the cleanest data and clearest mode shapes were from a combination of tests O-17 and V-37. These were used for mode matching and creating the beam model. Configuration O was a 45º shake on the aft wing tip, while configuration V was a vertical shake on the horizontal stabilizer. Table 1 below shows a small number of the frequencies (only up to 14 Hz) from these two data sets. It should be noted that the frequencies from testing are with aircraft on jacks and not in a free-free boundary condition. The bolt frequencies in the table were used for mode matching.

The F-15B airplane baseline ground vibration test frequencies.

Mode #	Aft Wing Tip 45º Config. O – t 17 Freq. (Hz)	Horz Stab Vertical Config. V – t 37 Freq. (Hz)	F-15B Mode Shape Description
1	2.069	---	Aircraft Yawing
2	2.593	---	Aircraft Fwd/Aft, W1B sym
3	3.203	---	Aircraft Yawing, W1B antisym, some mid Fuselage Lat. Bending
4	5.939	6.628	Aircraft Roll
5	6.313	6.335	F1B Vertical
6	8.611	8.798	Lat. Boom, Fwd Fuselage Lat., V1B antisym
7	8.896	9.034	Lt. V1B, some Rt. V1B sym, some Lat. Fwd Fuse, some W1B sym (out of phase)
8	9.233	9.222	W1B sym, V1B antisym, Rt. S1B, some Vertical Boom
9	9.615	9.621	Rt. V1B, some Rt. W1B (out of phase), some Rt. S1B, some Lat. Boom
10	10.520	10.683	W1B sym, some V1B sym, some S1B sym (out of phase), some F2B sym
11	12.597	12.665	S1B antisym, W1B antisym (out of phase), V2B antisym (out of phase)
12	13.839	13.982	W1B antisym, S1B antisym, Lat. Boom, some Fuse Tors. (out of phase)

Status

An analytical beam FEM of the F-15B airplane has been created. Several GVTs and FEM updates of both a mockup version of the QS and flight QS hardware have been conducted. A final mated QS and F-15B GVT remain to be preformed along with the flutter analysis. The QS experiment is expected to fly in late 2005 or early 2006.

Contacts

Natalie Spivey, DFRC, Code RS, (661) 276-2790

FLUTTER ANALYSIS FOR THE CENTERLINE INSTRUMENTED PYLON (CLIP) WITH AIRDATA BOOM ATTACHMENT

Summary

A generic test fixture has been designed and is being fabricated to conduct aerodynamic tests on the F-15B (McDonnell Douglas Corporation, St. Louis, Missouri) test bed airplane. This Centerline Instrumented Pylon (CLIP) flight test fixture (fig. 1) is comprised of a modified centerline pylon and splitter plate to shield, as best possible, the test article from the F-15B underside flow disturbances. A finite element model of the CLIP was created from hand measurements to conduct the flutter analysis for flight clearance. The CLIP has the same attachment to the F-15B airplane as a previous Cone Drag Experiment (CDE) which was analytically modeled, ground vibration tested (GVT), and model validated using the GVT data. The validated spring constants that defined the connection from the CDE to the F-15B were used in the CLIP analytical model. With this important structural information there was confidence in a flutter analysis for CLIP using only an analytical model. The flutter analysis showed over a 200 percent flutter margin which permitted no GVT validation. The mode matching technique used for the previous CDE model validation saved time for analyzing the CLIP flight test fixture by eliminating the need for a GVT and real-time monitoring in the control room.

Objective

The mode matching capability used in the structural dynamics group has proved to save time by creating reusable models with less validation. With aircraft at the NASA Dryden Flight Research Center being used for more than one experiment, it is worth the time to create an analytical model of that vehicle and validate it using GVT data once. If the aircraft has only minor structural modifications, analytical changes need to be made. For more complex modifications, only a small scale GVT needs to be conducted. If the vehicle has different stores to be flown, a small GVT is required to verify the stiffness connection between the aircraft and store.

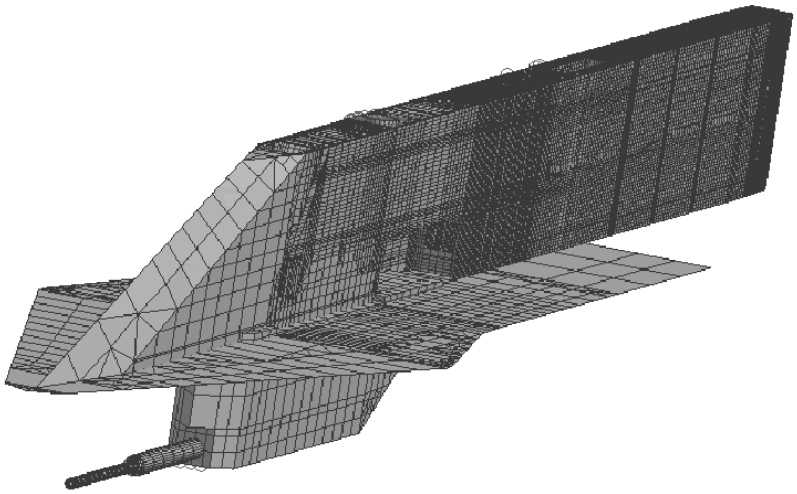

Figure 1. The centerline instrumented pylon finite element model.

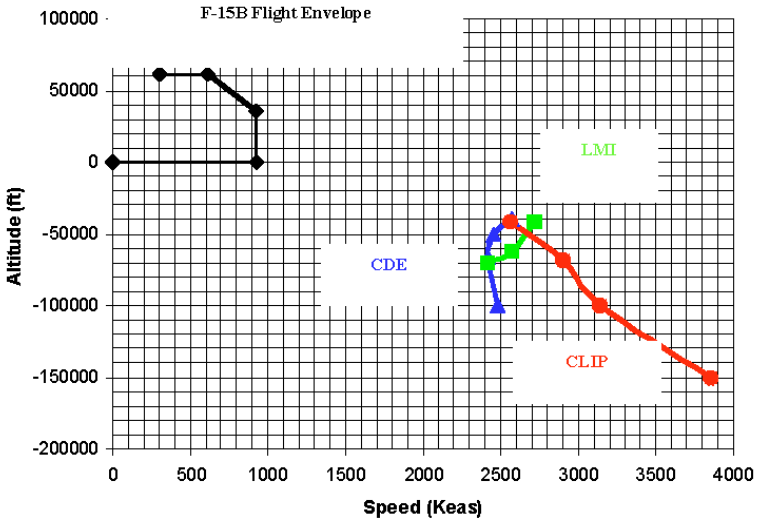

Figure 2. The F-15B airplane flight envelope compared to three different external store flutter points.

Approach

With past flutter analysis experience for stores on the F-15B airplane, the critical flutter mode is usually defined by the attachment stiffness from the store to the airplane (unless the store is less stiff than the connection stiffness). With this assumption, the spring constants validated in the CDE model were used in the CLIP analytical model [NASA Structural Analysis (NASTRAN)] and flutter analysis (ZONA Technology, Inc., Scottsdale, Arizona). The first analytical frequency of the CLIP was 20 Hz and flight data showed the first mode recorded with the accelerometers was 29 Hz, a slightly stiffer connection point than predicted.

Status

The F-15B/CLIP flights started October 2005.

Contacts

Starr Ginn, DFRC, Code RS, (661) 276-3434

FULL FIELD THERMAL PROTECTION SYSTEM HEALTH MONITORING SYSTEM FOR CREW EXPLORATION VEHICLES

Summary

The thermal protection system (TPS) of a space vehicle is a very critical system, as the tragic Space Shuttle Columbia accident highlighted. Currently there is no system to monitor the health of a TPS. The instrumentation in use on flight vehicles today consists of traditional sensor systems: thermocouples, strain gages, pressure transducers, and a few others. These sensor systems are all far too heavy to consider for use in implementing a full field health monitoring system using current technology. Fiber optic sensors (specifically fiber Bragg grating (FBG) sensors), however, are extremely lightweight, and have the capability of multiplexing many sensors on one fiber, minimizing system weight and complexity.

Objective

The objective of this research effort is to develop a prototype TPS Health Monitoring System (HMS) for a crew exploration vehicle (CEV) or equivalent flight vehicle with insulated structures (that is, using some form of a TPS). In addition to the sensors and system development effort, an algorithm will be developed to interpret the data and determine TPS health.

Approach

The FBG sensors, along with colocated thermocouples and strain gages, will be embedded in the room temperature vulcanizing (RTV) bond layer between the aluminum substrate and high temperature ceramic tile. A series of tests will be performed to determine sensor sensitivity, system feasibility, and algorithm efficacy.

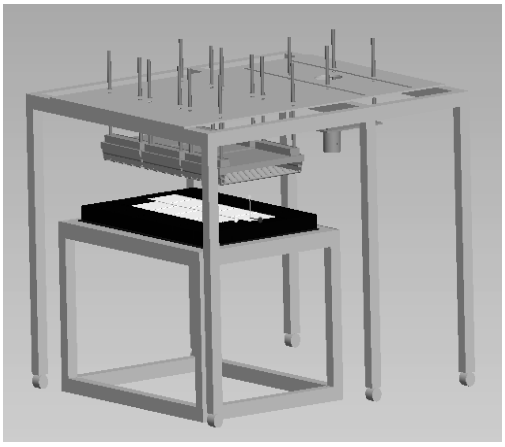

Test setup design featuring quartz lamps and impact fixture mounted to wheeled superstructure over test article and stand.

Status

The effort began with an extensive literature survey of impact testing and research that had been done, as well as Space Shuttle tile thermal properties and vehicle implementation. The testing methodology has been outlined, and test setup fabrication has commenced. The test article design for each phase of testing is nearly complete.

Contacts

Christopher Kostyk, DFRC, Code RS, (661) 276-5443

DISPLACEMENT THEORIES FOR INFLIGHT DEFORMED SHAPE PREDICTIONS OF A LONG SPAN FLYING WING

Summary

Displacement equations have been developed for describing the deformed shapes of a highly-flexible span-loaded high-aspect-ratio wing, typical of many unmanned aerial vehicle (UAV) designs. The displacement equations are expressed in terms of bending and distortion strains to be measured at multiple strain sensing stations on the wing spar surface. The bending and distortion strain data can then be input into the displacement equations for the calculations of slopes, deflections, and twisting of the wing spar at the strain sensing stations for generating the deformed shapes of the wing spar. The displacement equations are validated on a representative thin-walled composite tube using both conventional and fiber optic sensors. Fiber optic strain sensors, along with the computationally-efficient strain-displacement algorithm, form a powerful tool for inflight deformation monitoring of the Helios (AeroVironment, Inc., Monrovia, California) flying-wing-class vehicles.

Objective

By installing multiple strain sensors at discrete sensing stations on a cantilever wing spar, it is our goal to use the resulting strain sensor data to calculate the deflections and twists of the wing spar during flight. The purpose is to monitor the inflight deformed shape of the remote-controlled highly flexible extraordinary long span flying wing. This research represents the first step toward controlling the wing shape of highly flexible wings in flight.

Approach

Using classical beam theory, the theoretical slope equations, deflection equations, and cross-sectional twist equations were developed and written in terms of the strains. The measured strain data can be input into those equations for the calculations of deformed wing shape.

Status

The displacement equations were developed from classical beam theory and finite-element solutions and successfully validated for their accuracy during extensive ground testing. The displacement theory and the associated strain sensing system (for example, fiber optic sensors) form a powerful tool for monitoring the inflight deformed shapes of the long span flying wing. The calculated deformation data can ultimately be visually displayed to the ground based pilot who can monitor the inflight deformed shape of the large flying wing.

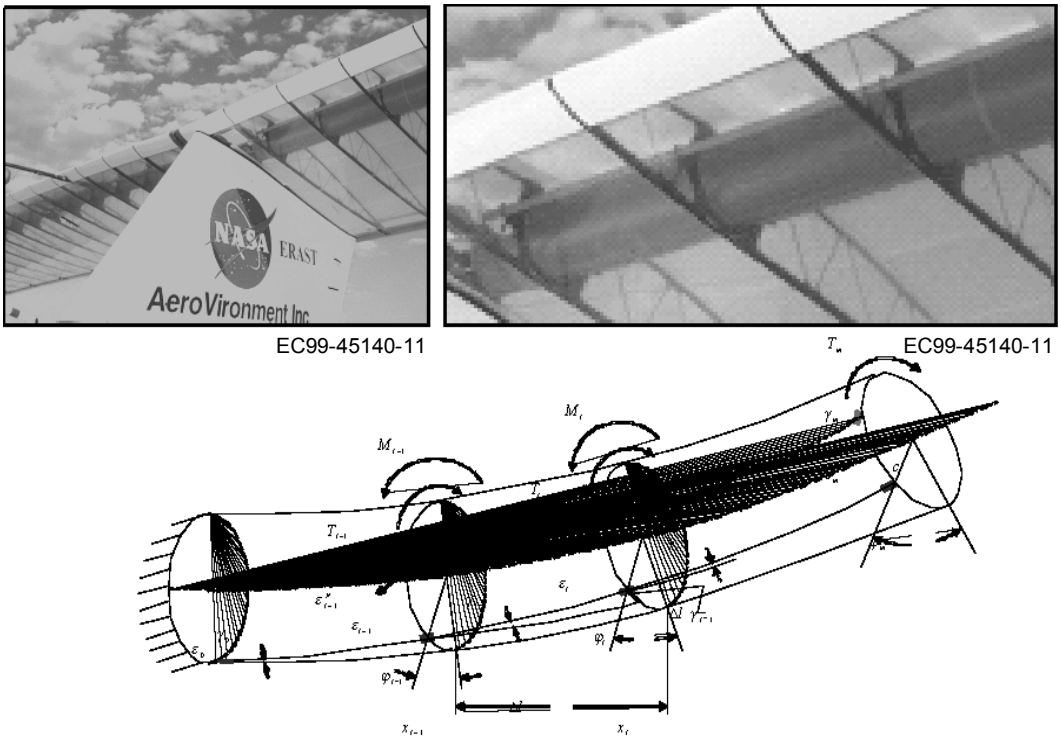

Figure 1. Helios wing structure (upper left) closeup showing spar detail (upper right), and tubular spar bending diagram (lower).

Photo courtesy Lance Richards

Figure 2. Composite tube during test.

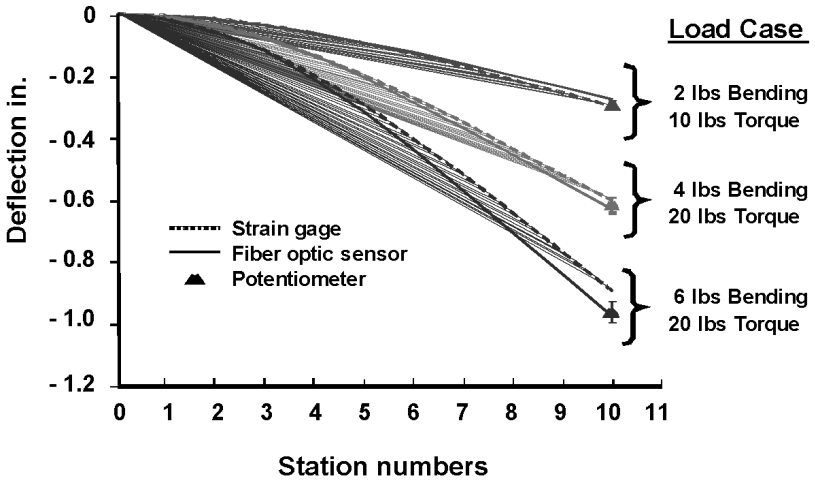

Figure 3. Load case test results.

Contacts

Dr. William L. Ko, DFRC, Code RS, (661) 276-3581
W. Lance Richards, DFRC, Code RS, (661) 276-3562

SIMULTANEOUS FLIGHT DEMONSTRATION OF THREE WING DEFLECTION MEASUREMENT APPROACHES

Summary

This work produced a demonstration of three simultaneous, independent wing elastic structural deflection measurement methods. The deflection measurement methods used were: 1) the electro-optical flight deflection measurement system (FDMS), 2) a standard video-based measurement method, and 3) a digital still-camera-based approach. These systems were flown on the Active Aeroelastic Wing (AAW) F/A-18 (McDonnell Douglas Corporation, St. Louis, Missouri and Northrop Corporation, Newbury Park, California) research airplane shown in figure 1. The focus of the AAW flight research project was to use wing torsional elasticity as an aid to roll control using modified flight control laws. The left wing upper surface was viewed and tracked by all three systems. Data were produced for steady 1*g* level cruise, 5*g* wind-up-turns, and 360-deg rolls.

EC02-0264-19

Figure 1. The NASA Active Aeroelastic Wing F/A-18 airplane in flight.

Objective

The objective of this research was to produce flight data from each system for performance comparisons. Measurement hardware size, weight, cost, installation complexity, data rate, precision, data availability, and other requirements were noted as well.

Approach

The data from the FDMS is used as the truth standard in this study. The FDMS has been used in various versions on several flight research projects including the Highly Maneuverable Aircraft Technology (HiMAT), the X-29A (Grumman Aerospace Corporation, Bethpage, New York) Forward Swept Wing aircraft, and the Advanced Fighter Technology Integration F-111 (General Dynamics, Falls Church, Virginia) AFTI Mission Adaptive Wing aircraft. The FDMS was used as the primary wing deflection research measurement on the AAW. The FDMS data operated at one data sample every 5 ms and was available in real time through the telemetry data stream.

The video-based deflection measurement study made use of a standard analog flight-qualified video camera positioned so that the upper surface of the left wing was viewed, as shown in figure 2. The inflight video signal was sent to the ground station through a telemetry channel and was monitored in real time. The original intent for this camera was for real time situational awareness for the mission control room team. Digital processing of the video frames has allowed the production of deflection data.

An off-the-shelf commercial digital still camera, shown in figure 3, was used for the third data system. It was mounted coaxially with the other two systems. The shutter was commanded manually by a trigger switch on the pilot's flight control stick. The images were recorded in electronic memory within the camera itself and were downloaded and processed postflight.

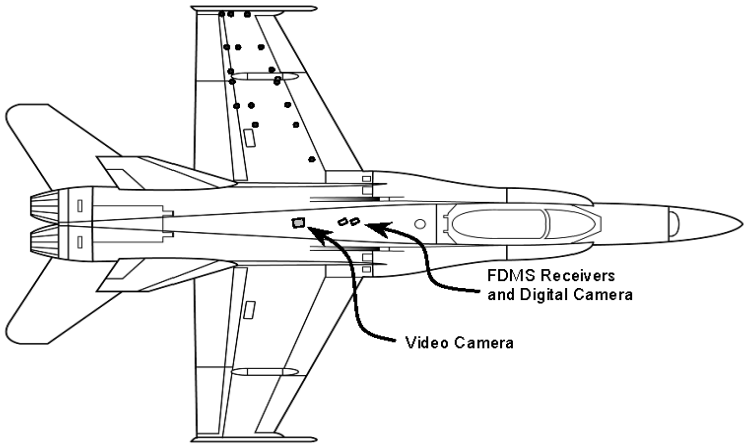

Figure 2. Measurement systems locations.

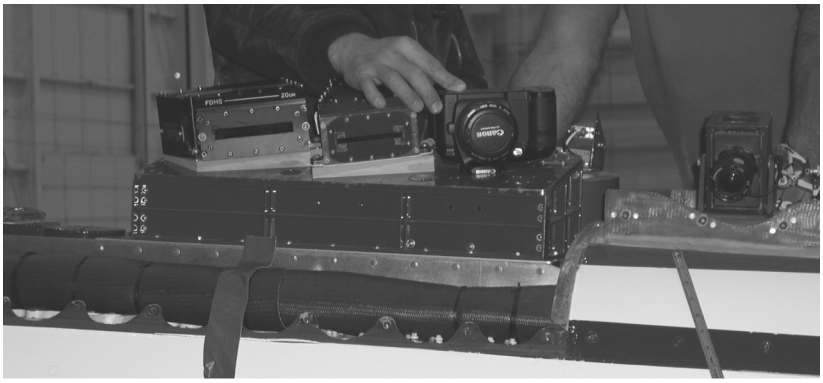

Photo courtesy James Mills

Figure 3. Flight deflection measurement system receivers, digital camera, and video camera.

Status

Flight data from all three systems were collected. The FDMS data have been reduced. Still camera images and video data will be processed next, leading to direct comparison of all three systems.

Contacts

William A. Lokos, DFRC, Code RS, (661) 276-3924
Danny A. Barrows, LaRC, Code D304, (757) 864-8158

NONLINEAR AEROELASTIC SYSTEM IDENTIFICATION WITH APPLICATION TO EXPERIMENTAL DATA

Summary

Research is under way to identify and represent nonlinear aeroelastic systems as Nonlinear AutoRegressive Moving Average model with eXogenous variables (NARMAX). A nonlinear difference equation describing a simple nonlinear aeroelastic aircraft model was derived theoretically and shown to be of the NARMAX form. Identification methods for NARMAX models are being applied to aeroelastic dynamics, and their properties demonstrated via continuous-time simulations of experimental conditions. Simulation results show that the outputs of the NARMAX model match closely those generated using continuous-time methods and that NARMAX identification methods applied to aeroelastic dynamics provide accurate discrete-time parameter estimates. Application of NARMAX identification to experimental aeroelastic dynamics data gives a high-percent fit for cross-validated data.

Objective

This application of system identification in the aerospace and flight-test community is for the analysis of aeroelasticity. Previous approaches have modeled aeroelasticity with linear time-invariant (LTI) models. These linear models have been successful in providing approximate estimates of the response of an aircraft to gust, turbulence and external excitations; for very flexible aircraft at any flight condition, or aircraft at high subsonic or transonic Mach numbers, however, linear models no longer provide accurate predictions of the behavior of the aircraft. Some of the behavior that cannot be modeled linearly includes very flexible high altitude, long endurance (HALE) and unmanned aerial vehicle (UAV) dynamics and effects of transonic dip, air flow separation, and shock oscillations which can induce nonlinear phenomena such as limit cycle oscillations (LCO). The onset of LCO has been observed on several aircraft such as the F-16C (Lockheed Martin Corporation, Bethesda, Maryland) or F/A-18 (The Boeing Company, Chicago, Illinois) and cannot be modeled properly as a LTI system. This has necessitated the application of nonlinear identification techniques to accurately model LCO dynamics.

Approach

Nonlinear models offer the advantage of covering a wider range of system dynamics than linear models, which could allow for faster envelope expansion. Using LTI models for envelope expansion requires the dynamics to be re-estimated as flight conditions change, because as a function of flight condition, the system will operate over a different region of the nonlinearity. With nonlinear identification, the model and hence its parameters, are valid over a larger operating regime since the model explicitly accounts for nonlinear effects. These nonlinear effects are modeled as nonlinear input–output terms. Identification of nonlinear models, which are linear-in-the-parameters, is more efficient than developing a set of LTI models which may be valid over only a small operating regime. Only one model is needed to describe the complex underlying dynamics with a NARMAX approach, as opposed to possibly many LTI models, over a given operating regime. Using nonlinear models to characterize aeroelastic phenomena can provide significant time and cost savings for test and development of aerospace vehicles. Moreover, the discrete nonlinear models of pitch–plunge provide excellent predictions which could be used for control synthesis, and statistical studies of NARMAX coefficients may be of direct relevance for health monitoring of aerostructures.

Status

The NARMAX modeling describes nonlinear systems in terms of linear-in-the-parameters difference equations relating the current output to (possibly nonlinear) combinations of inputs

and past outputs. It is suitable for modeling both the stochastic and deterministic components of a system and is capable of describing a wide variety of nonlinear systems. This formulation yields compact model descriptions that may be readily identified and may afford greater interpretability. The NARMAX model class offers an ideal framework for describing nonlinear behavior such as aeroelastic aircraft dynamics. The power of parametric nonlinear identification techniques in terms of NARMAX models is that these models can describe complex aeroelastic behavior over a large operating range, providing models that can be more robust and reduce development time.

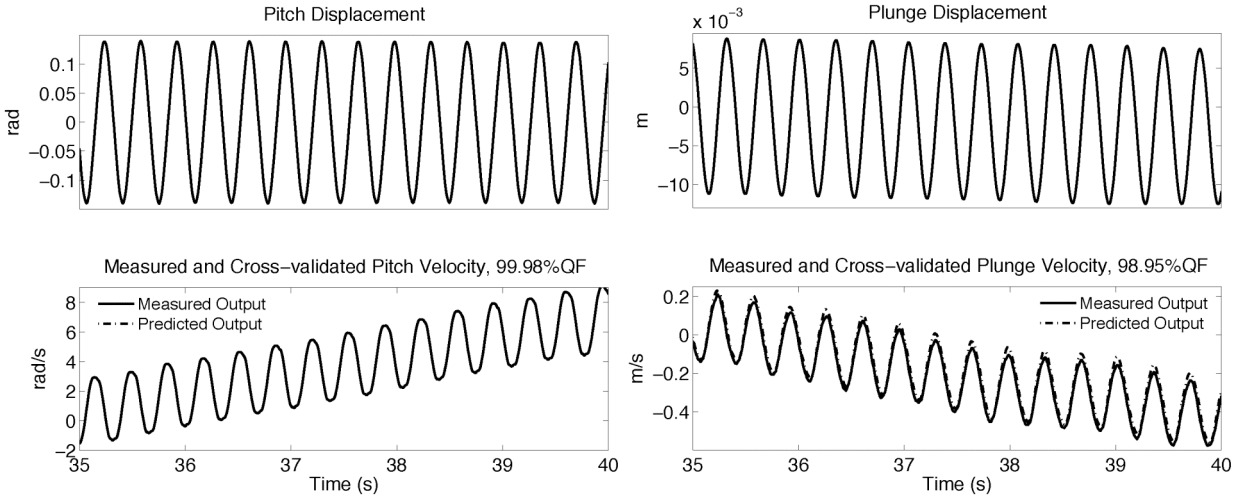

Pitch and plunge displacement and velocity.

Identification results illustrate that methods for identification of NARMAX models are well suited for identifying aircraft dynamics. Analysis of experimental data using NARMAX identification techniques provides a parameter set that explains the input–output data well. This research contributes to the understanding of the use of parametric identification techniques for modeling of aerospace systems. The main point here is that the NARMAX form is clearly amenable to the study of a wide range of aerospace systems, and could be computationally efficient. The NARMAX modeling and identification techniques should be examined further, especially in the case of severe nonlinear behavior.

Contacts

Sunil L. Kukreja, DFRC, Code RS (Aerostructures Branch, NRC postdoc),
Sunil.Kukreja@nasa.gov, (661) 276-2788
Marty Brenner, DFRC, Code RS (Aerostructures Branch), Martin.J.Brenner@nasa.gov,
(661) 276-3793

A LEAST ABSOLUTE SHRINKAGE AND SELECTION OPERATOR (LASSO) FOR NONLINEAR SYSTEM IDENTIFICATION

Summary

Identification of parametric nonlinear models involves estimating unknown parameters and detecting the underlying structure. Structure computation is concerned with selecting a subset of parameters to give a parsimonious description of the system, which may afford greater insight into the functionality of the system or a simpler controller design. In this research, a least absolute shrinkage and selection operator (LASSO) technique is being investigated for computing efficient model descriptions of nonlinear systems. The LASSO minimizes the residual sum of squares by the addition of a 1-norm penalty term on the parameter vector of the traditional 2-norm minimization problem. Use of the LASSO for structure detection is a natural extension of the constrained minimization approach to linear regression problems, which produces some model parameters that are exactly zero and, therefore, yields a parsimonious system description. The performance of this LASSO structure detection method was evaluated by using it to estimate the structure of two nonlinear polynomial models. The applicability of the method to more complex systems, such as those encountered in aerospace applications, was shown by identifying a parsimonious system description of the F/A-18 (McDonnell Douglas Corporation, St. Louis, Missouri and Northrop Corporation, Newbury Park, California) Active Aeroelastic Wing (AAW) airplane using flight test data.

Objective

Discrete-time nonlinear polynomials are often useful to describe the input-output behavior of complex systems encountered in many control engineering, aerospace engineering and biological science applications. These polynomial mappings describe the dynamic relationship of a system by expanding the present output value in terms of present and past values of the input signal and past values of the output signal. These models are popularly known as polynomial Nonlinear AutoRegressive Moving Average model with eXogenous variables (NARMAX). Many systems are described by these polynomial models having only a few terms. However, even if the system order is known through some a priori knowledge, a full expansion of this model representation yields a large number of candidate terms that may be required to represent the system dynamics. Often many of these candidate terms are insignificant and, therefore, can be removed. Hence, the structure detection problem is that of selecting a subset of candidate terms that best predicts the output while maintaining an efficient system description. The relevance of structure computation is, for example, controller design and study of aerospace vehicle dynamics. For control, a parsimonious system description is essential for many control strategies. In modeling, the objective is often to gain insight into the function of the underlying system.

There are two fundamental approaches to the structure detection problem: 1) exhaustive search, in which every possible subset of the full model is considered, or 2) parameter variance, in which the covariance matrix based on input-output data and estimated residuals is used to assess parameter relevance. Both have problems. Exhaustive search requires a large number of computations and parameter variance estimates are often inaccurate when the number of candidate terms is large.

Approach

For many practical systems, collecting large data records may be financially or technically infeasible, or both. Nonlinear aeroelastic dynamics of aircraft are highly complex processes likely involving a large number of candidate terms (such as high order terms) which may not be accurately characterized by current NARMAX identification approaches. The application of a

novel method for NARMAX model identification via LASSO is being researched. This approach permits identification of NARMAX models in situations in which current methods cannot be applied.

Often in aerospace applications, the model order is not well known a priori but can be bounded by some upper limit. In this research it is assumed that the system order can be bounded. The nonlinearity order (for polynomial models) can often be upper bounded as third order since models of higher nonlinear order can be decomposed to second or third order.

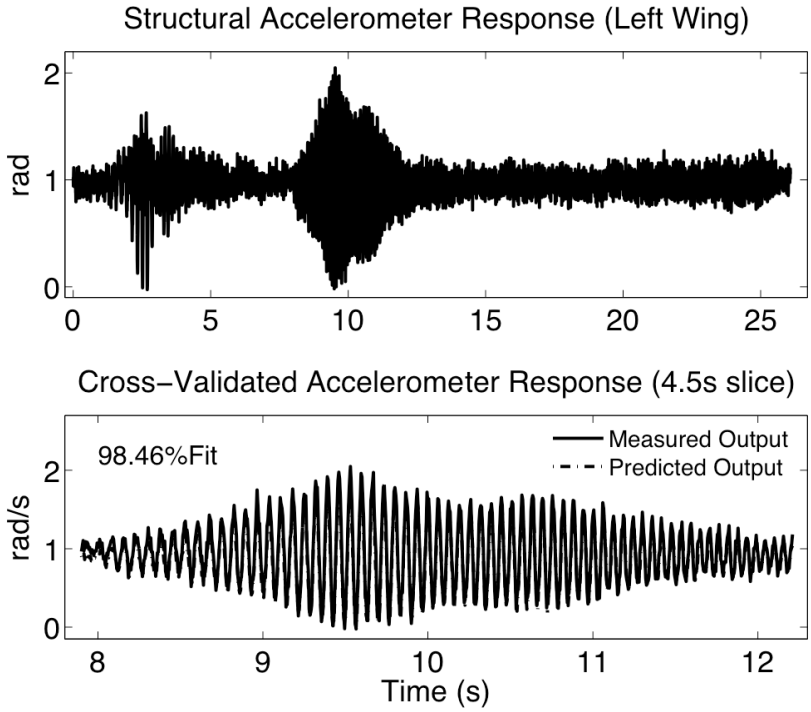

Accelerometer responses.

Status

The LASSO technique yields good results for structure detection of highly overparameterized polynomial NARMAX models in the presence of additive output noise. Application of structure computation to aeroelastic modeling using flight test data from the F/A-18 AAW airplane was shown to yield a parsimonious model structure while maintaining a high-percent fit to cross-validation data. The LASSO technique is a novel approach for detecting the structure of highly overparameterized nonlinear models in situations where other methods may be inadequate. The main point here is that the LASSO technique is clearly amenable to the study of a wide range of nonlinear systems. These results may have practical significance in the analysis of aircraft dynamics during envelope expansion and could lead to more efficient control strategies. In addition, this technique could allow greater insight into the functionality of various systems dynamics by providing a quantitative model which is easily interpreted.

Contacts

Sunil L. Kukreja, DFRC, Code RS (Aerostructures Branch, NRC postdoc),
Sunil.Kukreja@nasa.gov, (661) 276-2788
Marty Brenner, DFRC, Code RS (Aerostructures Branch), Martin.J.Brenner@nasa.gov,
(661) 276-3793

THE X-37 HOT STRUCTURE CONTROL SURFACE TESTING

Summary

Thermal-structural testing of three hot structure control surface subcomponent test articles (STA) designed for the X-37 (Boeing Phantom Works, Huntington Beach, California) Orbital Vehicle (OV) has been completed. The test articles were subcomponents of the X-37 OV bodyflap and flaperon control surfaces (figs. 1 and 2).

Figure 1. The X-37 Orbital Vehicle subcomponent test articles.

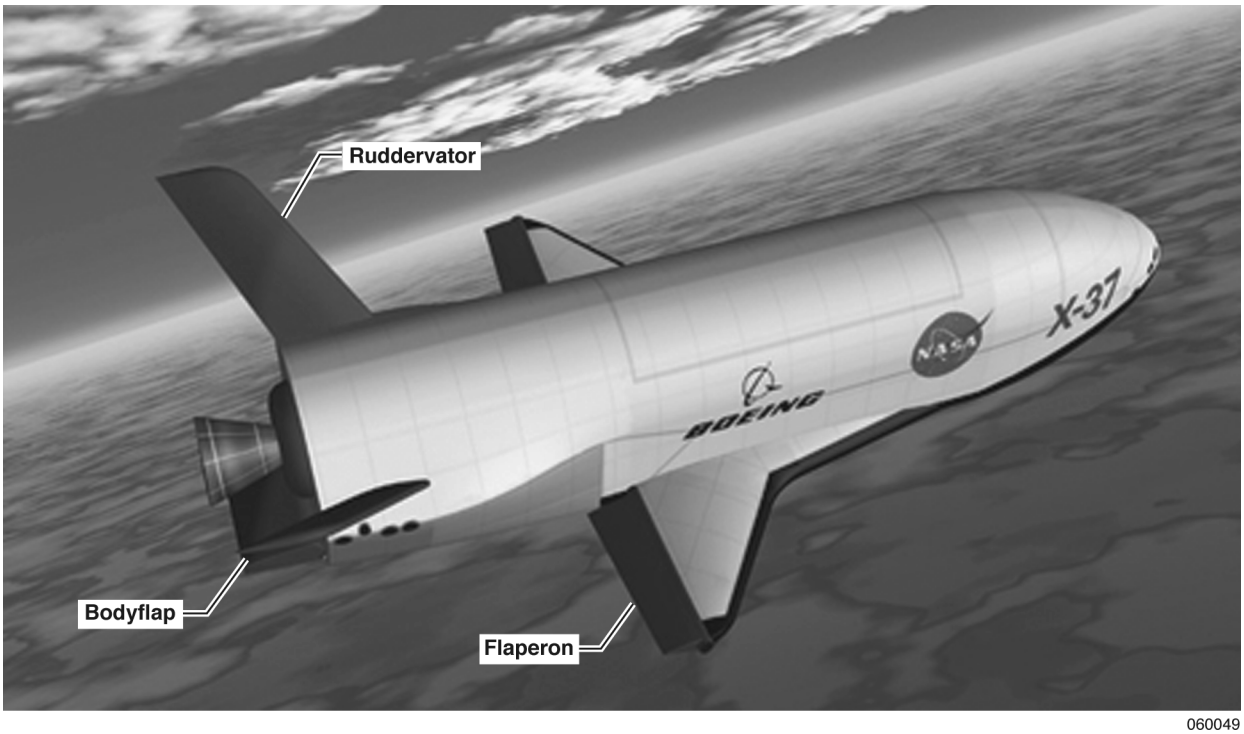

Figure 2. The X-37 Orbital Vehicle hot structure control surfaces.

The bodyflap STA was fabricated using carbon-silicon carbide (C/SiC). It had overall dimensions of approximately 24 in. L x 20 in. W x 4 in. H. The bodyflap STA was tested under combined thermal and structural loading to approximately 2100 °F and 100 percent of the design limit load (DLL) with no observable damage.

A C/SiC and carbon-carbon (C/C) flaperon STA was also tested under thermal and structural loading. Each STA utilized the same X-37 OV aerodynamic heating and loading profile information. Each STA also included a titanium spindle and an Inconel® Huntington Alloy Products Division, International Nickel Company, Huntington, West Virginia, outboard hinge pin.

The C/SiC Flaperon STA had overall dimensions of approximately 14 in. L x 30 in. W with a leading edge to trailing edge taper of 5 in. to 2 in. The STA was thermally and structurally loaded to 2400 °F and 100 percent DLL, respectively. It was also tested under combined structural and thermal loading and experienced 50 percent DLL at approximately 1800 °F. A final test to failure was performed at room temperature, which resulted in the C/SiC STA failing at 170 percent DLL.

The C/C flaperon STA had overall dimensions of approximately 19 in. L x 37 in. W with a leading edge to trailing edge taper of 5 in. to 1 in. The C/C STA was thermally and structurally loaded to 2300 °F and 100 percent DLL, respectively. A final test to 200 percent DLL was performed at room temperature, which resulted in the C/C STA showing no indications of failure.

Objective

The overall objective of the STA testing was to acquire structural ground test data on the performance of C/SiC and C/C hot structure control surfaces while being subjected to the simulated re-entry thermal and structural loading associated with the X-37 OV. The test data was used to verify the structural model and finite element analyses of each STA design.

Approach

Each STA was tested thermally in a nitrogen purged atmosphere (fig. 3). Structural loading was performed in air when not combined with thermal loading. Each STA was instrumented with high-temperature fiber optic strain sensors and thermocouples, both of which were bonded to the C/SiC and C/C substrates using the NASA Dryden Flight Research Center developed thermal-spraying techniques.

EC03-0275-03

EC04-0151-09

Photo courtesy of Larry Hudson

Figure 3. The X-37 Orbital Vehicle subcomponent test articles under test at NASA Dryden Flight Research Center.

Status

All STA testing has been completed and the test results have been documented, with the flaperon STA results being incorporated into the X-37 Flaperon Qualification Unit test program planned for completion in fiscal year 2005.

Contacts

Larry D. Hudson, DFRC, Code RS, (661) 276-3925
Craig A. Stephens, DFRC, Code RS, (661) 276-2028

TECH BRIEFS AND PATENTS

NASA Tech Briefs Articles

Casey Donohue
Role of Meteorology in Flights of a Solar-Powered Airplane
DRC-02-25

REPORT DOCUMENTATION PAGE

Form Approved
OMB No. 0704-0188

1. REPORT DATE *(DD-MM-YYYY)*	2. REPORT TYPE	3. DATES COVERED *(From - To)*
12-06-2006	Technical Memorandum	

4. TITLE AND SUBTITLE
2004 Research Engineering Annual Report

5a. CONTRACT NUMBER

5b. GRANT NUMBER

5c. PROGRAM ELEMENT NUMBER

6. AUTHOR(S)
Stoliker, Patrick; Flick, Bradley; and Cruciani, Everlyn

5d. PROJECT NUMBER

5e. TASK NUMBER

5f. WORK UNIT NUMBER
ES7

7. PERFORMING ORGANIZATION NAME(S) AND ADDRESS(ES)
NASA Dryden Flight Research Center
P.O. Box 273
Edwards, California 93523-0273

8. PERFORMING ORGANIZATION REPORT NUMBER
H-2638

9. SPONSORING/MONITORING AGENCY NAME(S) AND ADDRESS(ES)
National Aeronautics and Space Administration
Washington, DC 20546-0001

10. SPONSORING/MONITOR'S ACRONYM(S)
NASA

11. SPONSORING/MONITORING REPORT NUMBER
NASA/TM-2006-213677

12. DISTRIBUTION/AVAILABILITY STATEMENT
Unclassified -- Unlimited
Subject Category 99 Availability: NASA CASI (301) 621-0390 Distribution: Standard

13. SUPPLEMENTARY NOTES
Stoliker, Flick, and Cruciani, Dryden Flight Research Center
An electronic version can be found at the NASA Dryden Flight Research Center Web site, under Technical Reports.

14. ABSTRACT
Selected research and technology activities at Dryden Flight Research Center are summarized. These activities exemplify the Center's varied and productive research efforts.

15. SUBJECT TERMS
Aerodynamics, Flight, Flight controls, Flight systems, Flight test, Instrumentation, Propulsion, Structures, Structural Dynamics

16. SECURITY CLASSIFICATION OF:			17. LIMITATION OF ABSTRACT	18. NUMBER OF PAGES	19a. NAME OF RESPONSIBLE PERSON
a. REPORT	b. ABSTRACT	c. THIS PAGE			STI Help Desk (email: help@sti.nasa.gov)
U	U	U	UU	98	19b. TELEPHONE NUMBER *(Include area code)* (301) 621-0390